Subduction III
Regional subduction zone modeling

Thorsten W Becker
University of Southern California

Short course at Universita di Roma TRE
April 18 – 20, 2011

Reading

- King, S. (Elsevier Treatise, 2007)
- Billen, M. (Ann Rev, 2009)
- Becker & Faccenna (2009)

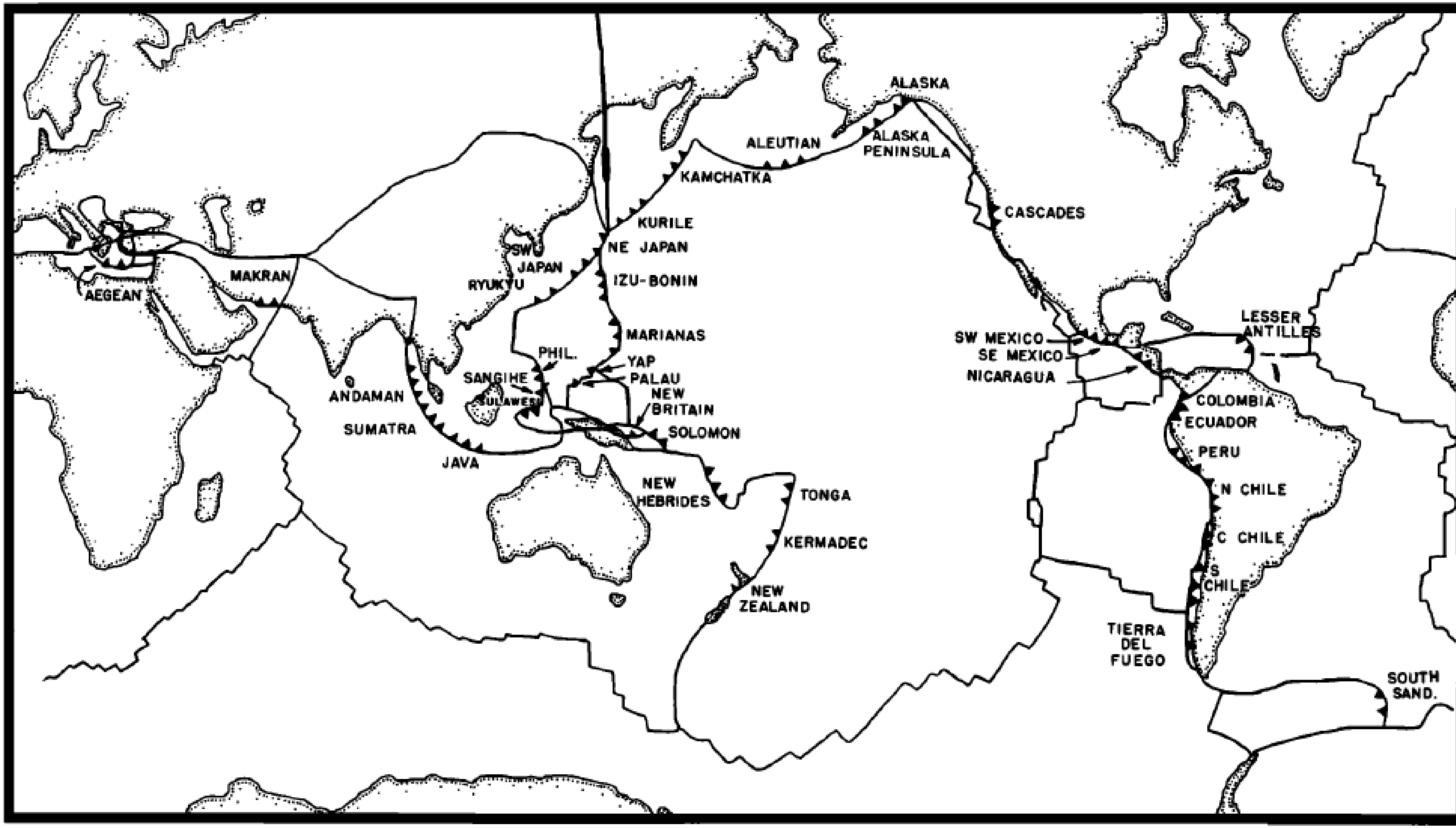

Jarrard (1986)

Figure 3 Covariance matrix for nine observations compiled from 39 modern subduction zones (Jarrard, 1986). The color scale represents the value of the correlation coefficient, with +1.0 being strongly correlated and −1.0 being strongly anticorrelated. Rollback is the rate of trench migration estimated from the global plate models (Minster and Jordan, 1978). Velocity is the velocity of the plate at the trench from the same global plate models. Slab age is the age of the plate entering the trench, and slab-tip age is calculated using the length of the slab and rate of change of the plate age for the plate entering the trench. The intermediate dip is calculated from the trench to the 100 km depth of the slab. The deep dip is calculated from the 100–400 km depth of the slab. The thermal parameter is the product of the slab age and the length of the slab.

King (2007)

Pre - Plate Tectonics

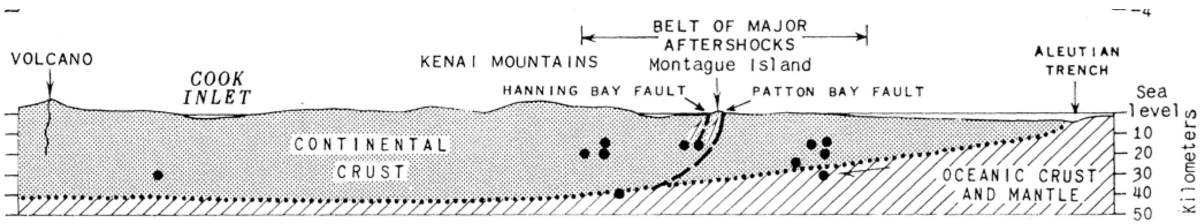

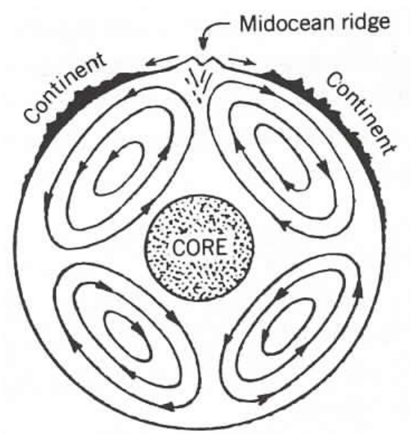

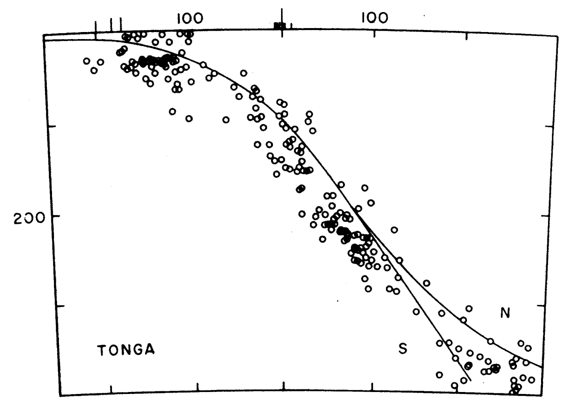

Internal deformation of subducted lithosphere.

- Isacks & Molnar, 1969

Deep planar fault zone

- Elsasser, 1968

Lithospheric thrusting

- Plafker, 1965

Mantle Convection

- Holmes, 1944

Mega-shear to 700 km

- Benioff, 1954

Crustal-scale thrusting

- Hess, 1962

1940s ***1950s*** ***1960s***

- ***Subduction into the mantle was one of the last pieces of the plate tectonics puzzle.***

Slide courtesy of M. Billen

Plate Tectonics: in the SZ

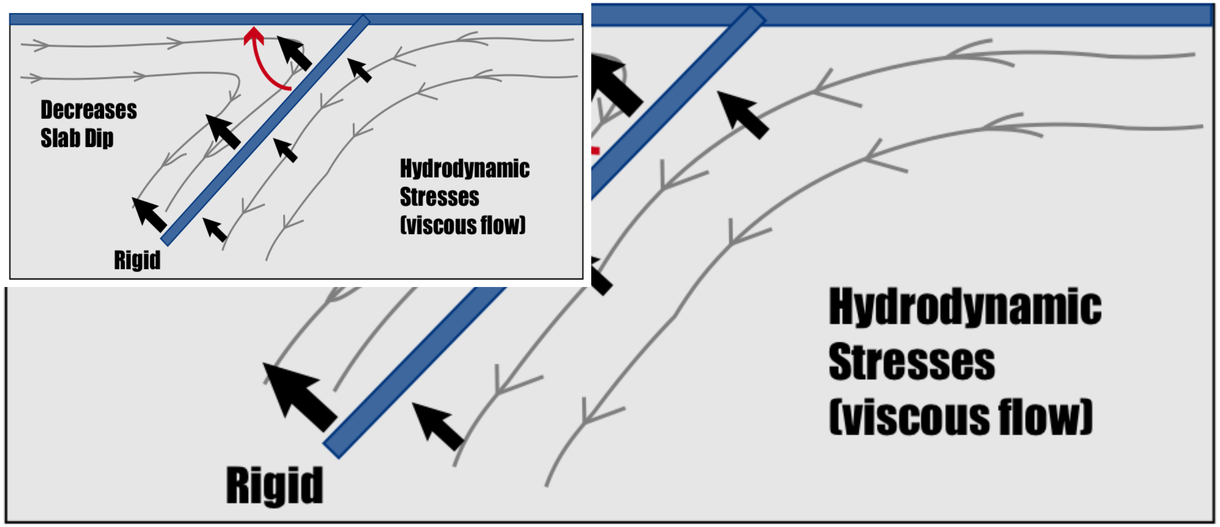

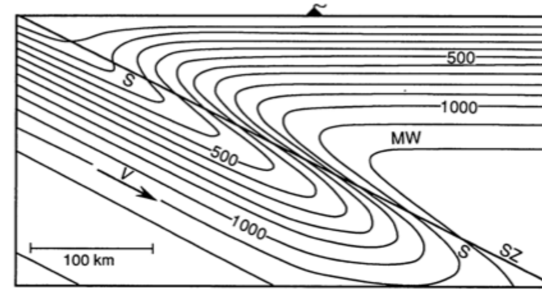

Linking slab temp. to mineralogy & petrology
- Peacock, 1990

- Yokokura, 1981

Corner-flow model.
- McKenzie, 1969

Dynamic topography from corner-flow
- Sleep, 1975

Slab thermal structure
-Toksov, 1971; 1973

1960s ***1970s 1980s*** ***1970s 1990s***

- ***Early analytic models capture major processes.***
  - ***Force balance on slab.***
  - ***Slab thermal structure.***

Slide courtesy of M. Billen

Kinematic Slab - Dynamic Wedge

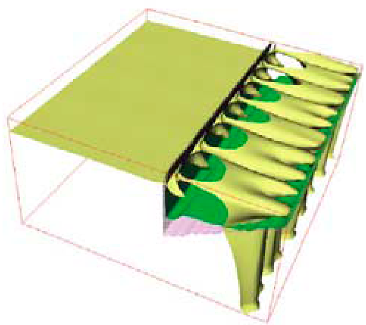

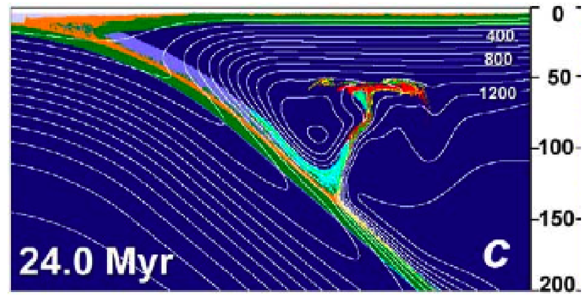

3D, anisotropy implication
- Kneller & van Keken, 2007

Non-linear viscosity
- Kneller et al., 2007

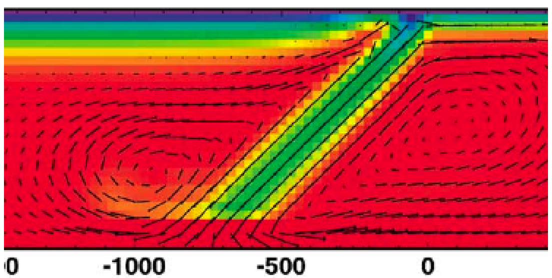

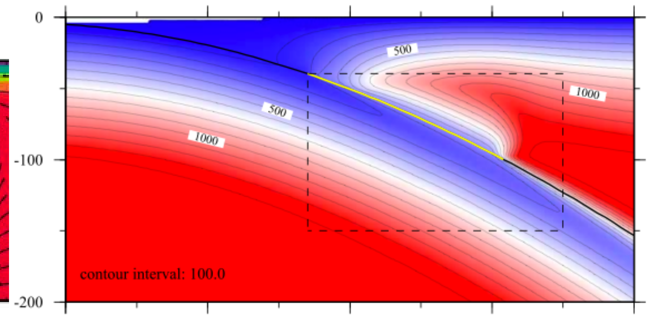

Compositional & phase: density & viscosity
- Gerya & Yuen, 2003

Low viscosity wedge
- Honda & Saito, 2003

Wedge/back arc flow
- Bodri & Bodri, 1978
- Toksov & Hsui, 1978

Convection in the wedge
- Ida, 1983
- Honda, 1985

Temperature-dep. visc.
- Eberle, 2001

1970s ***1980s*** ***1990s*** ***2000s***

- ***Slab & mantle wedge thermal/min./pet. structure.***
- ***Fluid transport***
- ***Seismic anisotropy.***

Slide courtesy of M. Billen

Observations

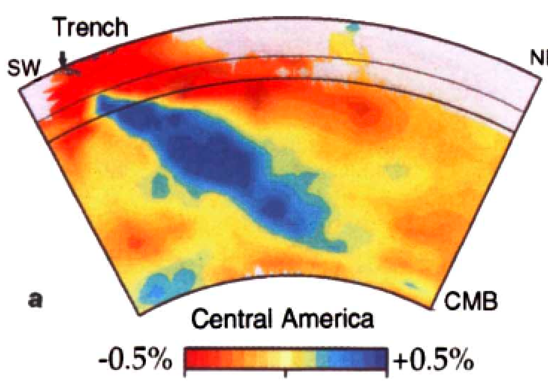

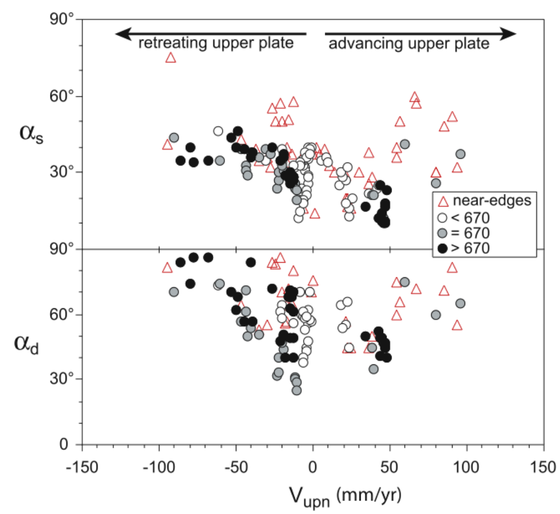

Plate kinematics & characteristics
- Mueller et al., 1997
- Lallemand et al., 2005

Seismic anisotropy
- Russo & Silver, 1994
- Fischer et al., 1998
- Long & Silver, 2008

Plate kinematics & characteristics
- Jarrard, 1986

Seismic tomography
- e.g., van der Hilst, 1997

Arc curvature, slab dip, subduction velocity.
- Tovish & Schubert, 1978

Geoid & dynamic topo.
- Hager 1984

Plate tectonic reconsts.
- e.g., DeMets, 1990

1970s

1980s

1990s ***2000s***

- ***Connecting kinematics to dynamics.***

Slide courtesy of M. Billen

Instantaneous (quasi) Dynamic

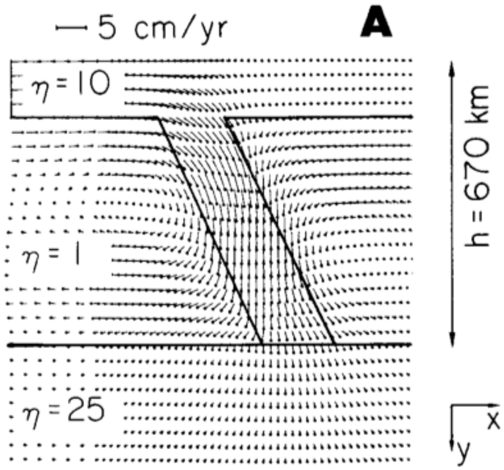

Stress-state in slab
- Vassiliou, 1984

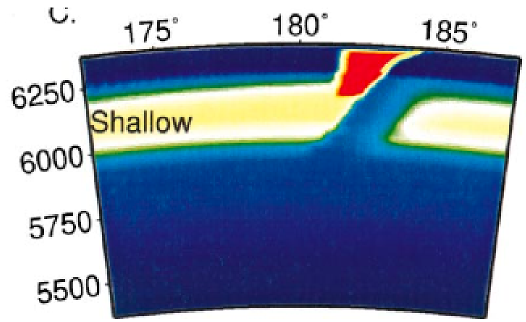

3D, Weak plate bndy, non-linear rheology
- Zhong & Gurnis, 1996

3D, Lateral (moderate) viscosity variations
- Moresi et al., 1996

2D, Faults & non-linear viscosity
- Zhong & Gurnis, 1992, 1994

2D, Overriding plate root geometry & slab suction
- Driscoll et al., 2009

3D, Slab strength effect toroidal & poloidal flow
- Piromallo et al., 2006

3D, Temp-dep, low viscosity wedge
- Billen & Gurnis, 2001

1980s ***1990s*** ***2000s***

- ***Rheologic Structure:***
  - ***mantle, slab, plate boundaries, wedge, crust...***
- ***Surface deformation:***
  - ***topography, geoid, stress-state.***

Slide courtesy of M. Billen

Fully Dynamic (t-dependent)

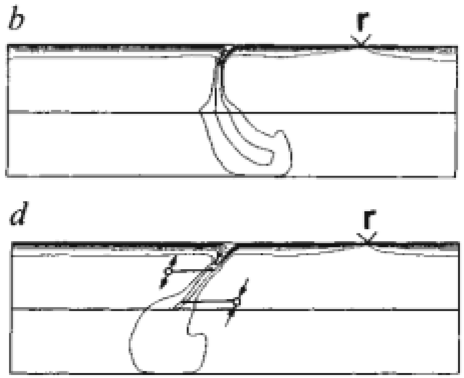

2D, Temp-dep,
- Gurnis & Hager 1988

2D, Phase trans. (mech)
- Christensen & Yuen, 1984

1980s

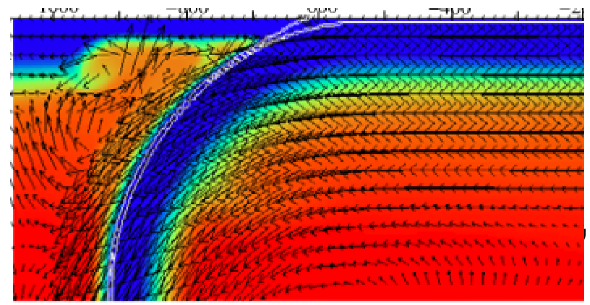

2D, Subduction initiation
- Toth & Gurnis, 1998

2D, Trench migration
- Olbertz et al., 1997
- Griffiths et al., 1995

2D, Phase trans. (T-dep. viscosity)
- King, 1991

1990s

2D, wedge rheology
- Arcay et al., 2008

3D, Slab width effects
- Stegman, 2006

2D, Slab detachment
- Gerya & Yuen, 2004

3D, Trench migration
- Funiciello et al., 2003

2D, Comp., grain-size-dep. slab visc
- Cizkova et al., 2002

2D, Oceanic plateaus
- van Hunen et al 2000

2000s

- ***Buoyancy forces: phase transition, slab, crust...***
- ***Rheologic structure: mantle, slab, wedge...***
- ***Geometry: 2-D, 3-D, slab edges, interactions...***

Slide courtesy of M. Billen

Fully Dynamic (t-dependent)

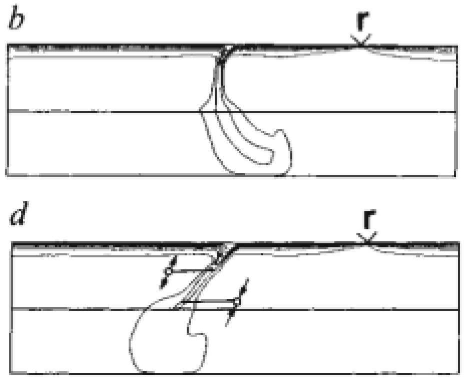

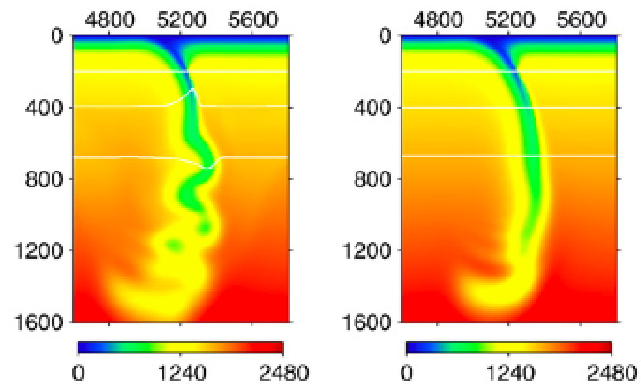

2D, Temp-dep,
- Gurnis & Hager 1988

2D, Phase trans. (mech)
- Christensen & Yuen, 1984

_1980s_

2D, Trench migration
- Olbertz et al., 1997
- Griffiths et al., 1995

2D, Phase trans.
(T-dep. viscosity)
- King, 1991

_1990s_

3D, Slab-edge flow & slab depth
- Honda, 2009

2D, Slab Buckling LM.
- Behounkova & Cizkova 2008

2D, Double-slab sub.
- Mishin et al., 2008

2D, 1-sided subduction
- Gerya et al., 2008

2D, Flat slabs & LVC
- Manea & Gurnis, 2007

2D, wedge rheology
- Arcay et al., 2008
3D, Slab width effects
2D, Slab detachment
- Stegman, 2006
3D, Trench migration
- Gerya & Yuen, 2004
2D, Comp., grain-size-dep. slab visc
- Funiciello et al., 2003
2D, Oceanic plateaus
- Cizkova et al., 2002
- van Hunen et al 2000

_2000s_

- ***Buoyancy forces: phase transition, slab, crust...***
- ***Rheologic structure: mantle, slab, wedge...***
- ***Geometry: 2-D, 3-D, slab edges, interactions...***

Slide courtesy of M. Billen

Fully Dynamic (t-dependent)

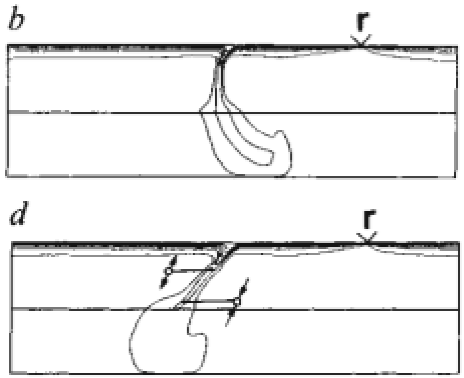

2D, Temp-dep,
- Gurnis & Hager 1988

2D, Phase trans. (mech)
- Christensen & Yuen, 1984

1980s

2D, Meta-stable olivine,
- Schmeling, 1999

2D, Subduction initiation
- Toth & Gurnis, 1998

2D, Trench migration
- Olbertz et al., 1997
- Griffiths et al., 1995

2D, Phase trans.
(T-dep. viscosity)
- King, 1991

1990s

2D, Compressibility
- Lee & King, 2009

2D, Ridge-trench int.
- Burkett & Andrews, 2009

2D, Coupled/uncoupled
continental collision
- Faccenda et al., 2009

3D, Slab-edge flow & slab depth
2D, Slab Buckling LM.
- Honda, 2009
2D, Double-slab sub.
- Behounkova & Cizkova 2008
2D, 1-sided subduction
- Mishin et al., 2008
2D, Flat slabs & LVC
- Gerya et al., 2008
- Manea & Gurnis, 2007

2D, wedge rheology
3D, Slab width effects
- Arcay et al., 2008
2D, Slab detachment
- Stegman, 2006
3D, Trench migration
- Gerya & Yuen, 2004
2D, Comp., grain-size-dep. slab visc
2D, Oceanic plateaus
- Funiciello et al., 2003
- Cizkova et al., 2002
- van Hunen et al 2000

2000s

- ***Buoyancy forces: phase transition, slab, crust...***
- ***Rheologic structure: mantle, slab, wedge...***
- ***Geometry: 2-D, 3-D, slab edges, interactions...***

Slide courtesy of M. Billen

Mineralogical-Petrological

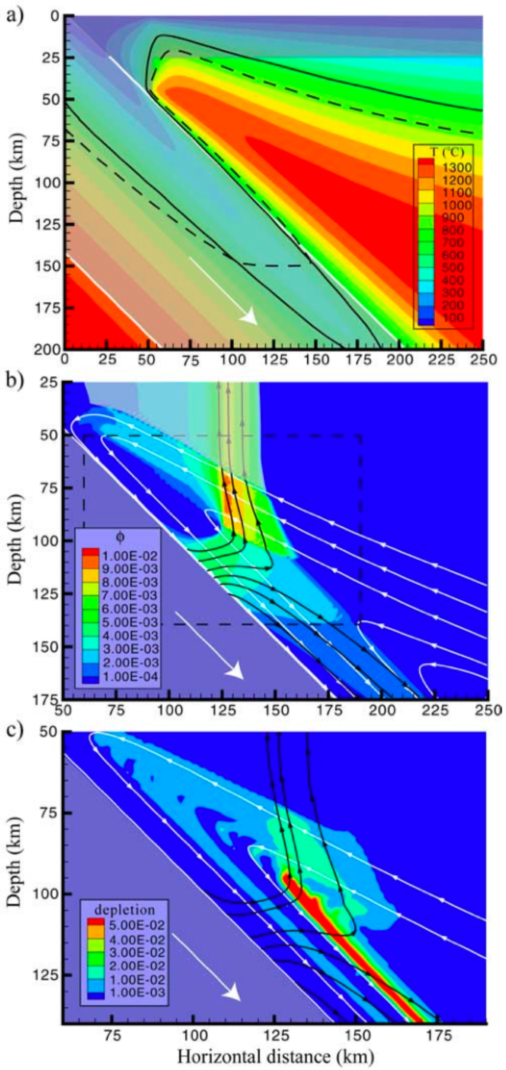

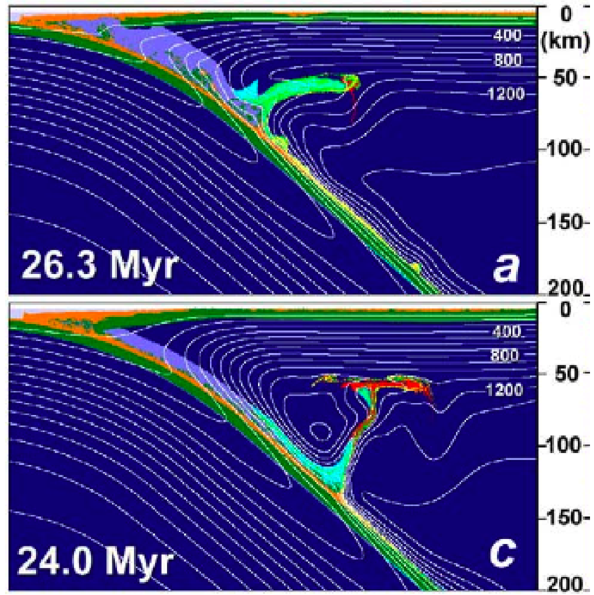

Fully-coupled mantle-wedge dynamics & petrology
- Baker-Hebert et al., 2009

Fluid transport, melting
- Cagniocle et al., 2007

Composite crust-mantle density & rheology in wedge
- Gerya & Yuen, 2003

Min./pet. implications
- Davies & Stevenson, 1992

1990s 2000s

- ***Need coupled solid & fluid flow, density & rheology, detailed tracking of composition & phase.***

Slide courtesy of M. Billen

A Multi-variate System

- ***Geometrical Variables***
  - 2D vs. 3D
  - Over-riding plate
  - Interaction w/ other plate boundaries.
- ***Mineral-/Petro-logical***
  - Compositional variation
    - Density
    - Rheology
- ***Physical Properties***
  - Rheology
  - Thermal parameters (α,κ)
  - Compressibility
- ***Coupled Systems***
  - Solid phase changes
  - Hydration/dehydration
  - Melting

Link to Observations & Time Evolution

Transform a kinematic theory to a <u>dynamic theory.</u>

Kinematic models

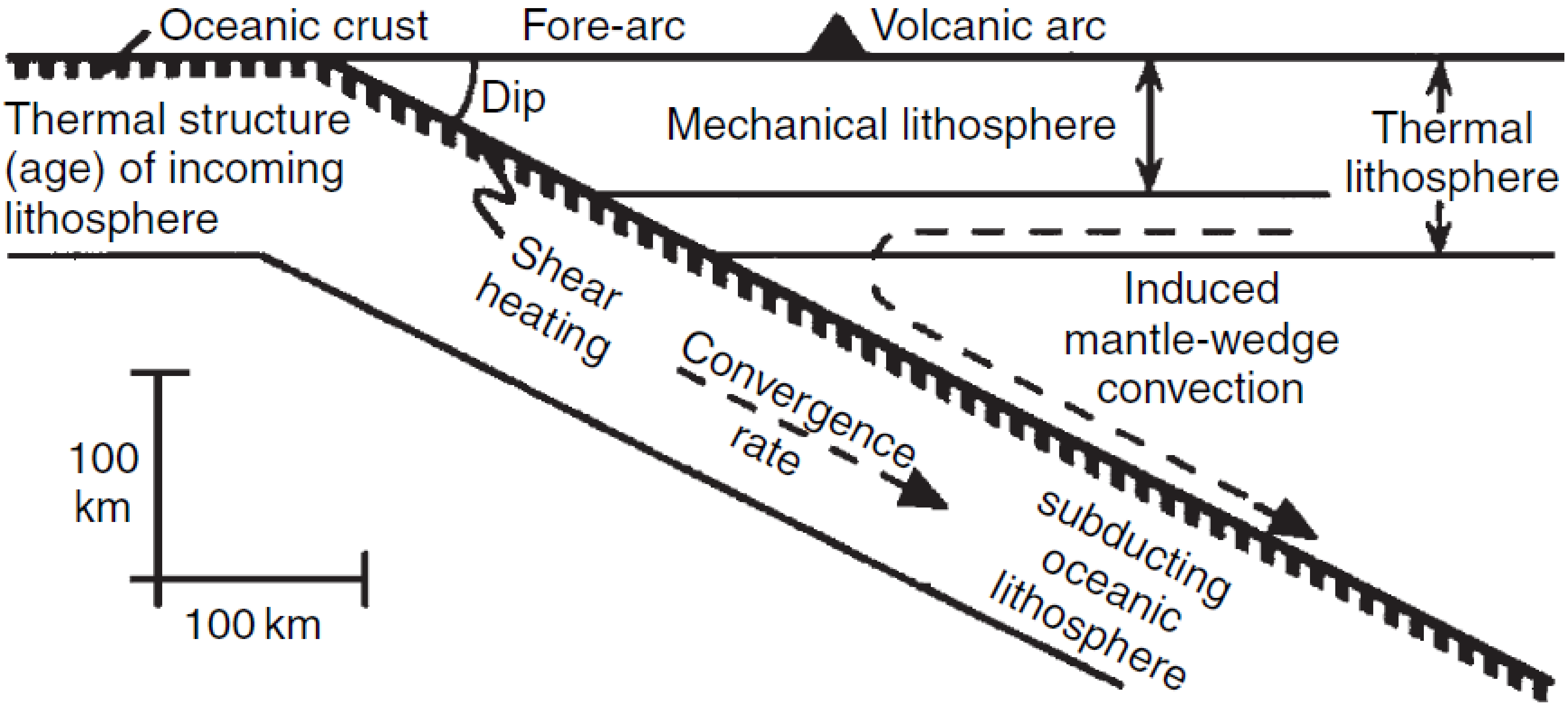

Peacock, 1996

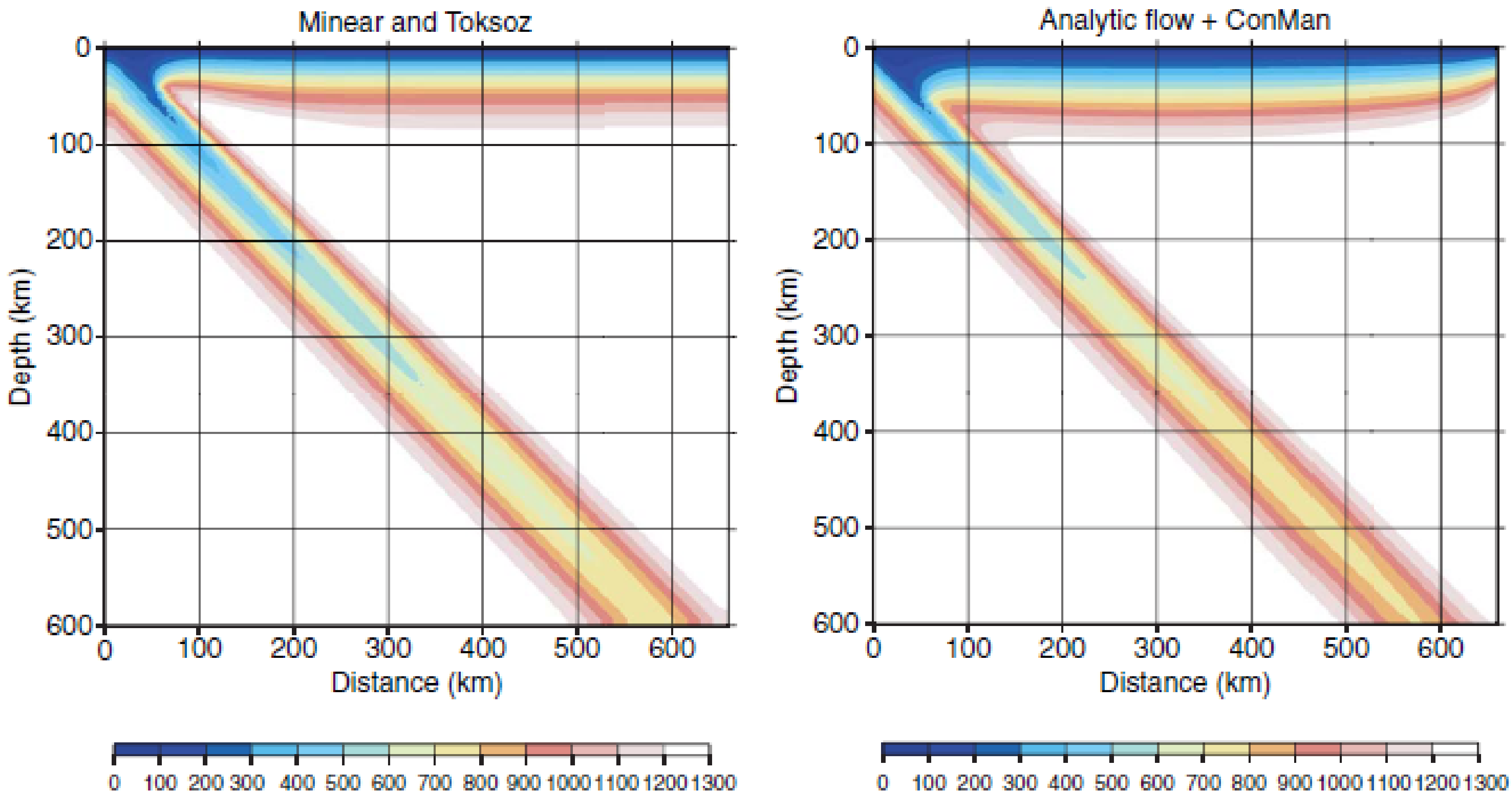

Figure 7 A comparison of slab thermal structures from a 50-Myr-old, 45° dipping slab descending at 5 cm yr^{-1} with kinematic slab approximations (left) (Minear and Toksöz, (1970) and (right) the analytic corner flow solution for flow and ConMan's temperature solver. Below 50 km depth, the Minear and Toksöz slab is colder than the corner flow plus ConMan solution.

King (2007)

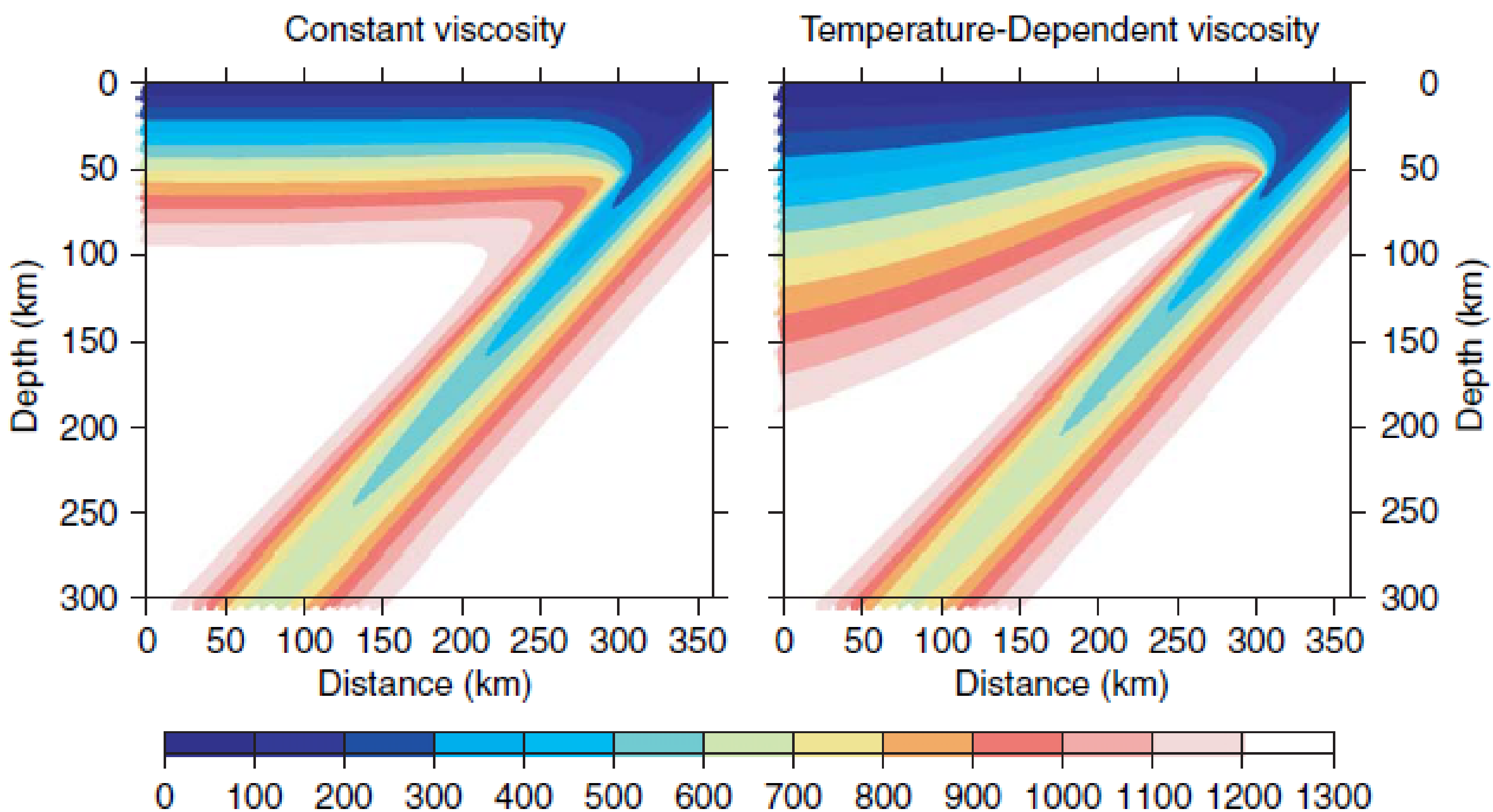

Figure 9 Thermal structure from two slab calculations using ConMan (King *et al.*, 1990). Both calculations have a slab descending at 45° at a fixed velocity of 5 cm yr^{-1}. The incoming plate material is 50 My old. The left image is a constant-viscosity mantle wedge and the right image is a temperature-dependent viscosity wedge, with an activation energy of 335 kJ mol^{-1}.

King (2007)

Heatflow

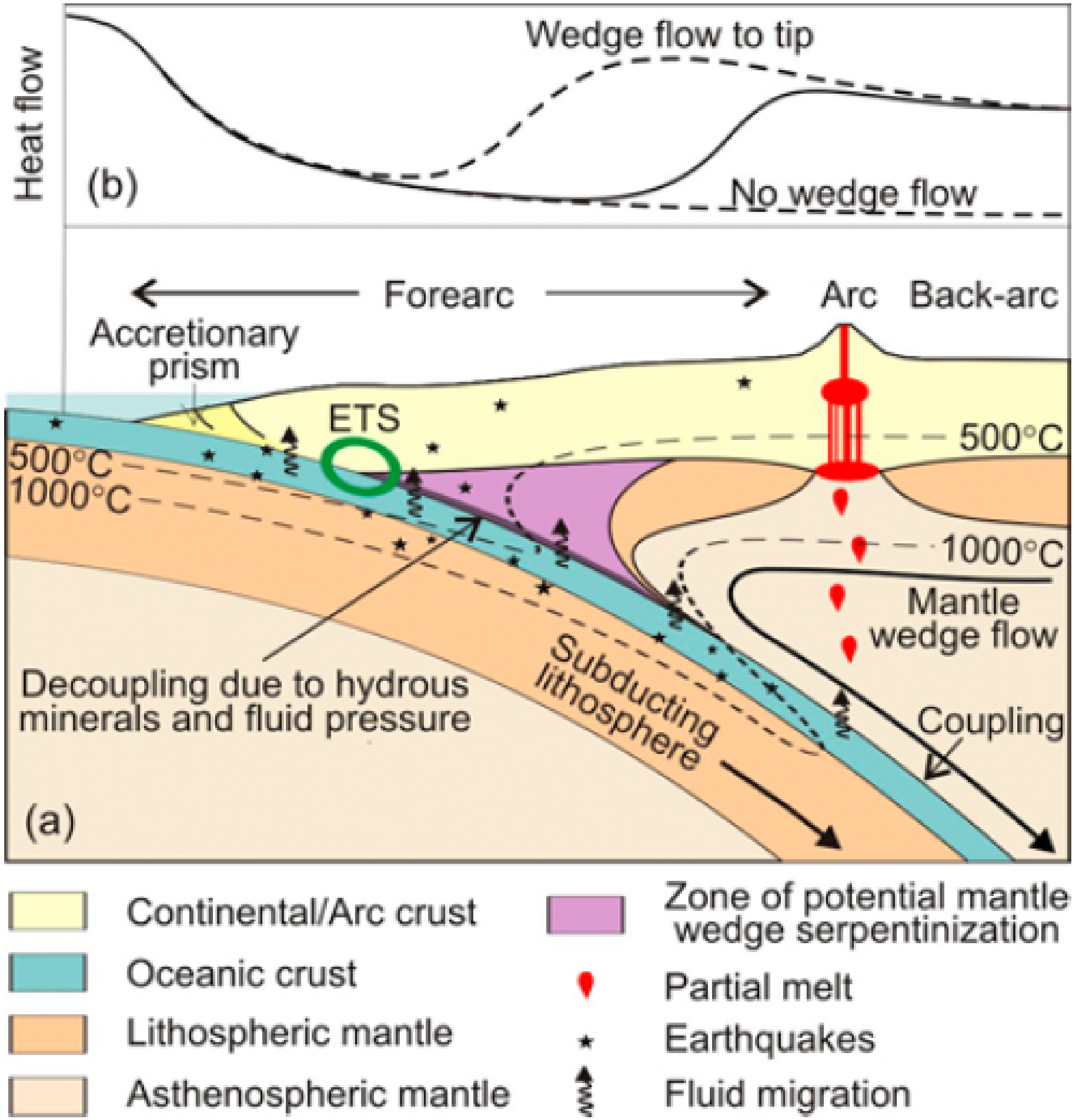

Wada and Wang, G3, 2009

Constraints on decoupling zone

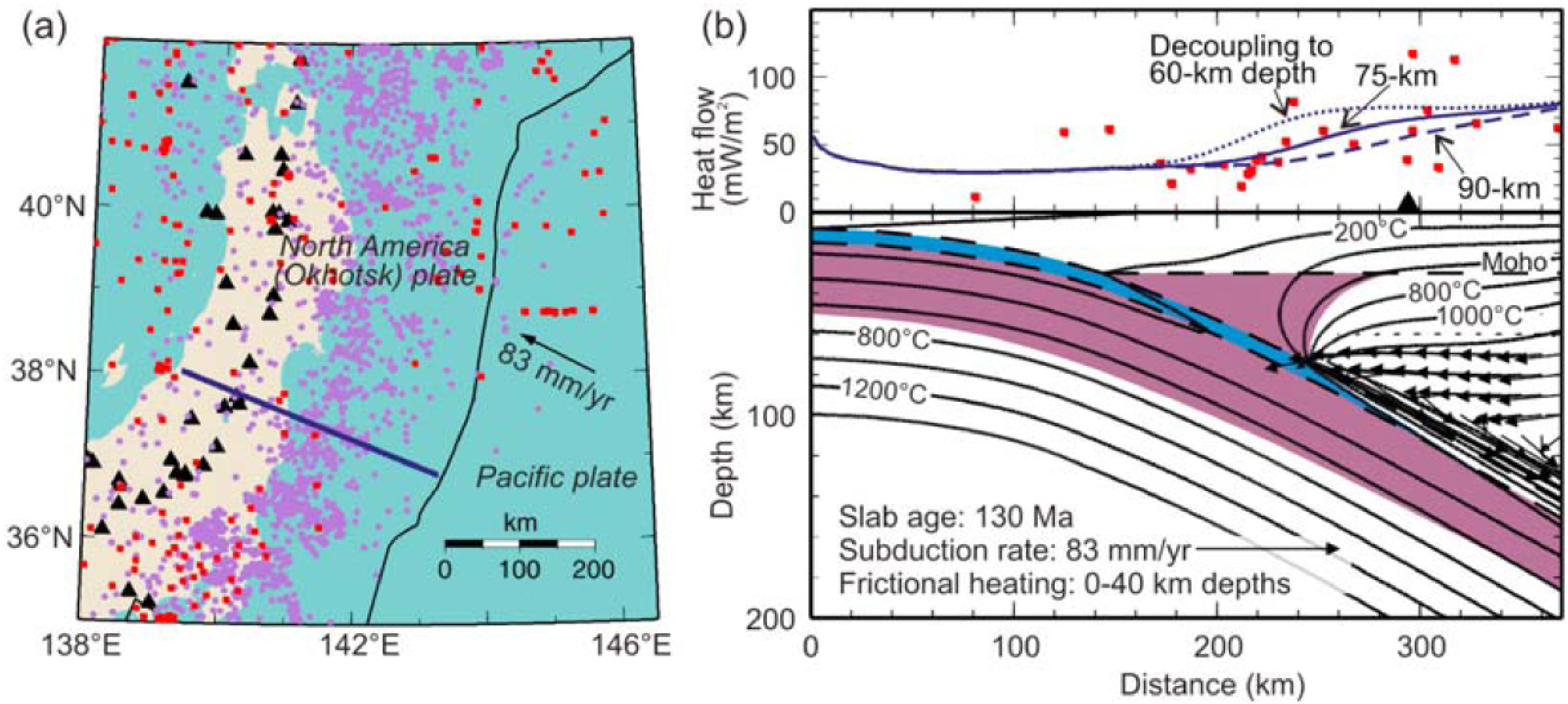

Wada and Wang, G3, 2009

Water flux

Water distribution in incoming slab

- Compacted sediments: 0.4-5 wt%
- Upper crust: few wt%
- Serpentinite in upper mantle: up to 2 wt%

Slab structure outboard of trench at Nicaragua (Ivandic et al., 2008)

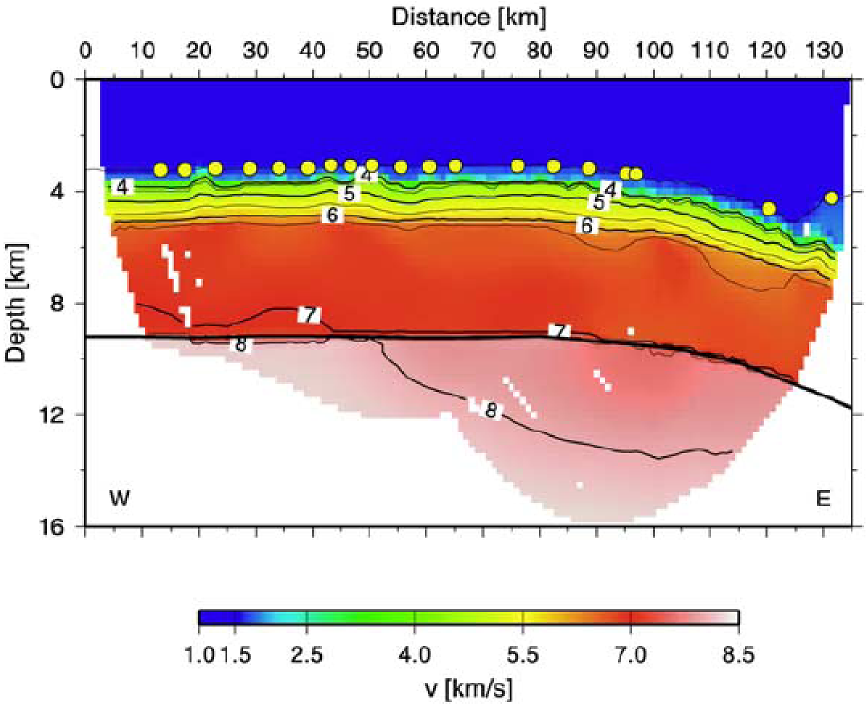

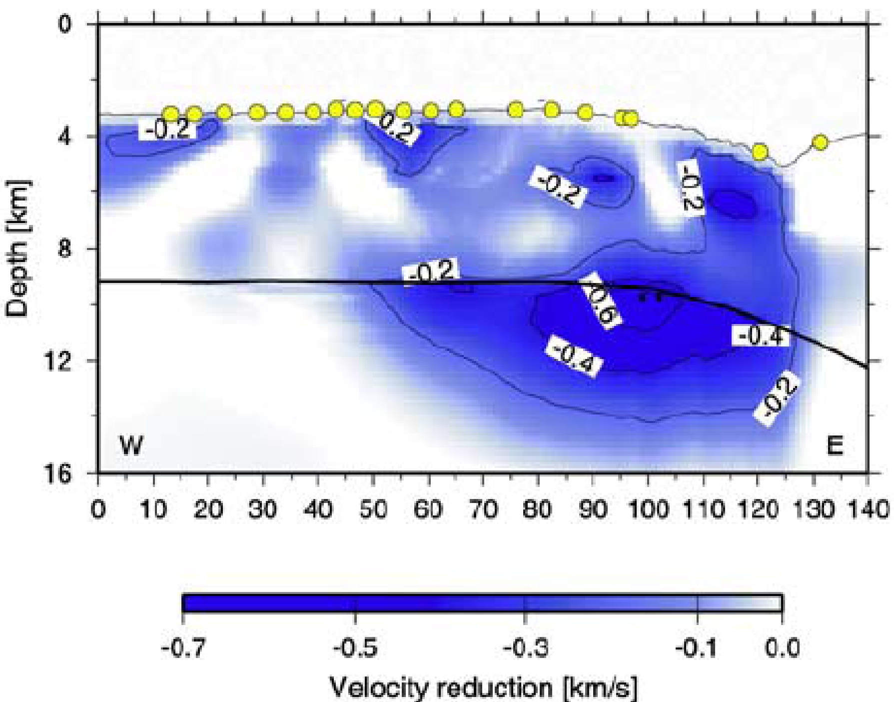

Slide courtesy of P. van Keken

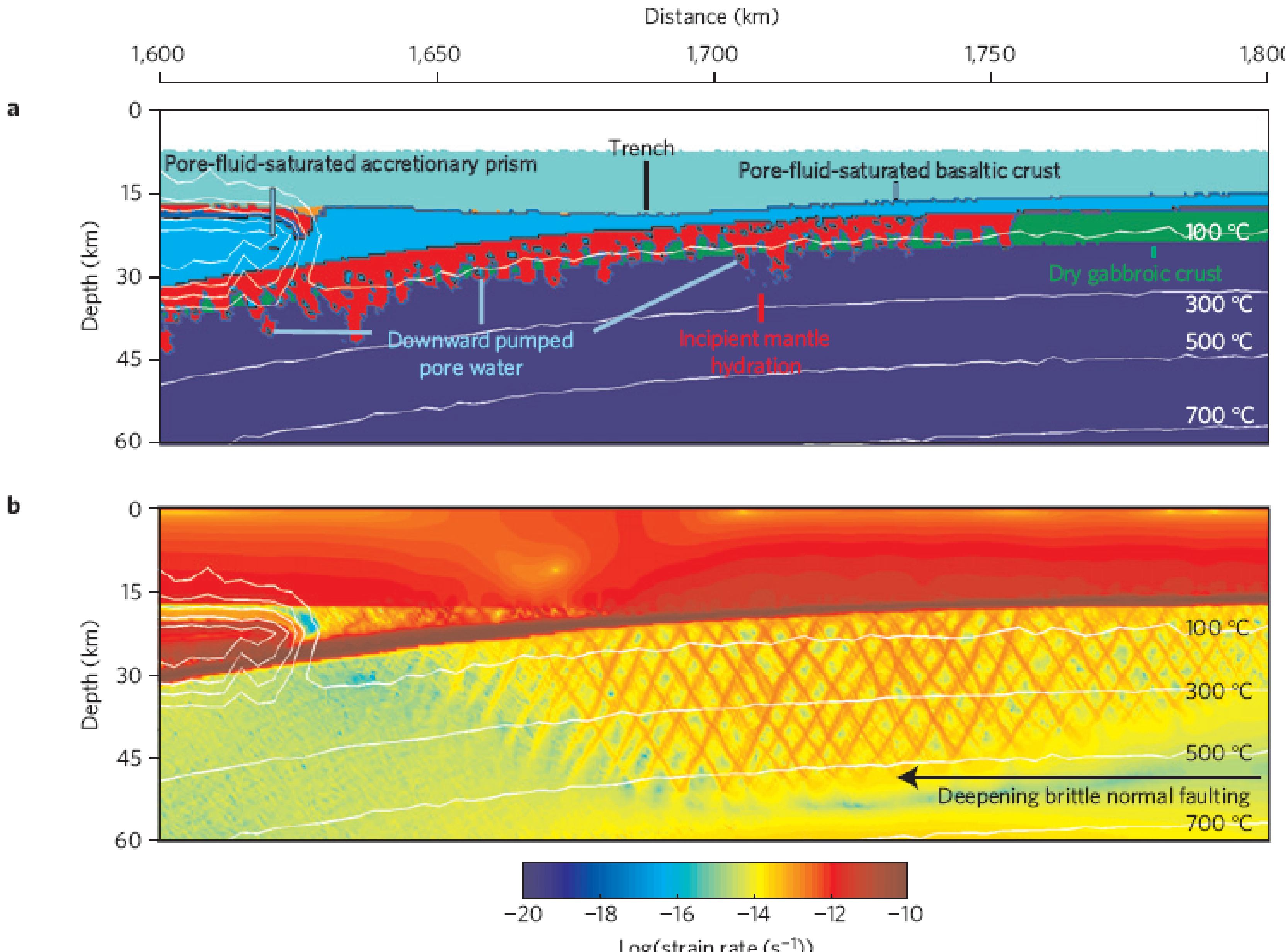

Faccenda et al. (2009)

Temperature in subducted oceanic crust

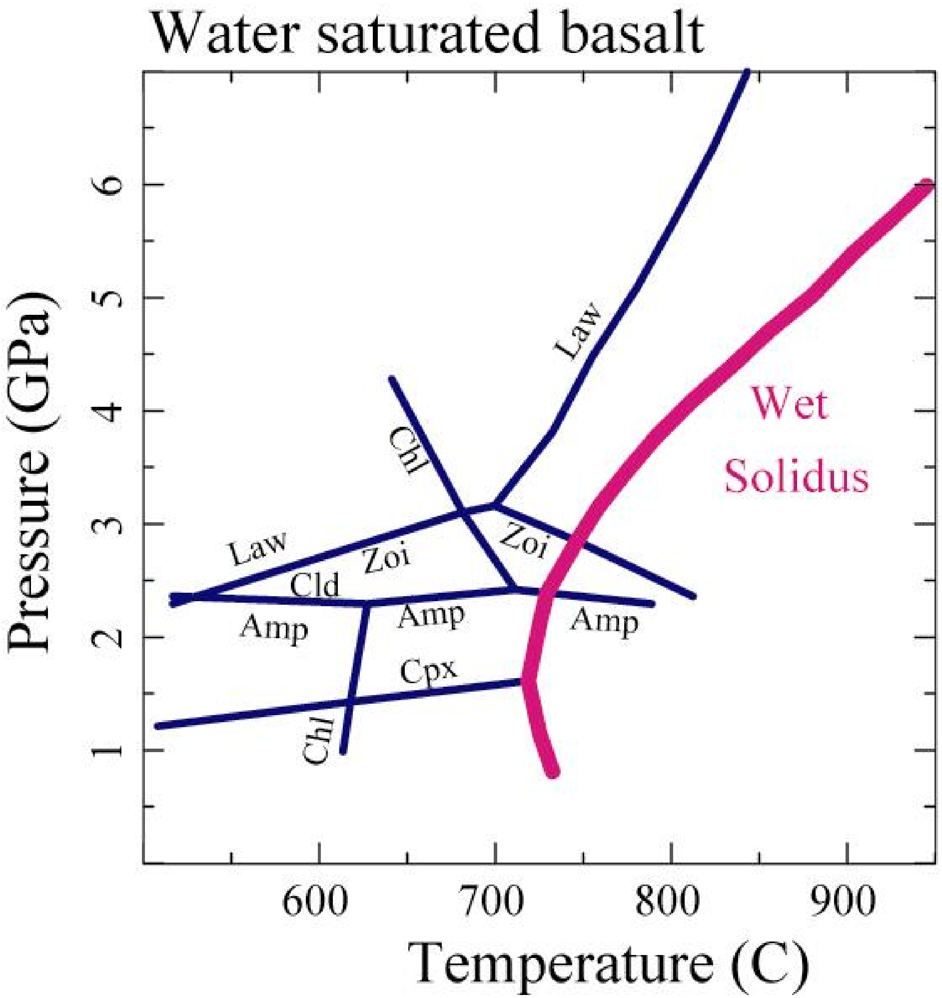

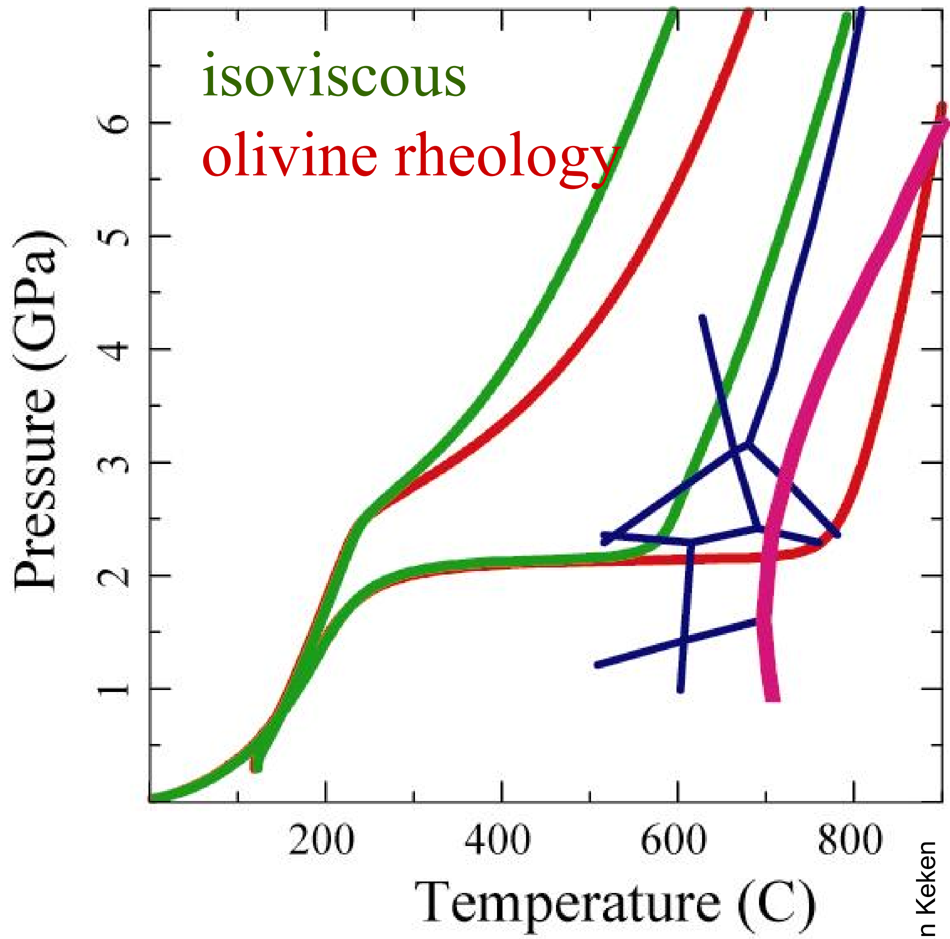

Van Keken et al., G³, 2002: model for Honshu
See also: Kelemen et al., 2003; Conder et al., 2003; Wada and Wang, 2008

Slide courtesy of P. van Keken

Update to Hacker, Gcubed, 2008
with full thermal models from Syracuse et al. (2010)

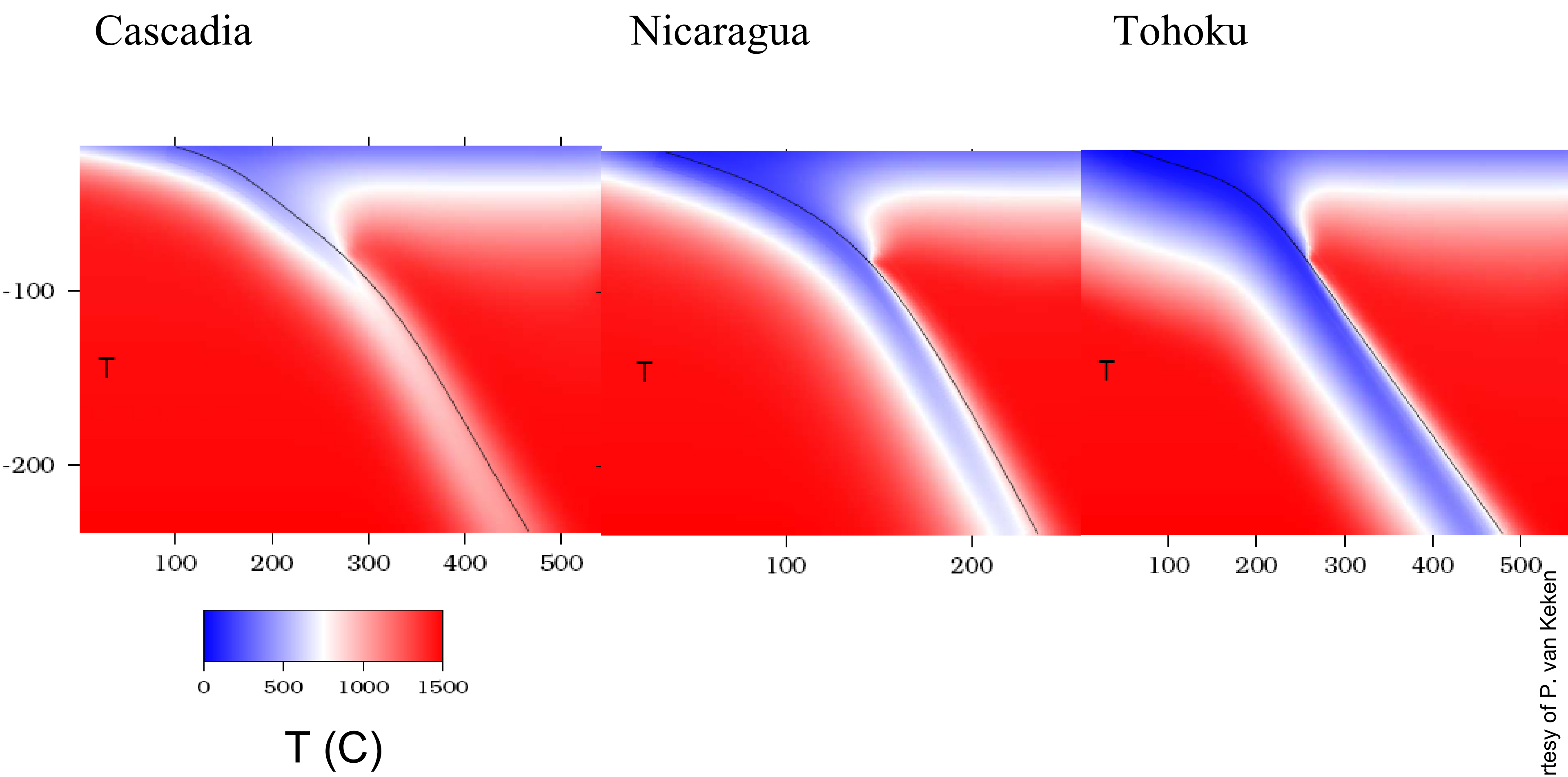

Slide courtesy of P. van Keken

Cascadia

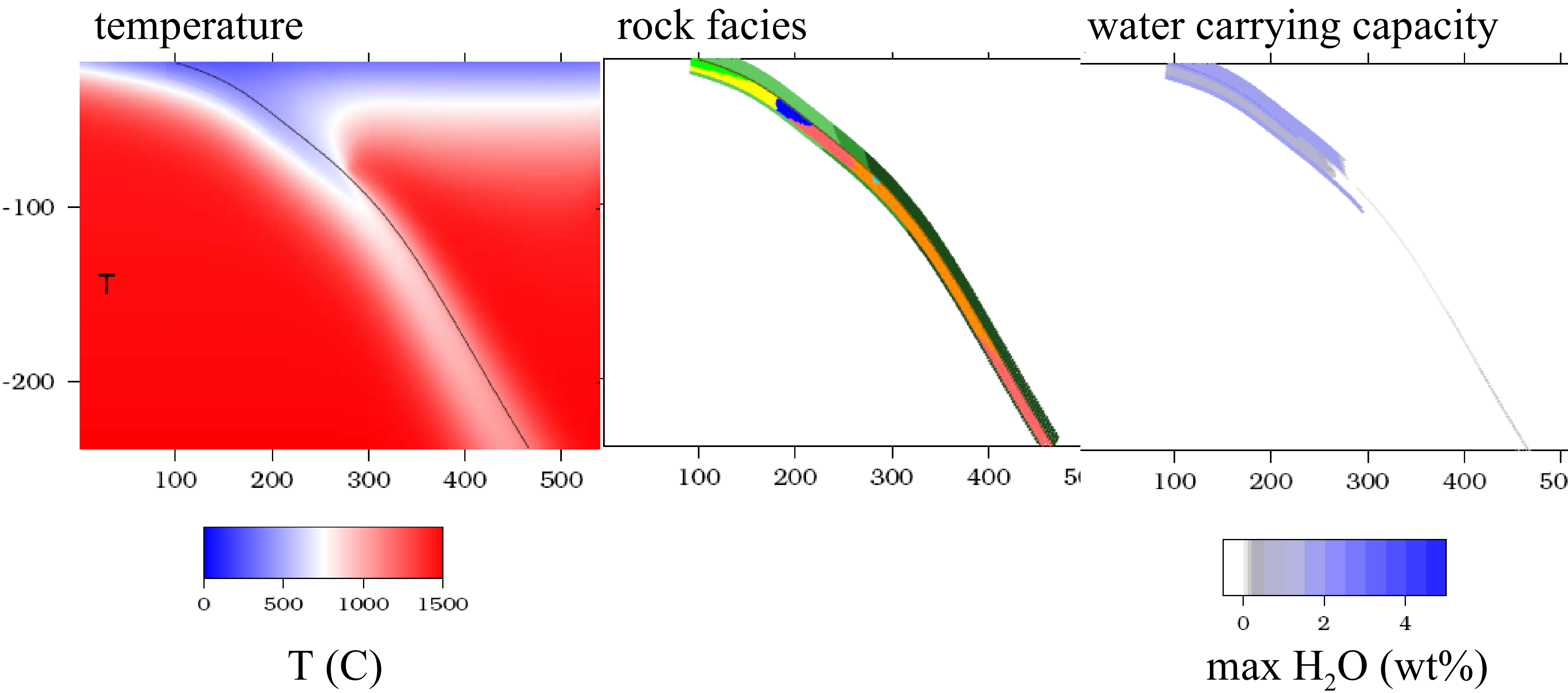

Syracuse et al. (2010)

Slide courtesy of P. van Keken

Tohoku

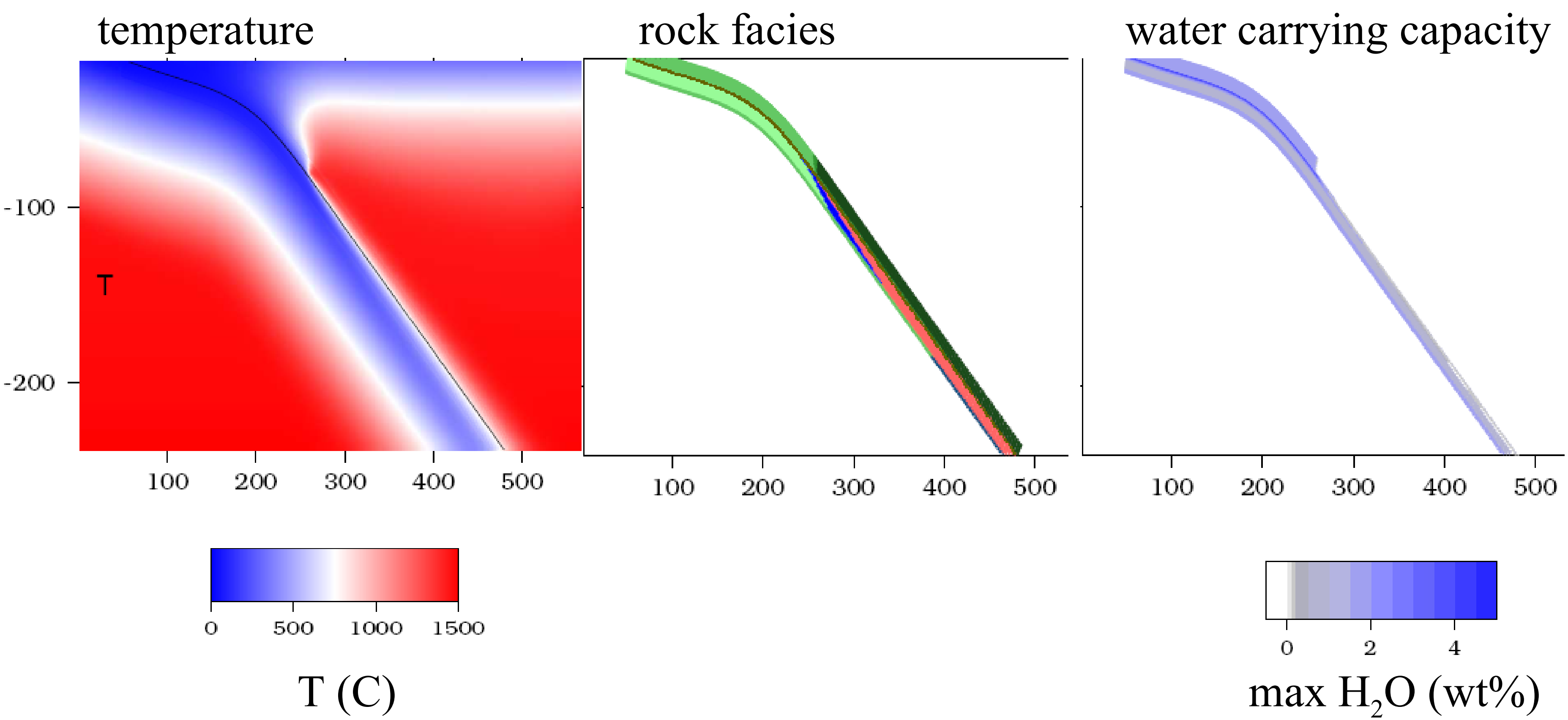

Syracuse et al. (2010)

Slide courtesy of P. van Keken

Coupled Solid-Fluid-Min.

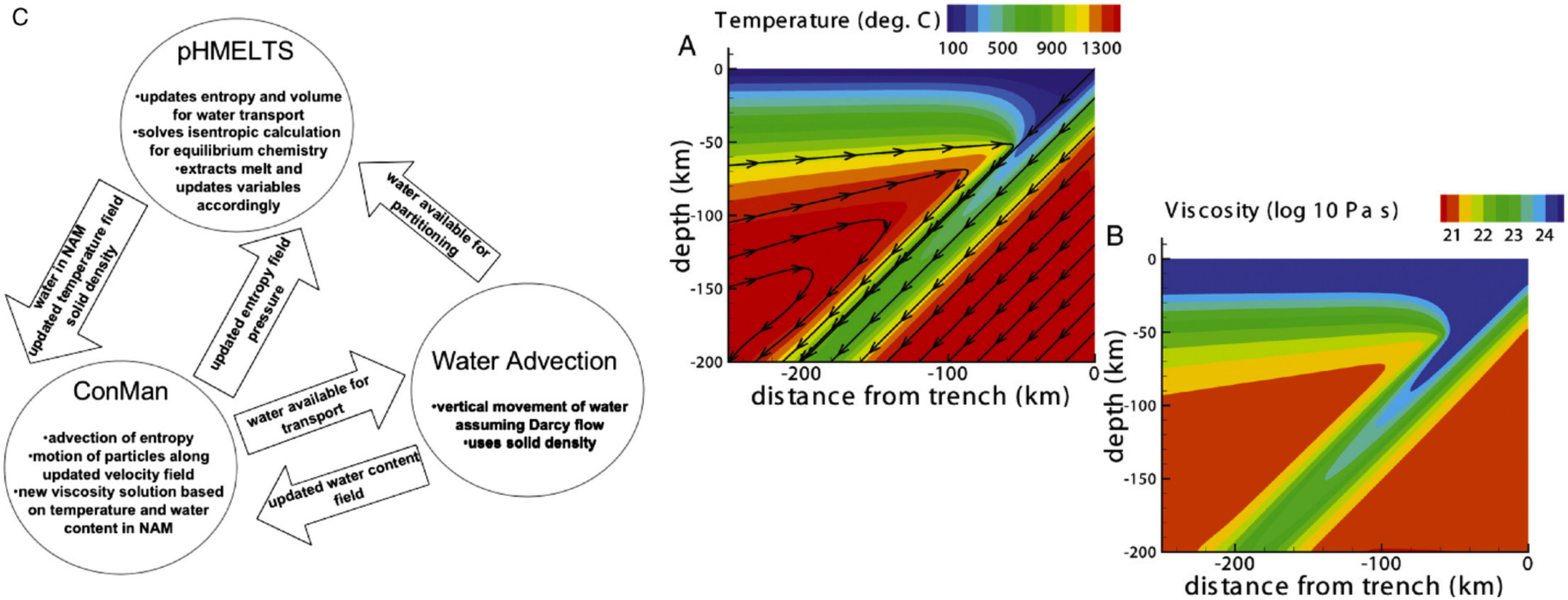

Hebert et al. (2009)

- Composition evolves including fluid & melt content.
  - Affects density (T, X) & rheology.
- Fluids move according to Darcy flow

Slide courtesy of M. Billen

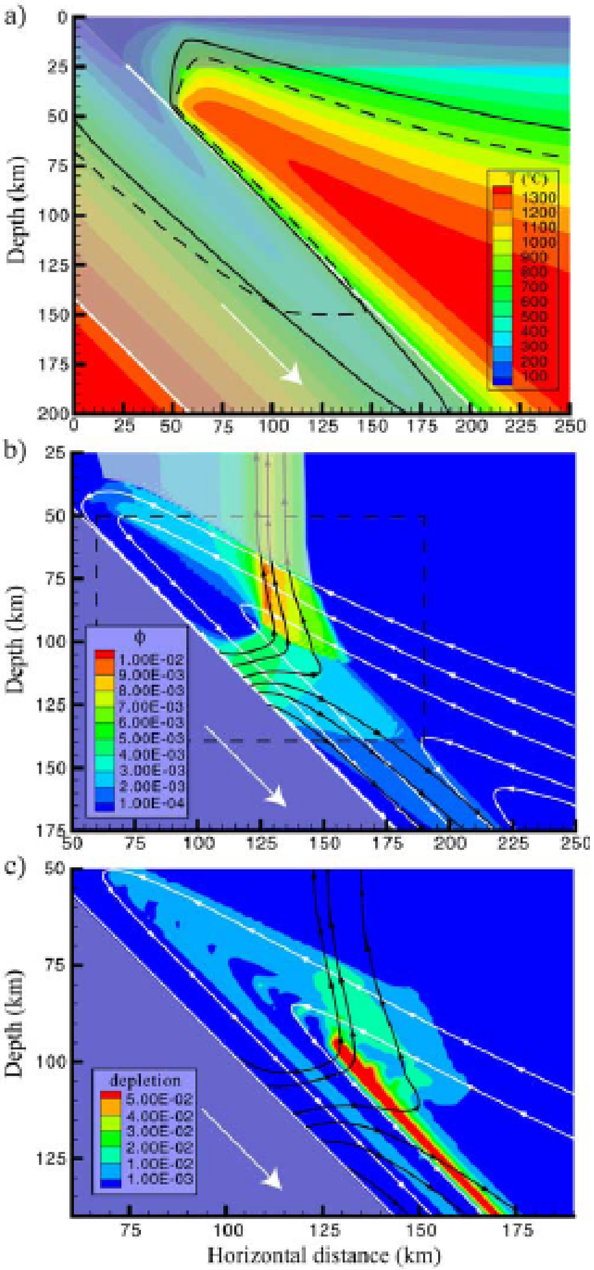

Cagnioncle et al. (2007)

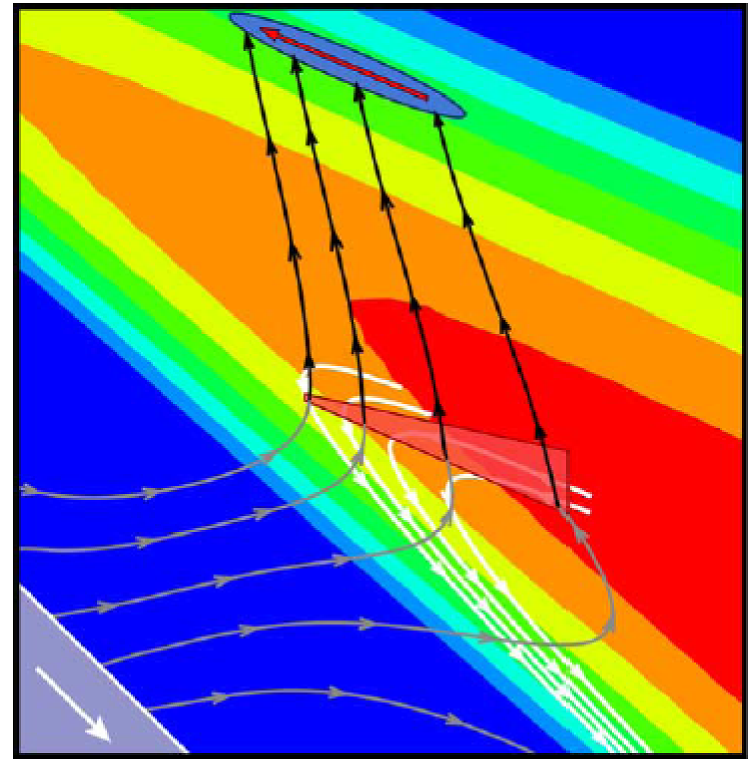

Figure 9. Schematic diagram of fluid migration at subduction zones. Hydrous fluids (grey streamlines) are released from the slab by dehydration reactions and rise buoyantly into the wedge. Fluids do not rise vertically into the wedge but are influenced by solid flow. A melting front (pale red triangle) develops where the water which was not advected to greater depth reaches a region hot enough to melt. The fluid is then a mixture of dissolved oxides and a hydrous component (black streamlines). The large fluid fraction after melting front prevents solid flow from affecting fluid migration, and fluids migrate vertically to the surface until they reach colder temperatures (pale blue ellipse). The present study does not explicitly treat the final fate of melt, but a potential melt transport mechanism, shown by the red arrow, is discussed in the text.

Fluids Affect Solid Flow.

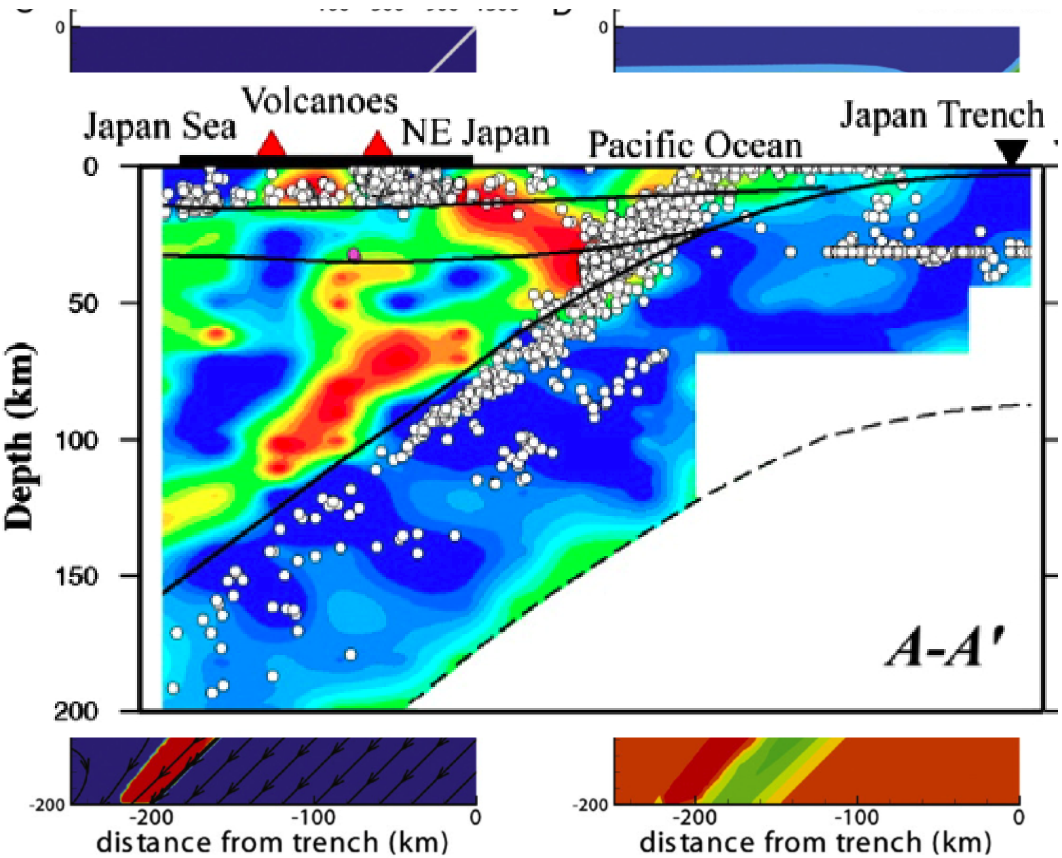

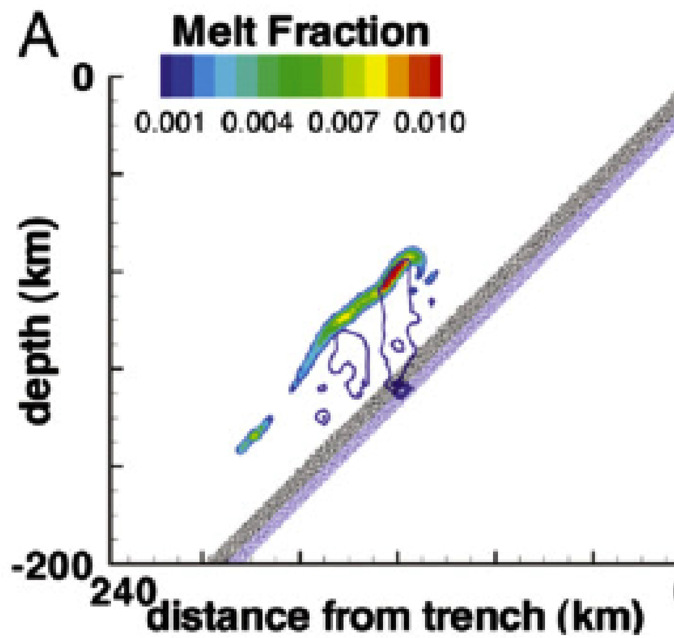

Hebert et al. (2009)

- ***Form low viscosity channel above slab.***
- ***Spatially & temporally variable melt fraction.***
  - ***Limits region of water effect on rheology.***

Slide courtesy of M. Billen

Semi-dynamic models

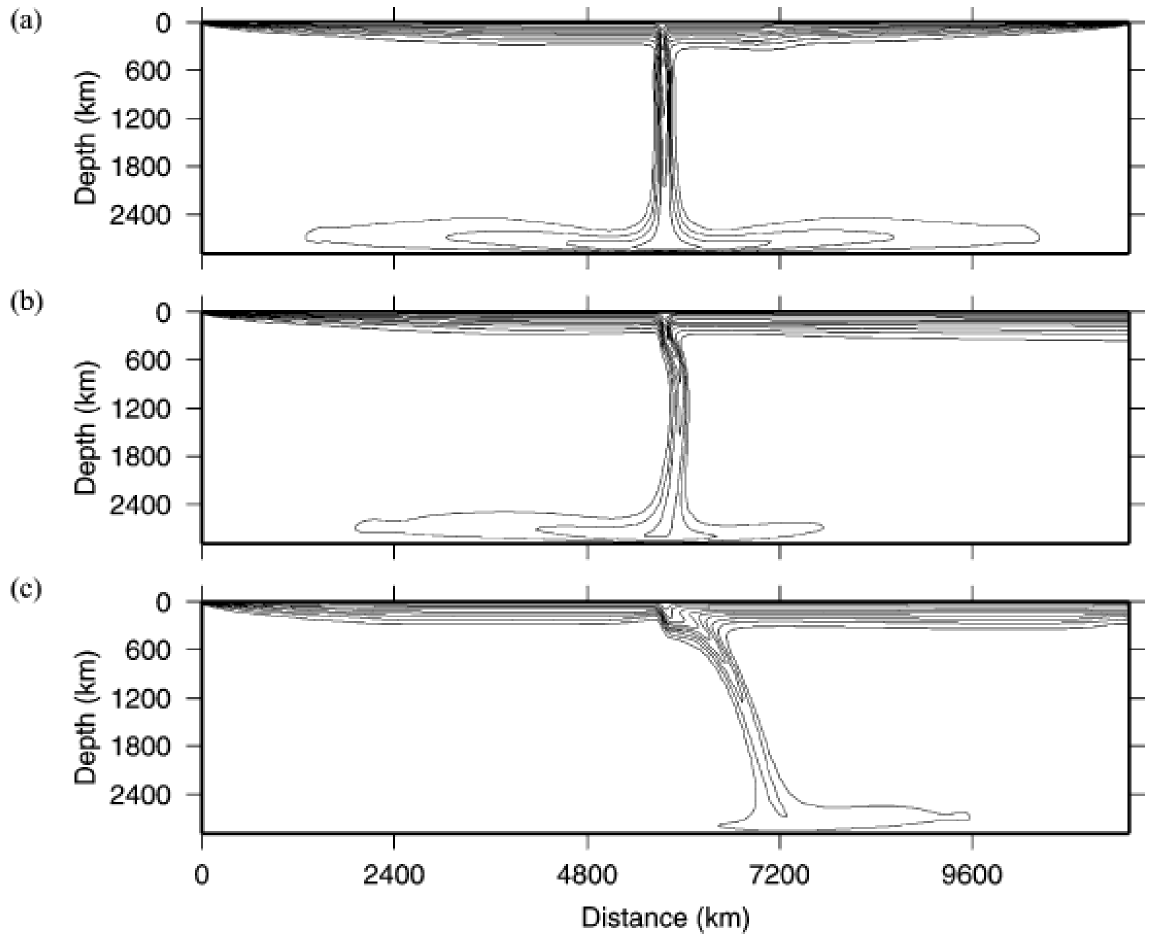

King (2001)

Fig. 1. Thermal fields from two convection calculations with plates. In both calculations the Rayleigh number is 10^6, the top and bottom are isothermal free-slip boundaries, the fluid is internally heated, and the viscosity is temperature dependent. The initial temperature field has a square root of age plate thermal field on the left side of the box and a uniform boundary layer on the right side of the box. Weak material zones allow the plate to deform at the trench and the ridge. The 'ridge' is in the left corner of the box and the 'trench' is in the center of the box. Further details on this type of calculation can be found in Chen and King (1998). (a) The side velocity boundary conditions are free-slip (material is free to move vertically along the edge). (b) Identical to (a) except that the velocity of a single node on the right-hand side is set to zero, breaking the symmetry of the top boundary layer velocities. (c) Identical to (b) except that the side velocity boundary conditions are an imposed horizontal velocity of 20 mm per year. This is identical to moving the trench and plate relative to the center of mass of the mantle.

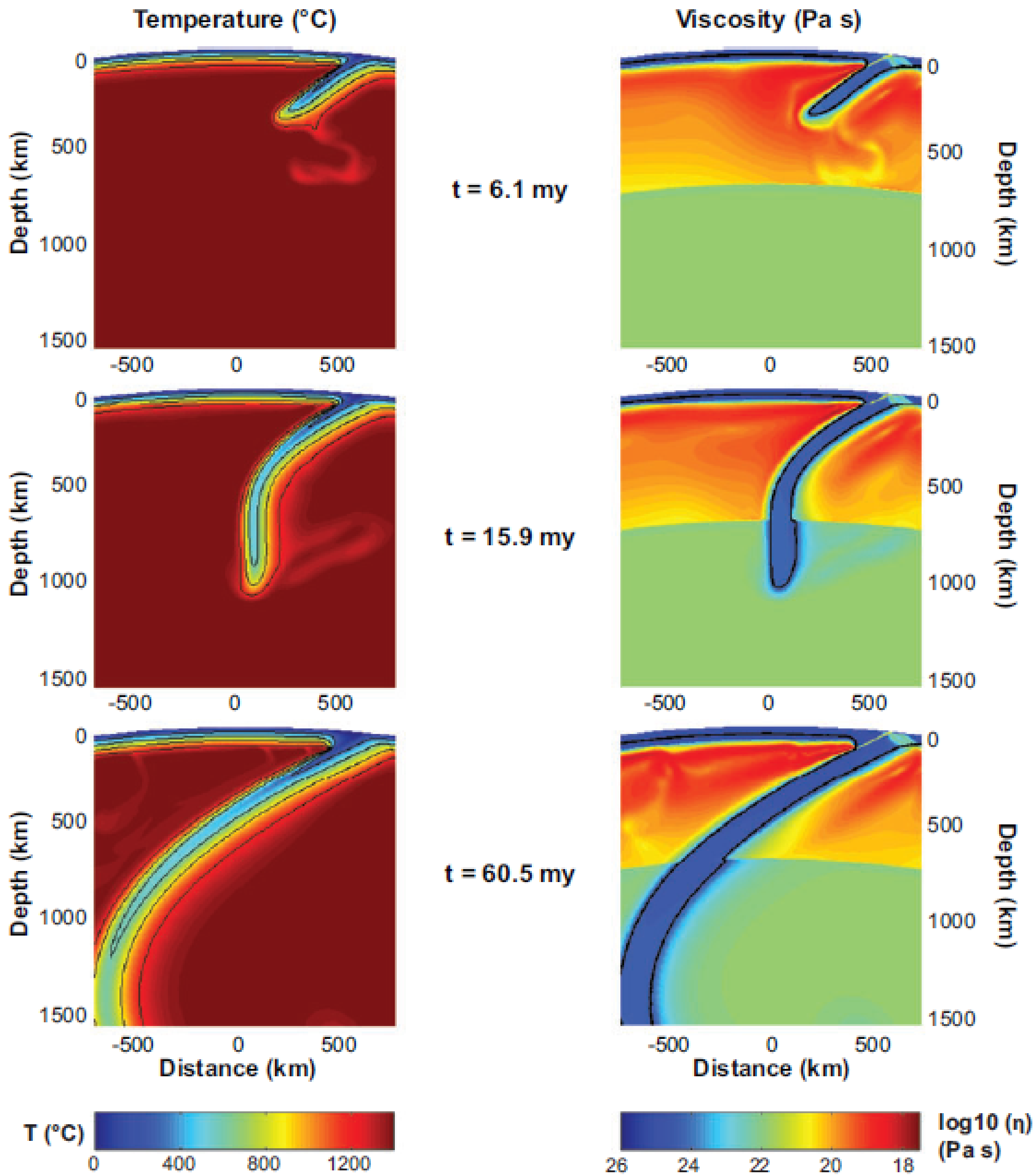
Temperature (°C)
Viscosity (Pa s)
t = 6.1 my
t = 15.9 my
t = 60.5 my
Depth (km)
Distance (km)
T (°C)
0
400
800
1200
log10 (η) (Pa s)
26
24
22
20
18

Billen (2009)

Grain size weakening at 410

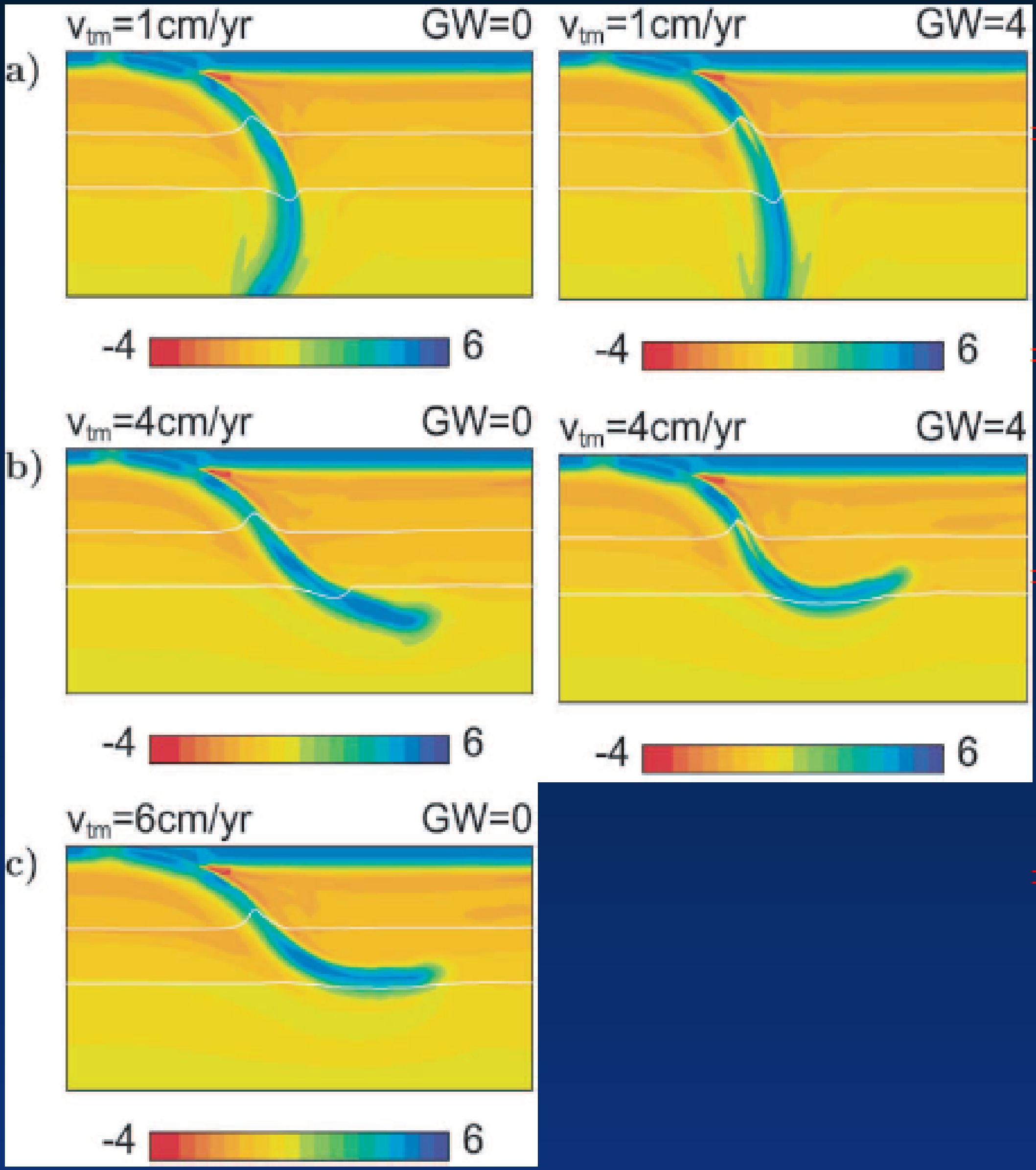

- ⇒ v_{trench} and GW varied à la van Hunen *et al.* (2002)
- ⇒ strong slabs penetrate (Davies, 1995)
- ⇒ GW could explain weak, bent slabs (*c.f.* Karato *et al.*, 2001)
- ⇒ alternatives: faults, η_y

Čížková *et al.* (2002)

Rollback and ponding

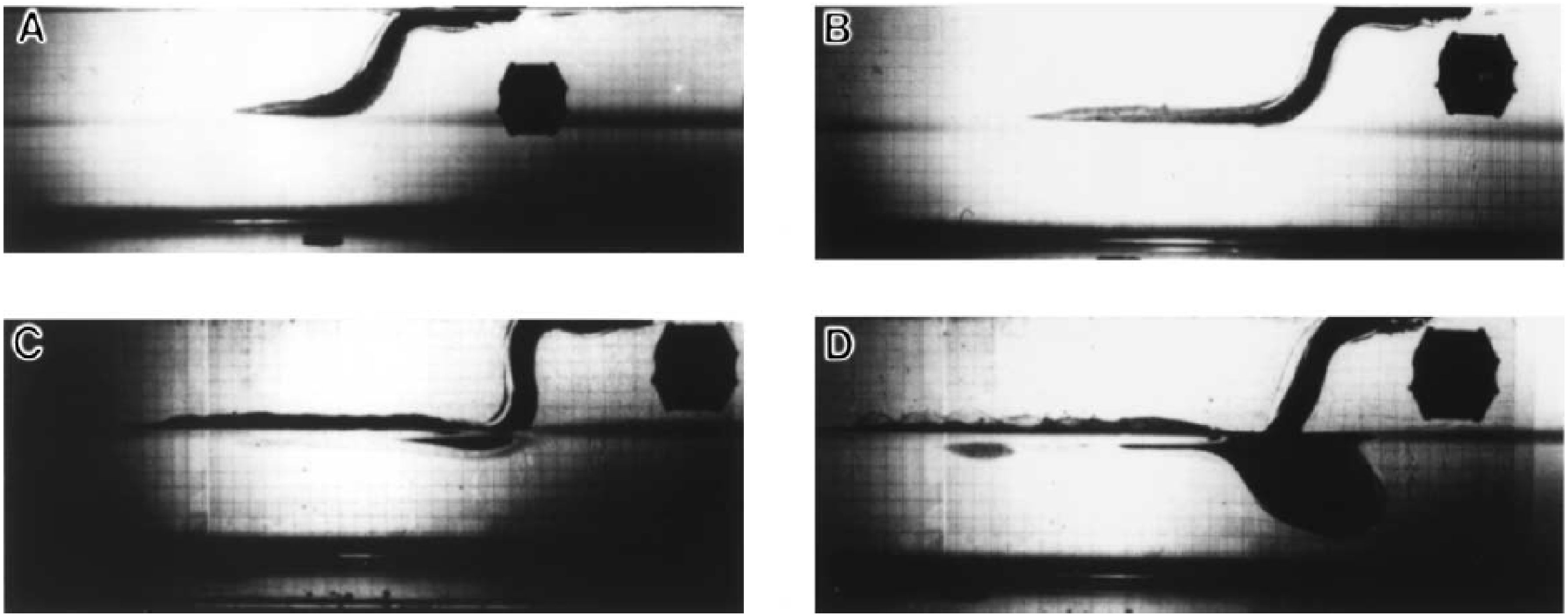

Fig. 1. Snapshots from a laboratory experiment by Guillou-Frottier et al. (1995). A sheet of chilled and dyed corn syrup is extruded into a tank with two layers of syrup. Initial rapid trench migration leads to a flat slab. After (B), trench-rollback is stopped and slab material accumulates in a pile that sinks into the lower layer. The whole sequence corresponds to approximately 400 million years of subduction.

Christensen (2001)

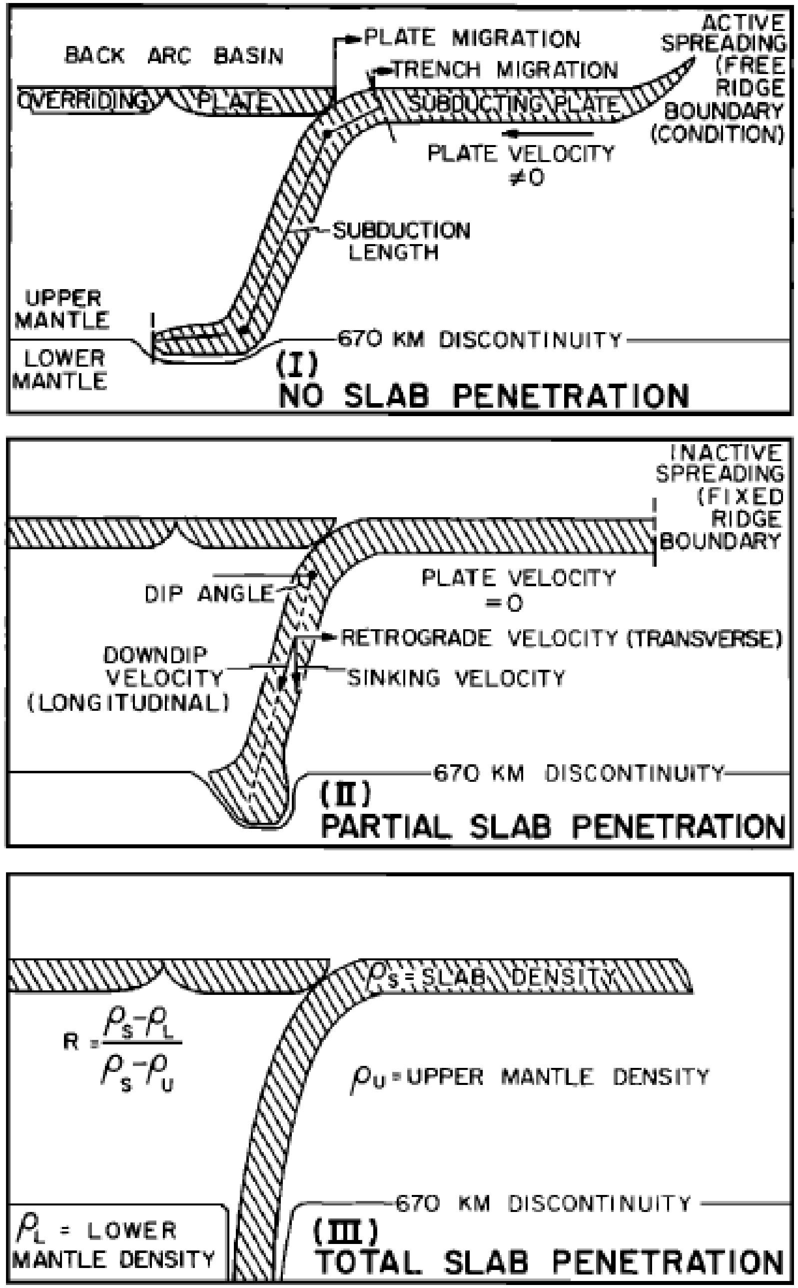

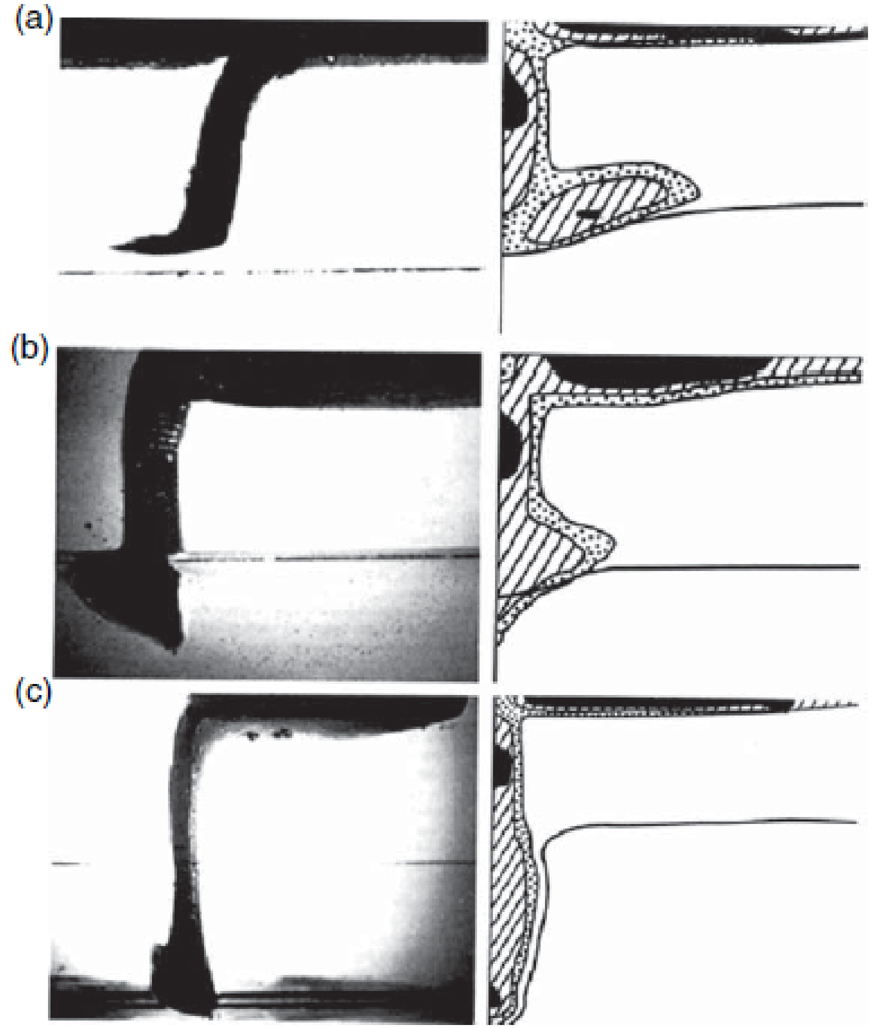

Figure 14 Experimentally observed styles of slab penetration through a density discontinuity (left) compared with 2-D calculation by Christensen and Yuen (1984) (right). (a) Slab deflection with $R \approx -0.2$. (b) Partial slab penetration with $R \approx 0.0$. (c) Complete slab penetration with $R \approx 0.5$. Reproduced from Kincaid C and Olson PL (1987). An experimental study of subduction and slab migration. *Journal of Geophysical Research* 92: 13832–13840, with permission from American Geophysical Union.

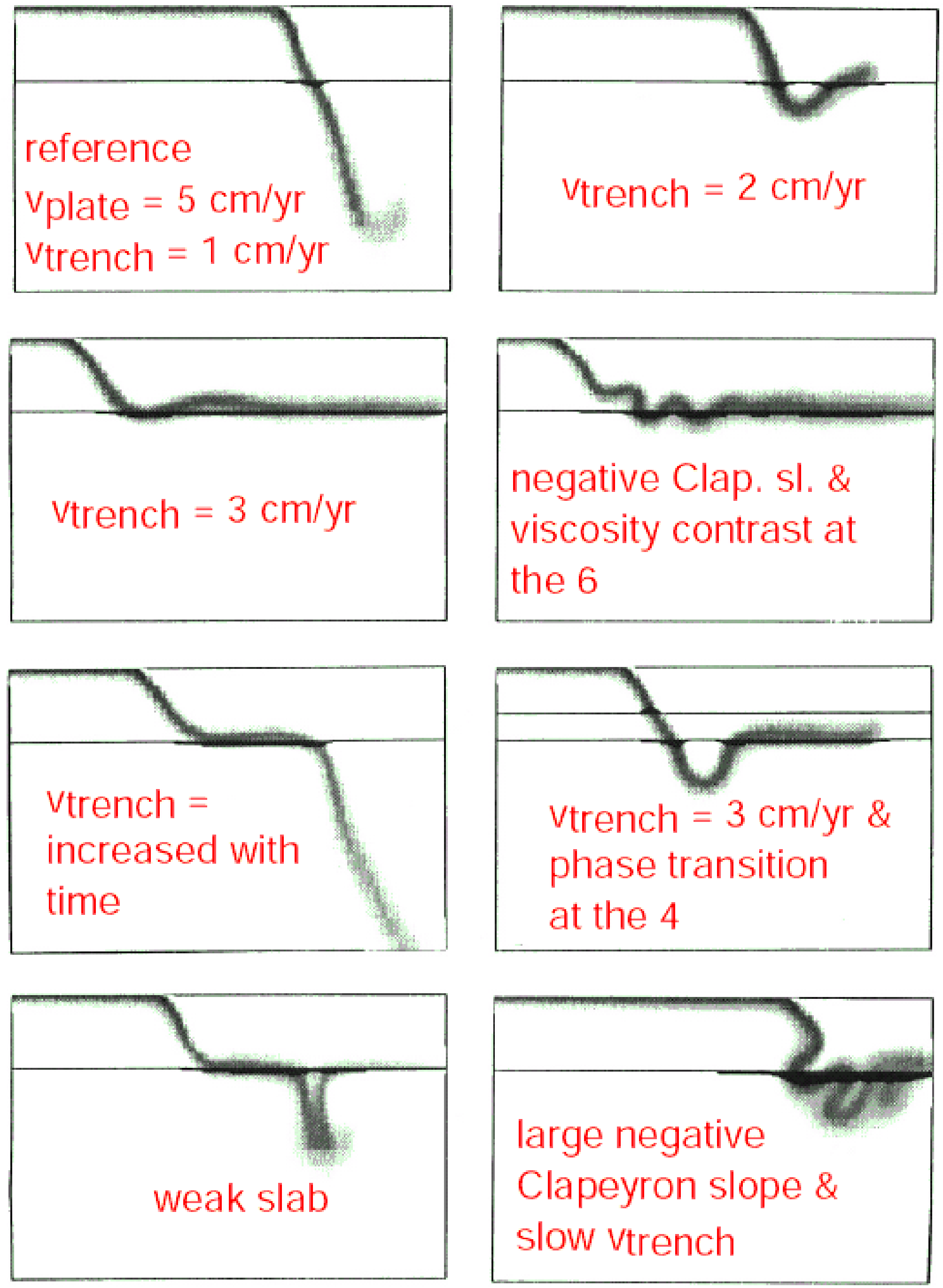

Christensen (1996)

Effect of negative Clapeyron slope on slabs and plumes

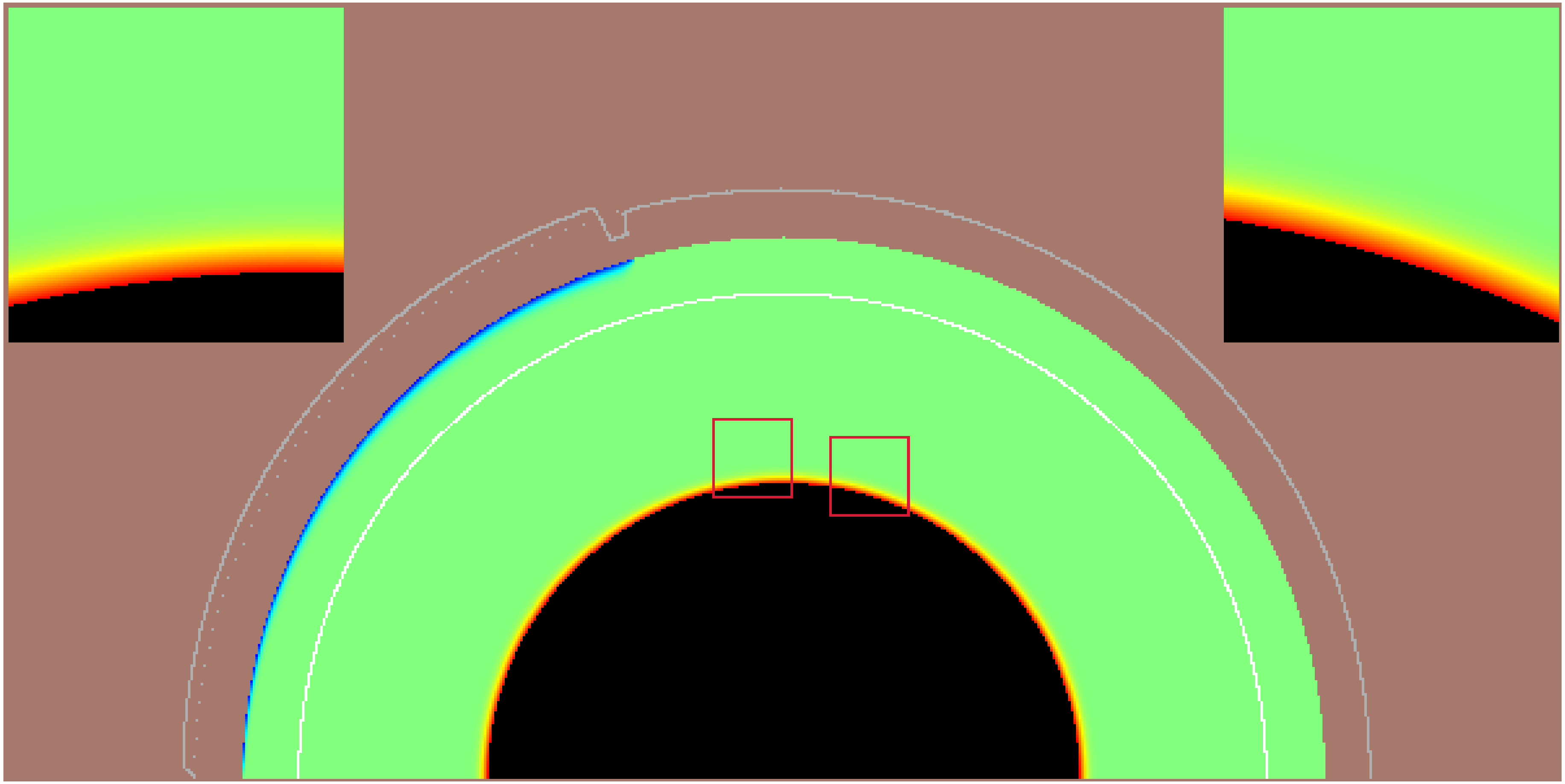

Tan et al. (2001)

Ponding as f(strength, rollback)

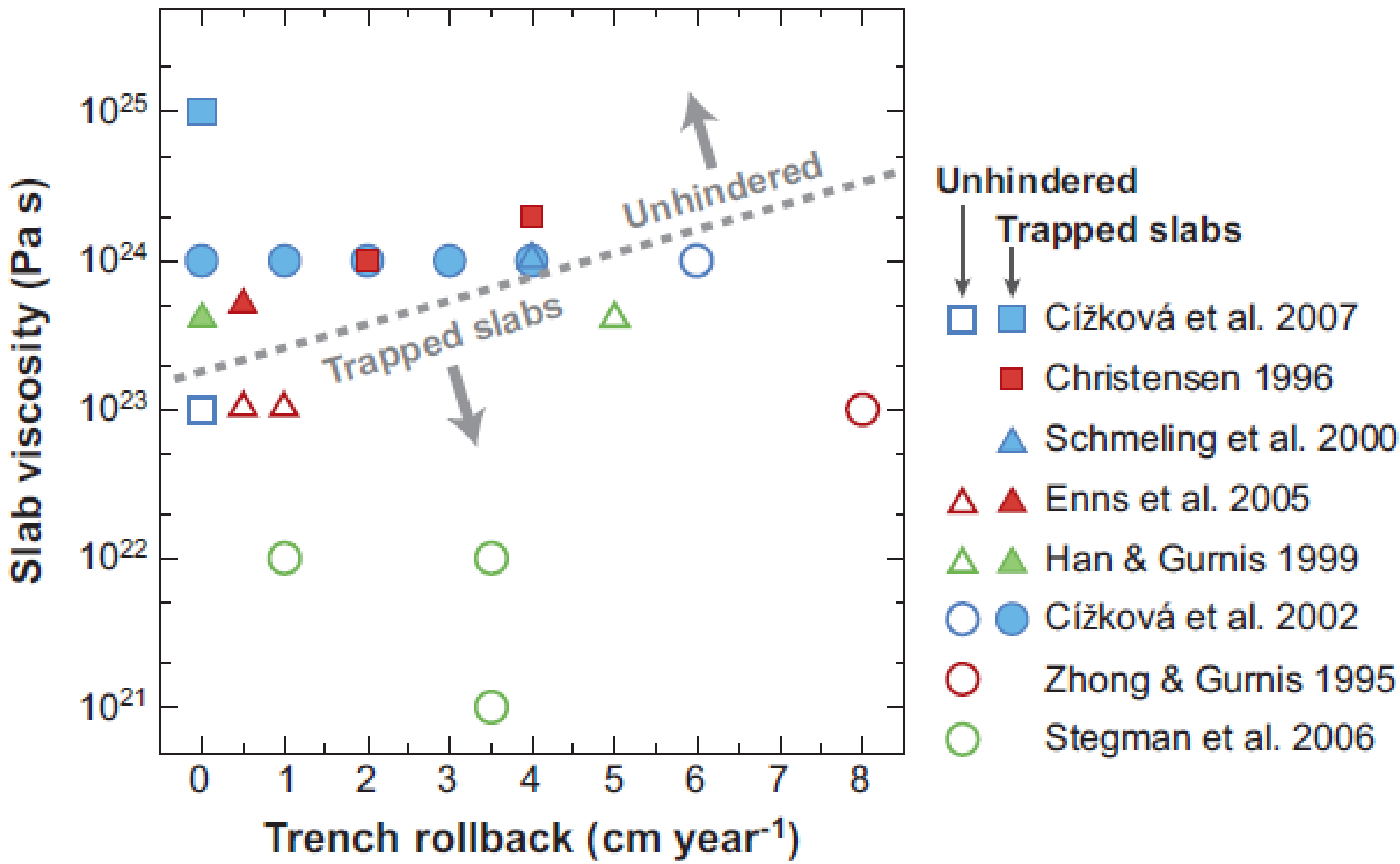

Billen (2009),
cf. Davies (1998)

Do slabs make it all the way to the CMB?

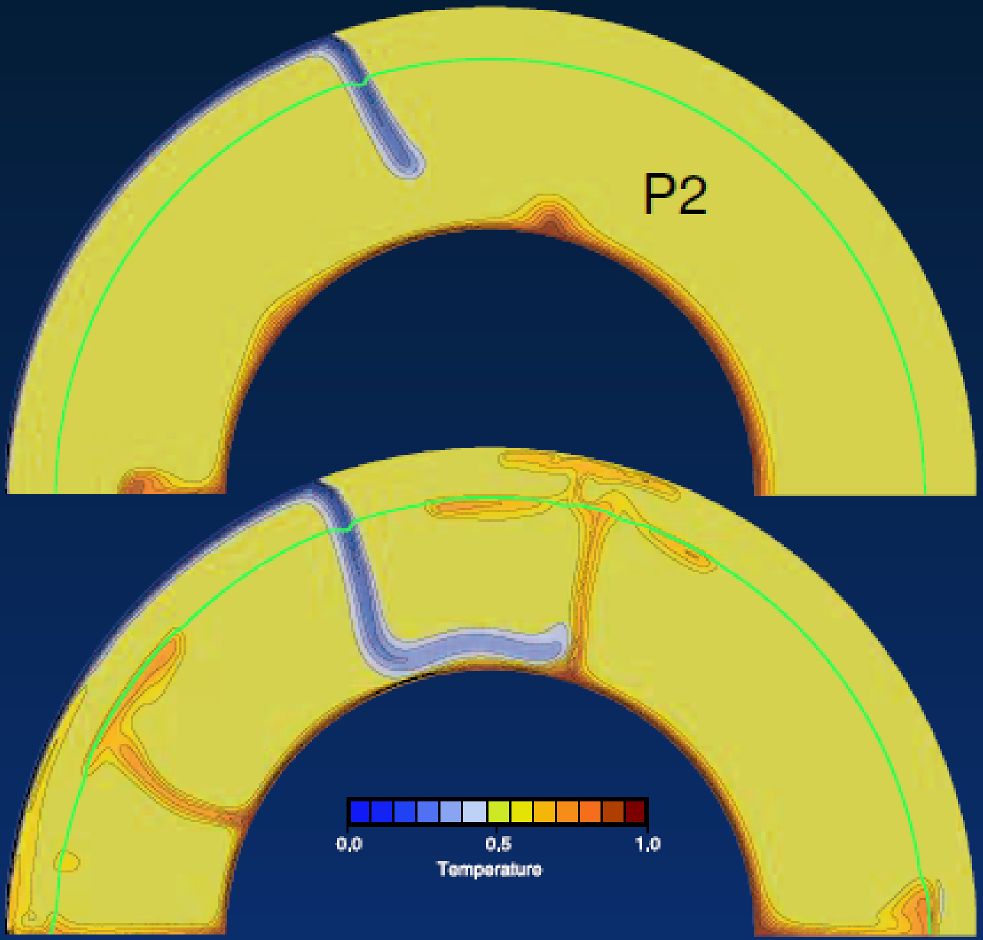

Yep.

$\Rightarrow$ $dp/dT| = -3$ MPa/K $\surd$

$\Rightarrow$ increase in κ with depth $\surd$

$\Rightarrow$ internal heating $\surd$

$\Rightarrow$ substantial (~ 500 K) anomaly at CMB

Tan *et al.* (2002)

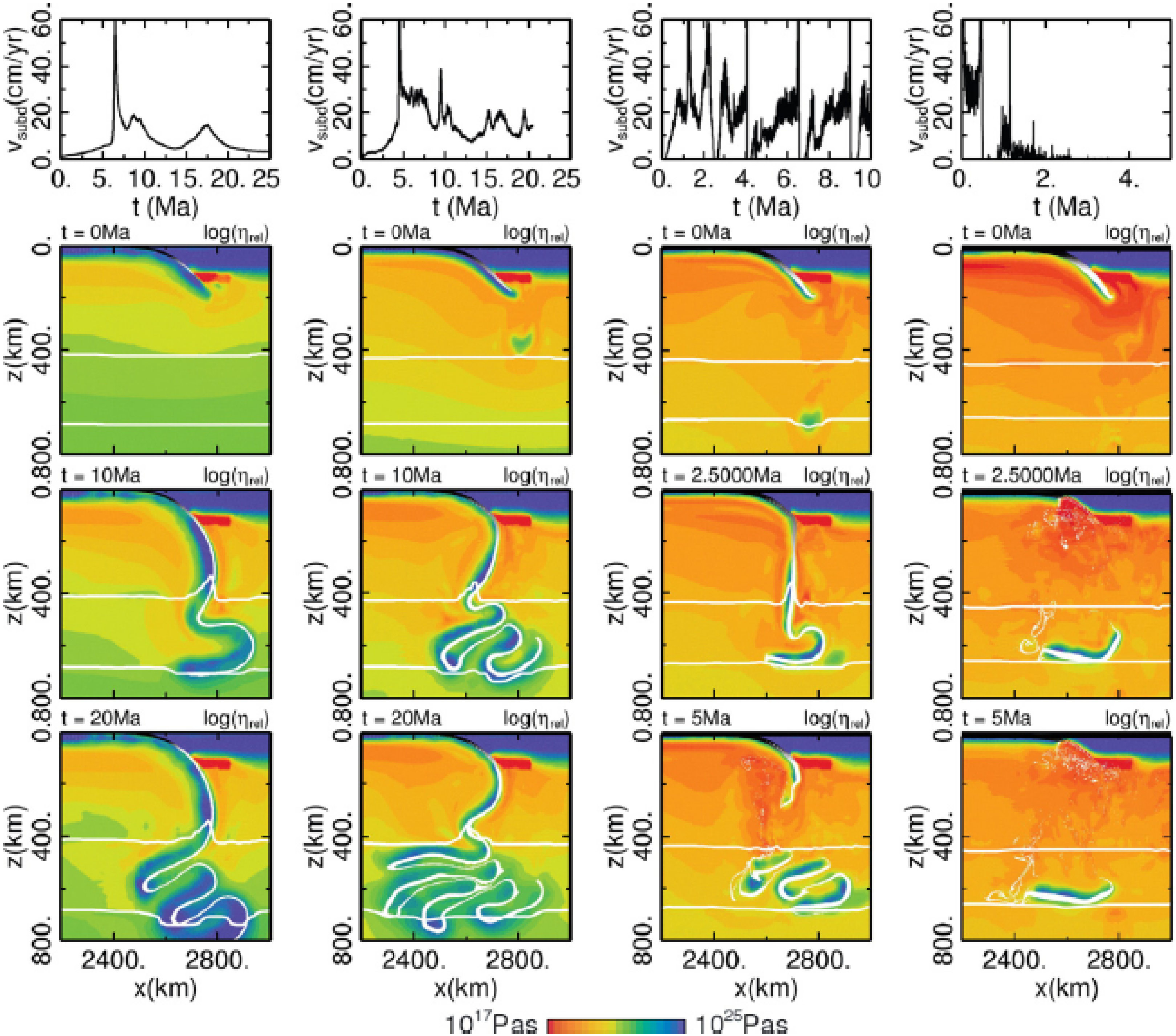

Van Hunen et al. (2007)

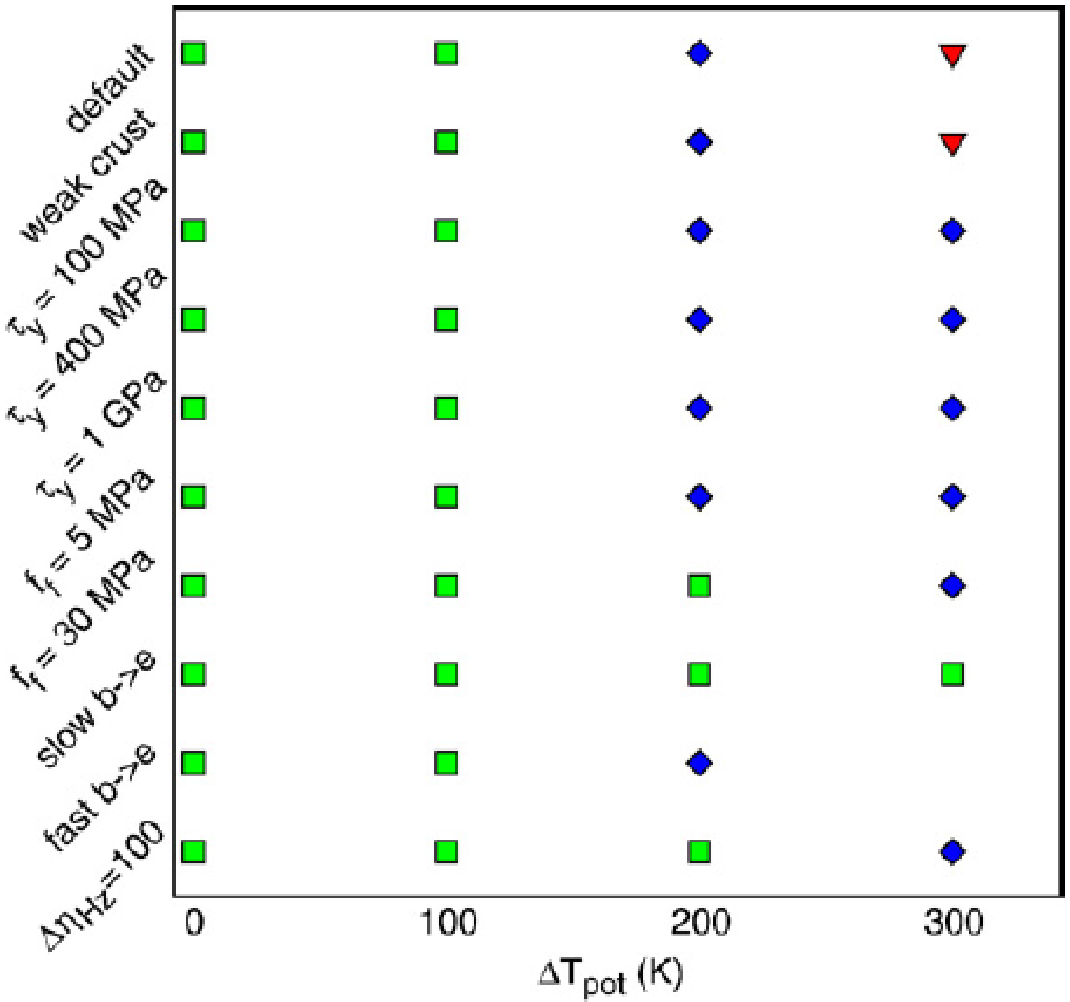

Fig. 10. Compilation of the subduction style of all presented calculations. Green blocks indicate a subduction style like at present. Blue diamond indicate frequent slab detachment events, and red triangles denote no continuing subduction.

Van Hunen et al. (2007)

Tomographic slabs and Stokeslets for a moving trench scenario

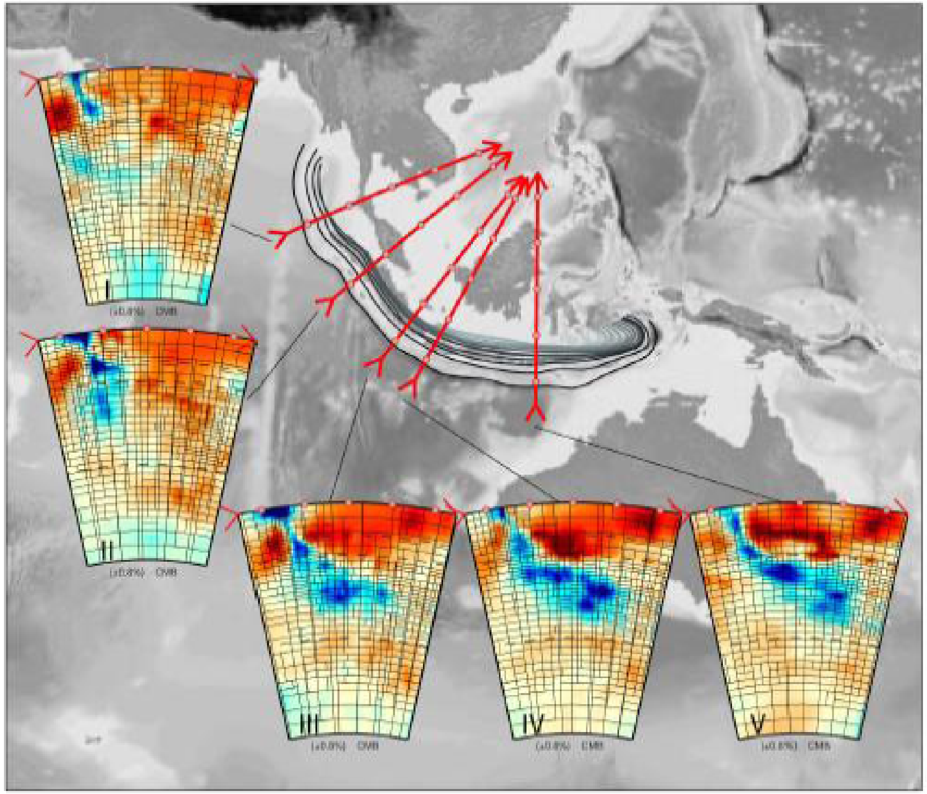

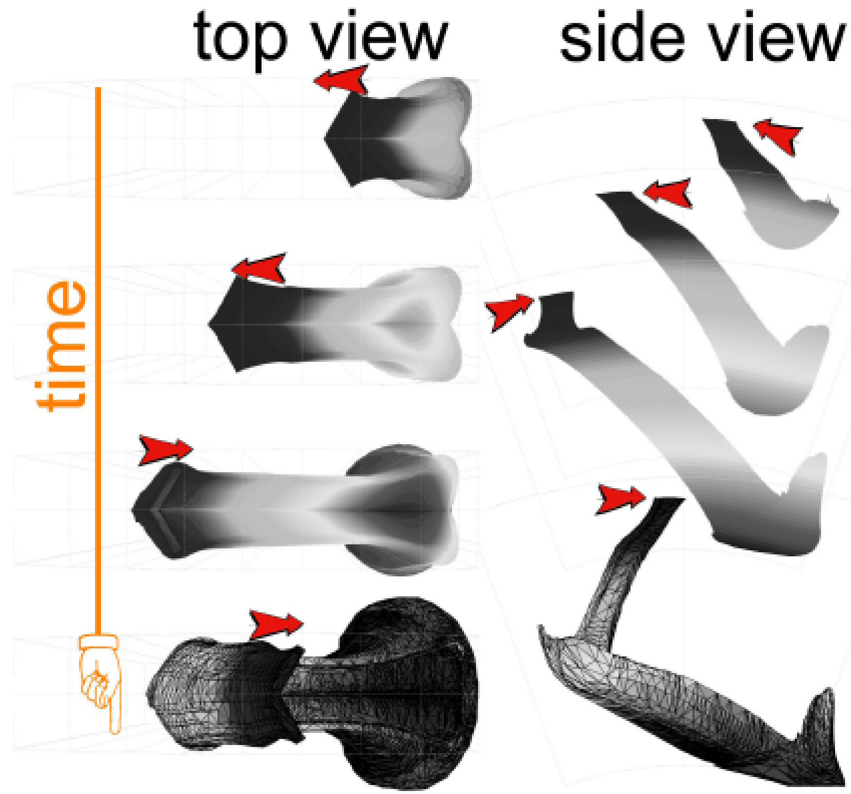

- Weak, fluid slab ($\eta' = \eta_{slab}/\eta_{mantle} = 1$) hits the 660
- Prescribed trench motion

Karason (2002)

Stokeslets and tomography

- Best fit for Sunda for a viscosity contrast between upper and lower mantle of > ~200
- Strong anchoring of weak slab
- cf. slablets of Morra et al.

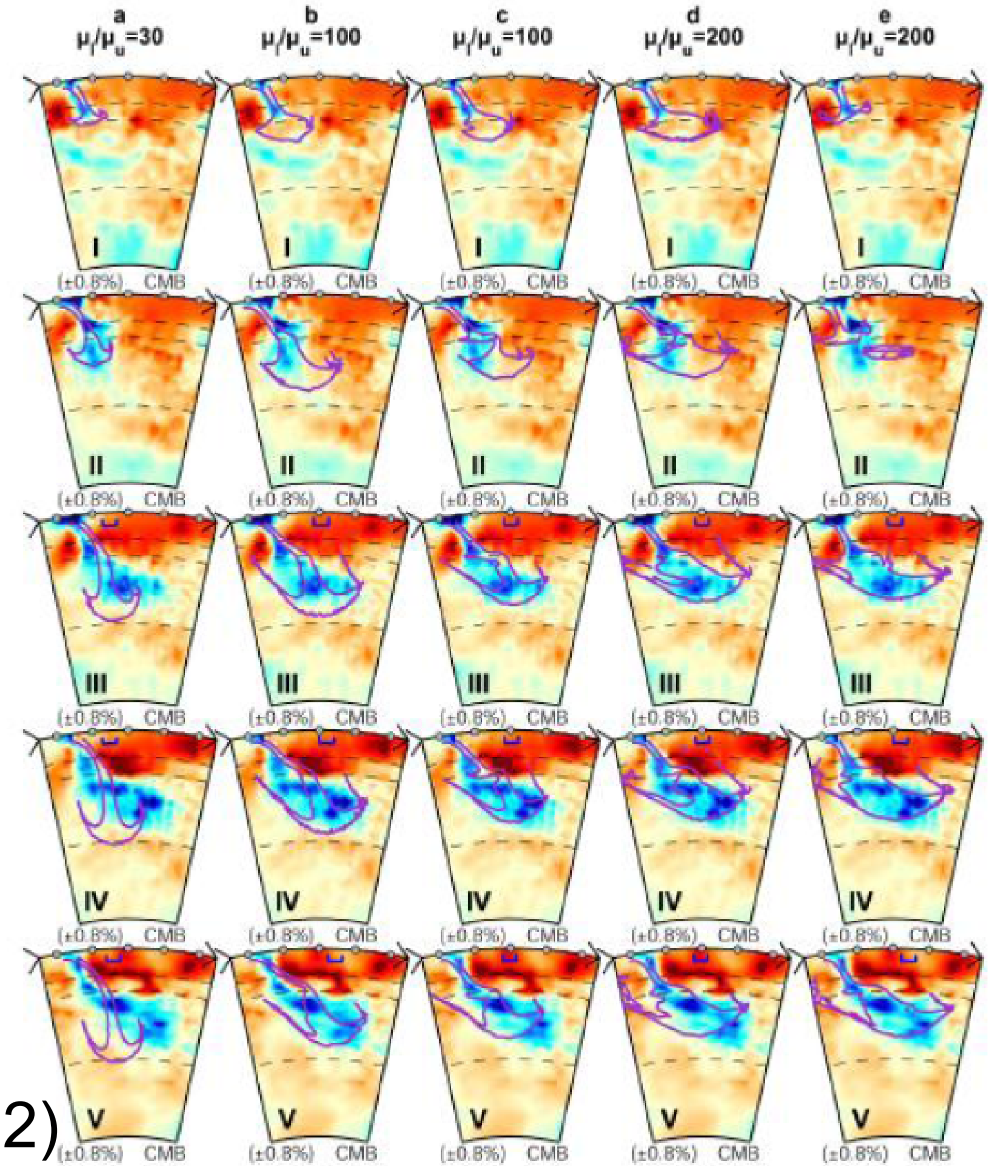

Karason (2002)

3D

Interactions: rollback and episodicity in 3D

laterally unconfined laterally confined

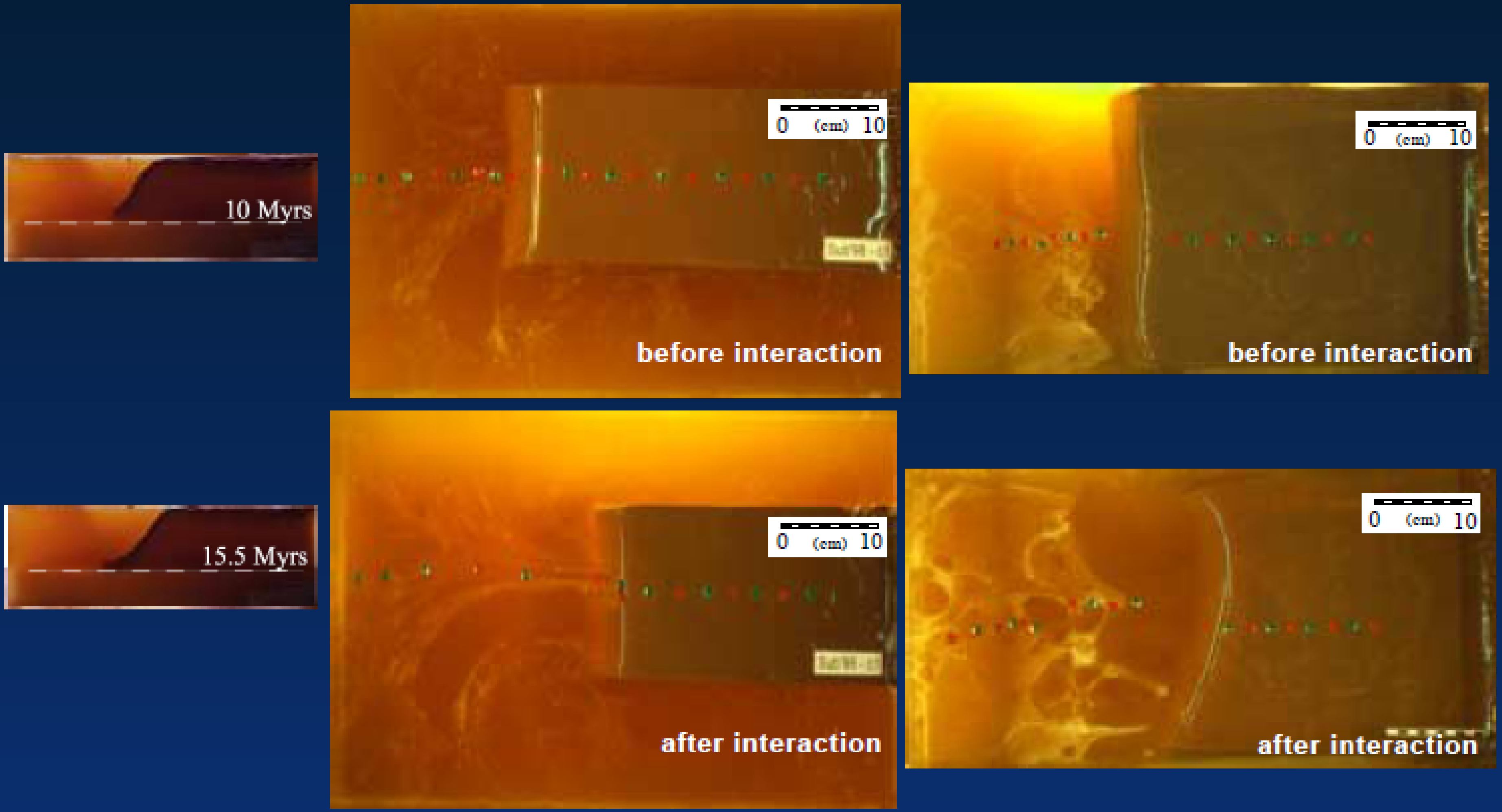

→ episodicity in case of lateral and vertical flow confinement

Funiciello *et al.* (2003)

Changes in plate motions

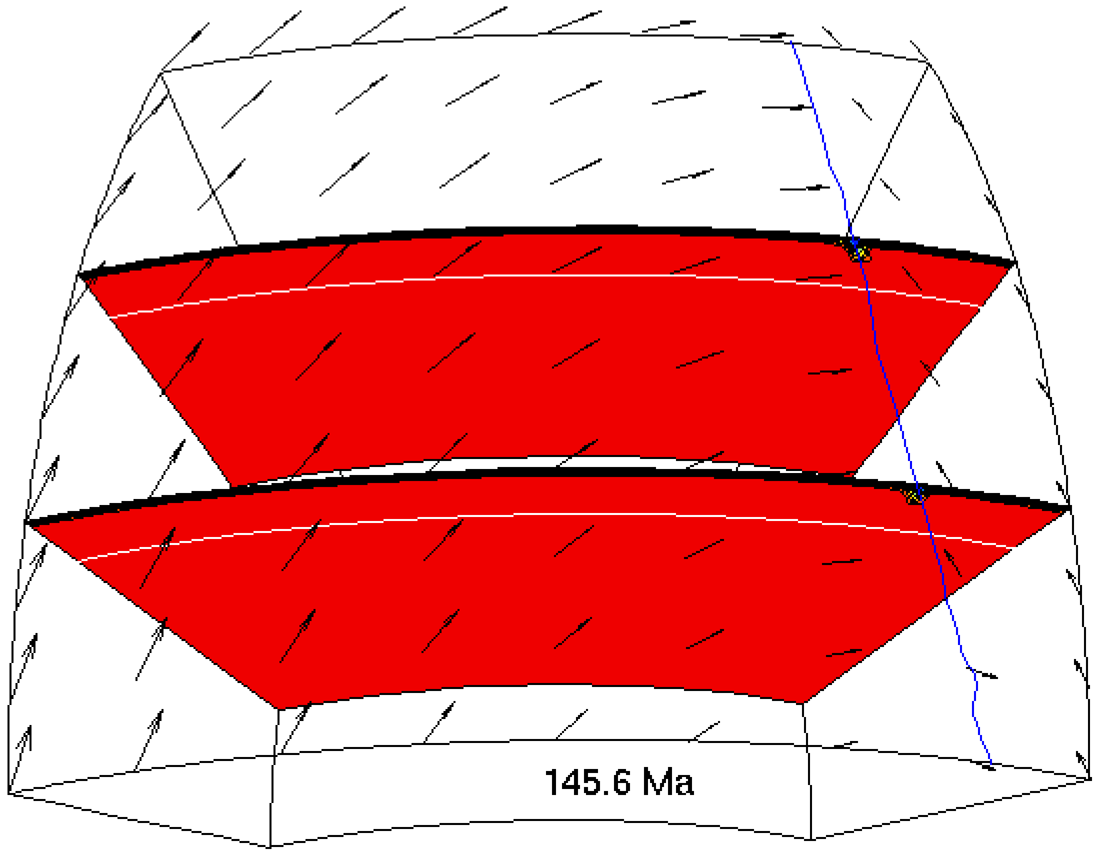

Tan and Gurnis (2002)

What should slabs look like in tomography?

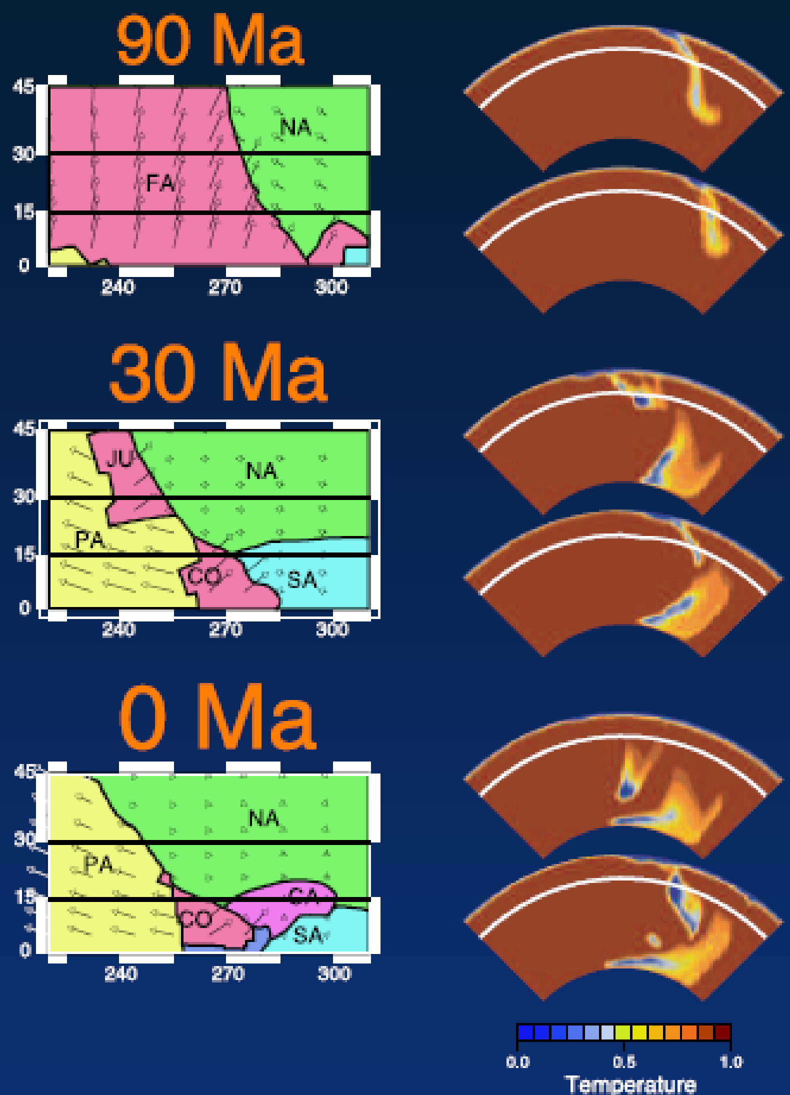

Complicated.

$\Rightarrow$ regional 3-D forward model

$\Rightarrow$ prescribed plate motions

$\Rightarrow$ slab segmentation expected

$\Rightarrow$ ambiguous cross-sections in tomography $\not\Rightarrow$ convection is layered

Tan *et al.* (2002)

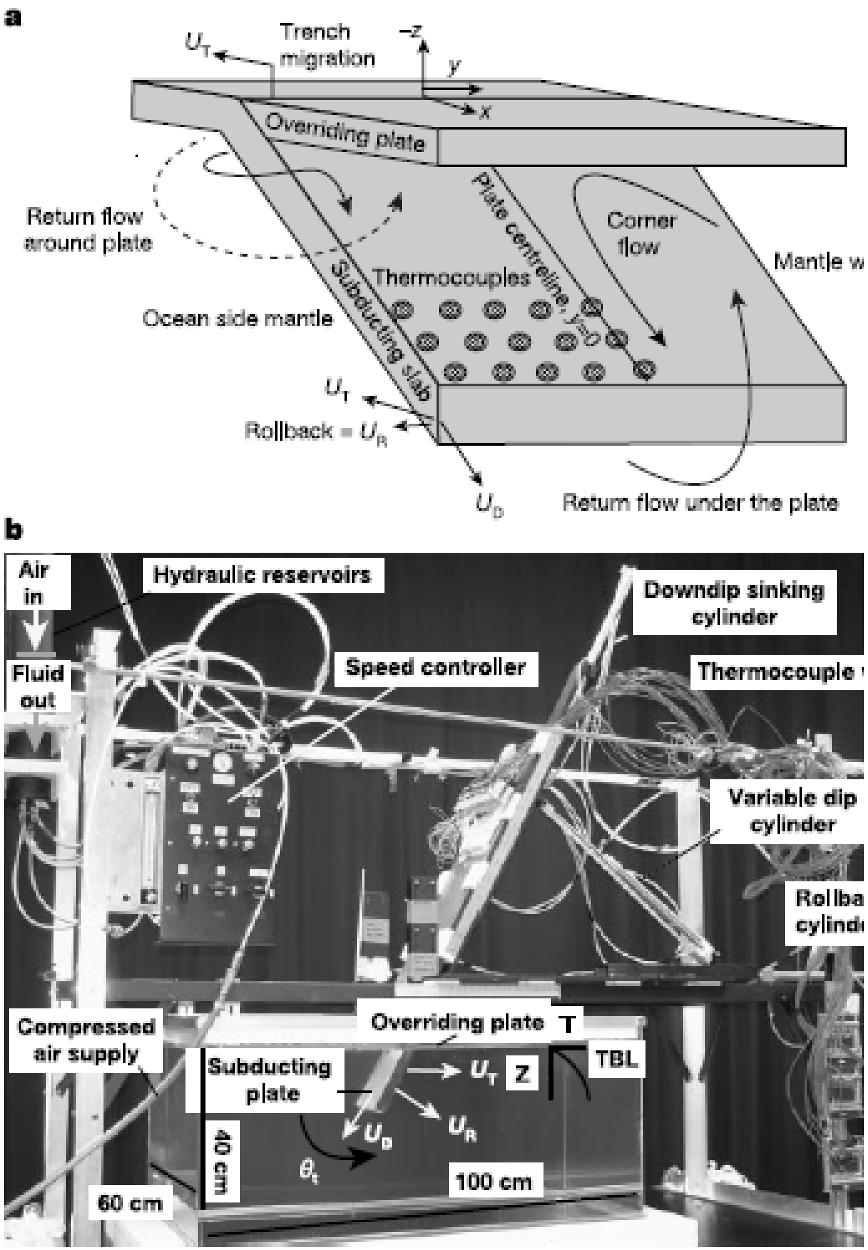

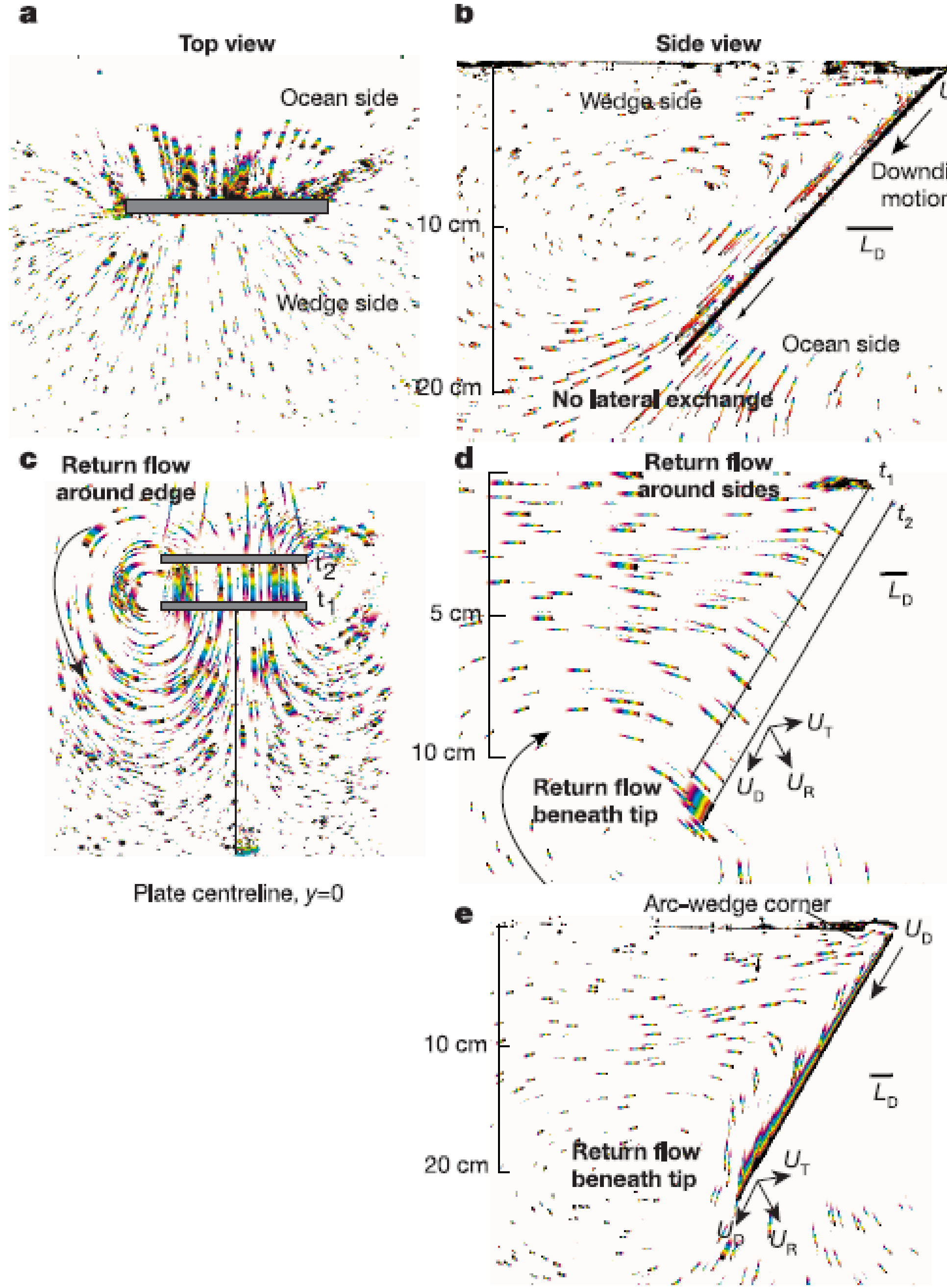

Kincaid & Griffith (2003)

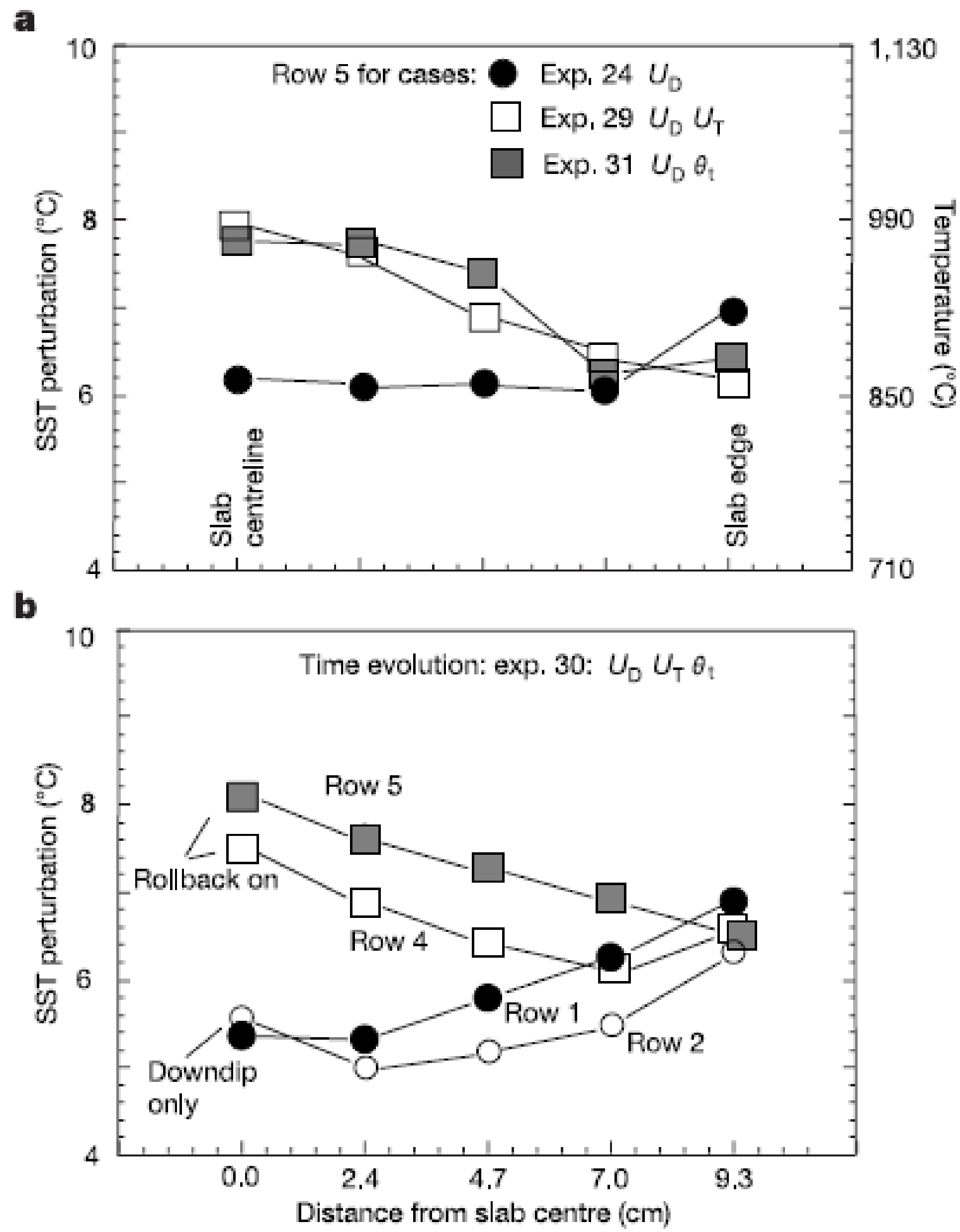

Kincaid & Griffith (2003)

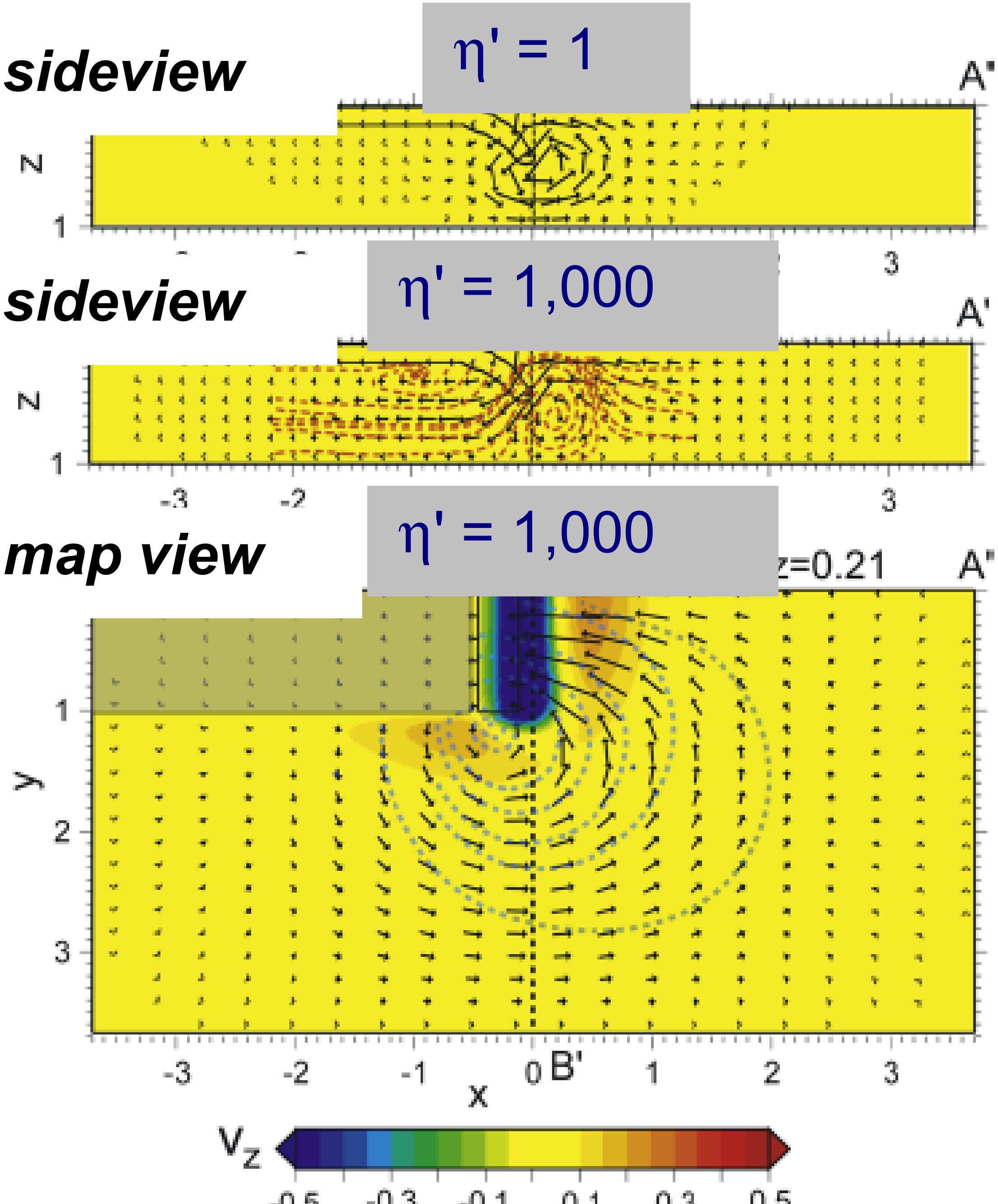

Piromallo et al. (2006)

Instantaneous toroidal partitioning

- Toroidal flow increases with slab width and peaks at moderate viscosity contrasts
- TPR increases with viscosity contrast

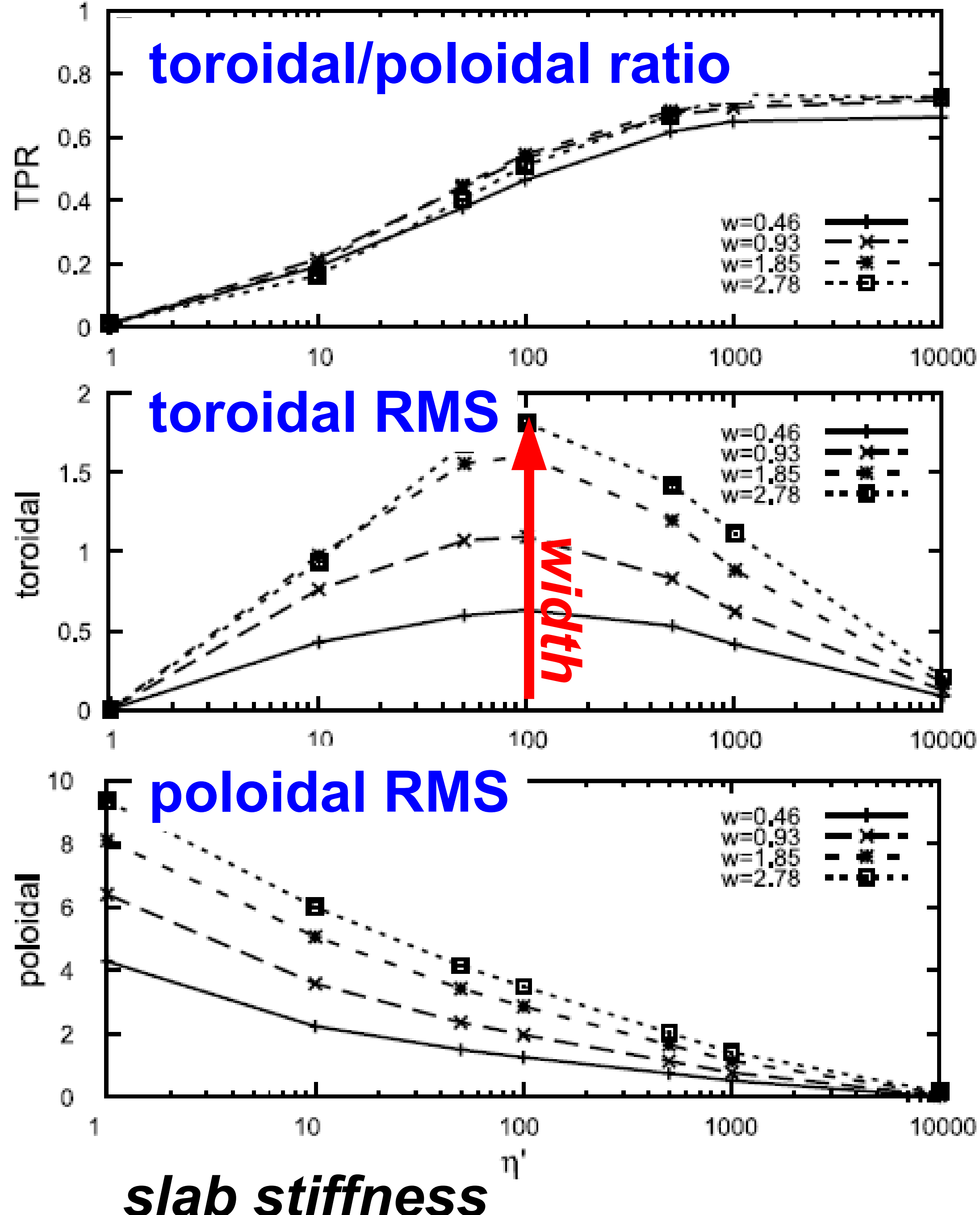

Piromallo et al. (2006)

Fully dynamic (free slab) models

Trench rollback

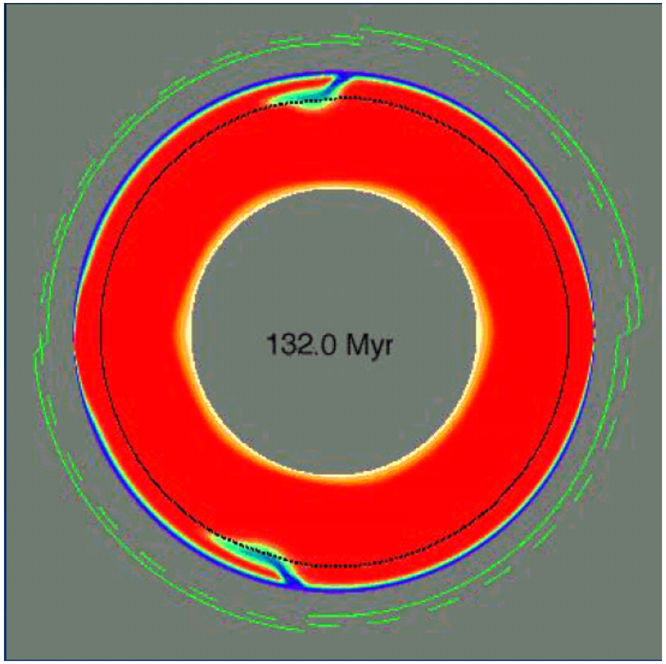

Zhong and Gurnis (1995)

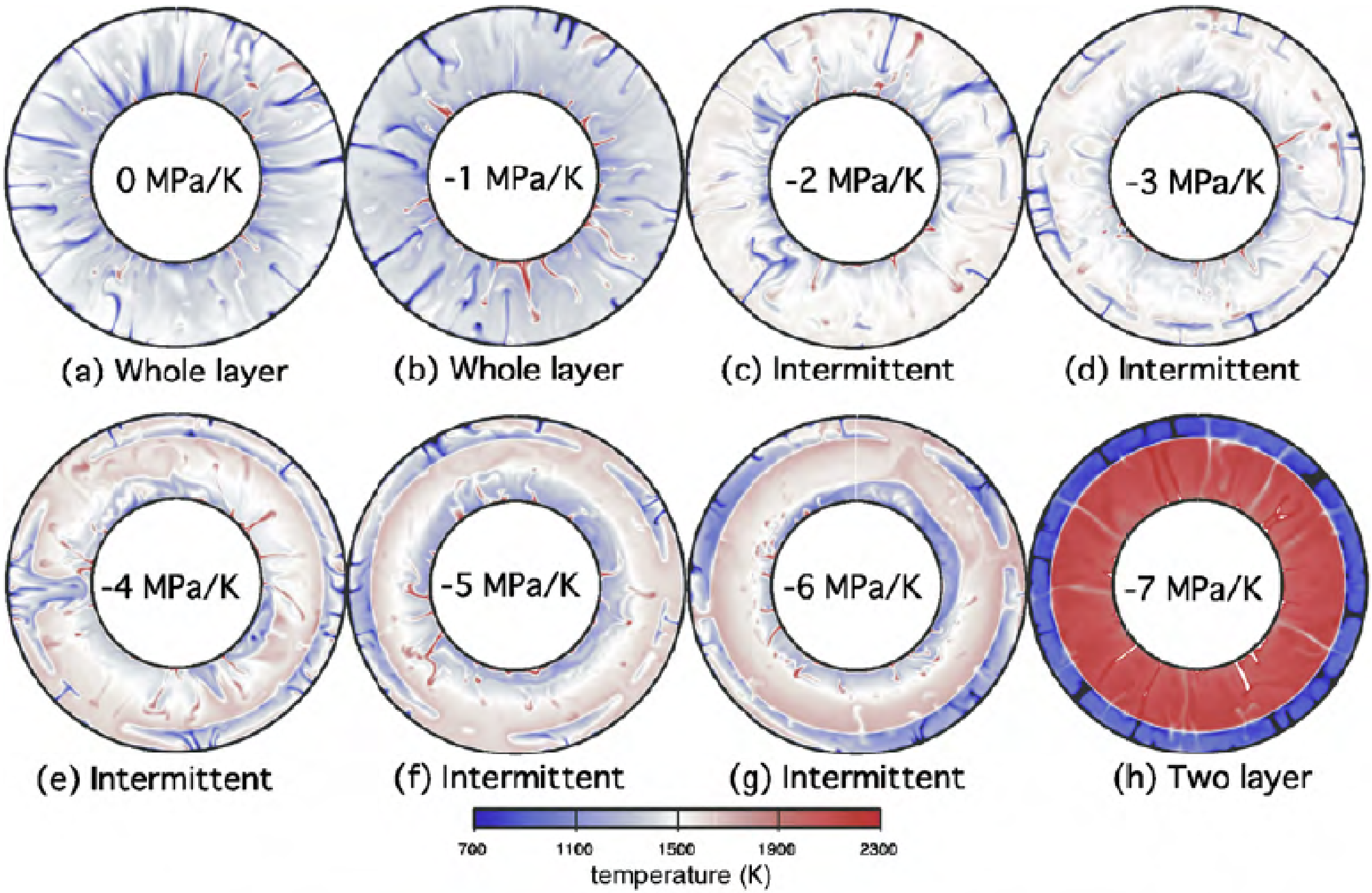

Yanigasawa et al. (2010)

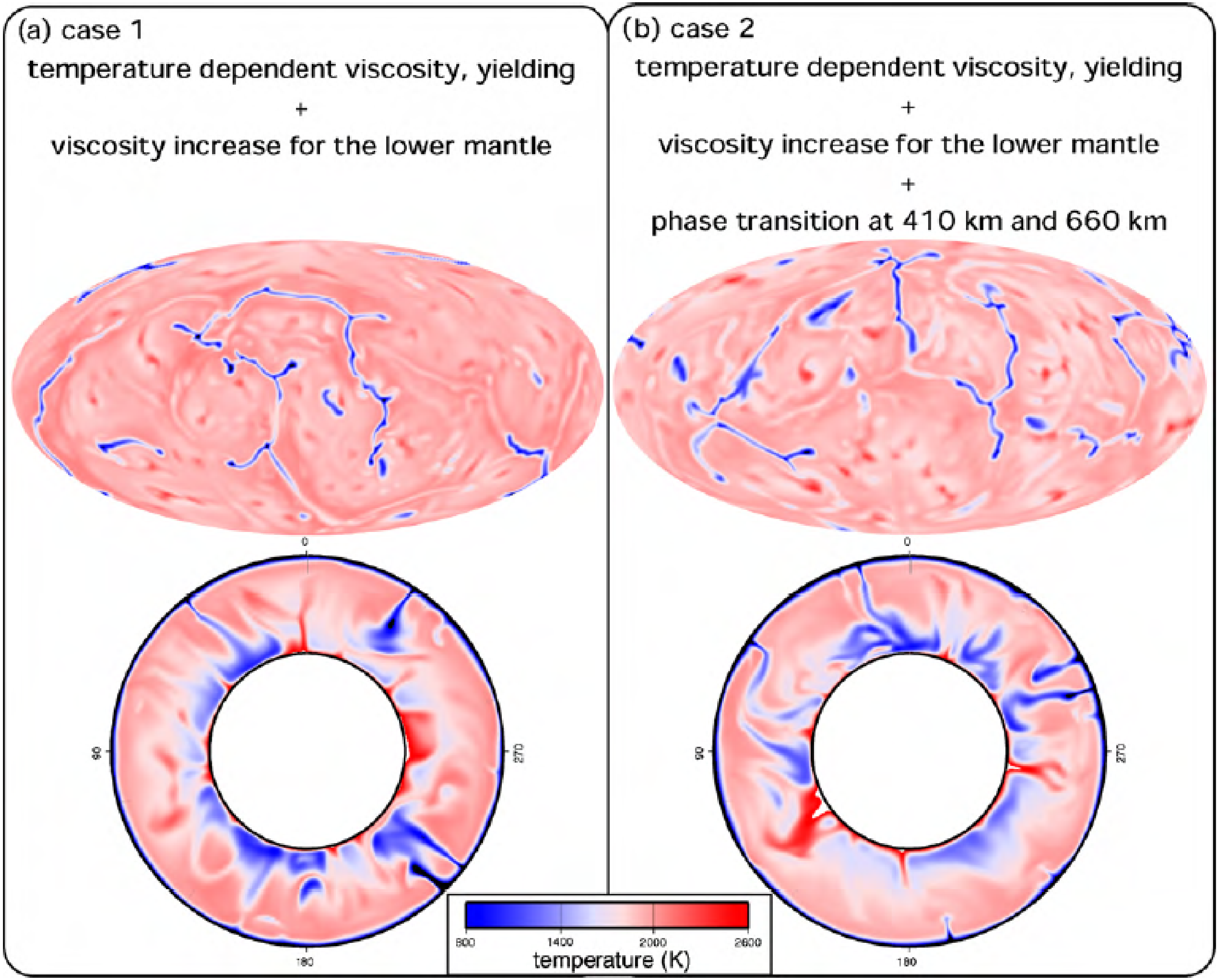

Yanigasawa et al. (2010)

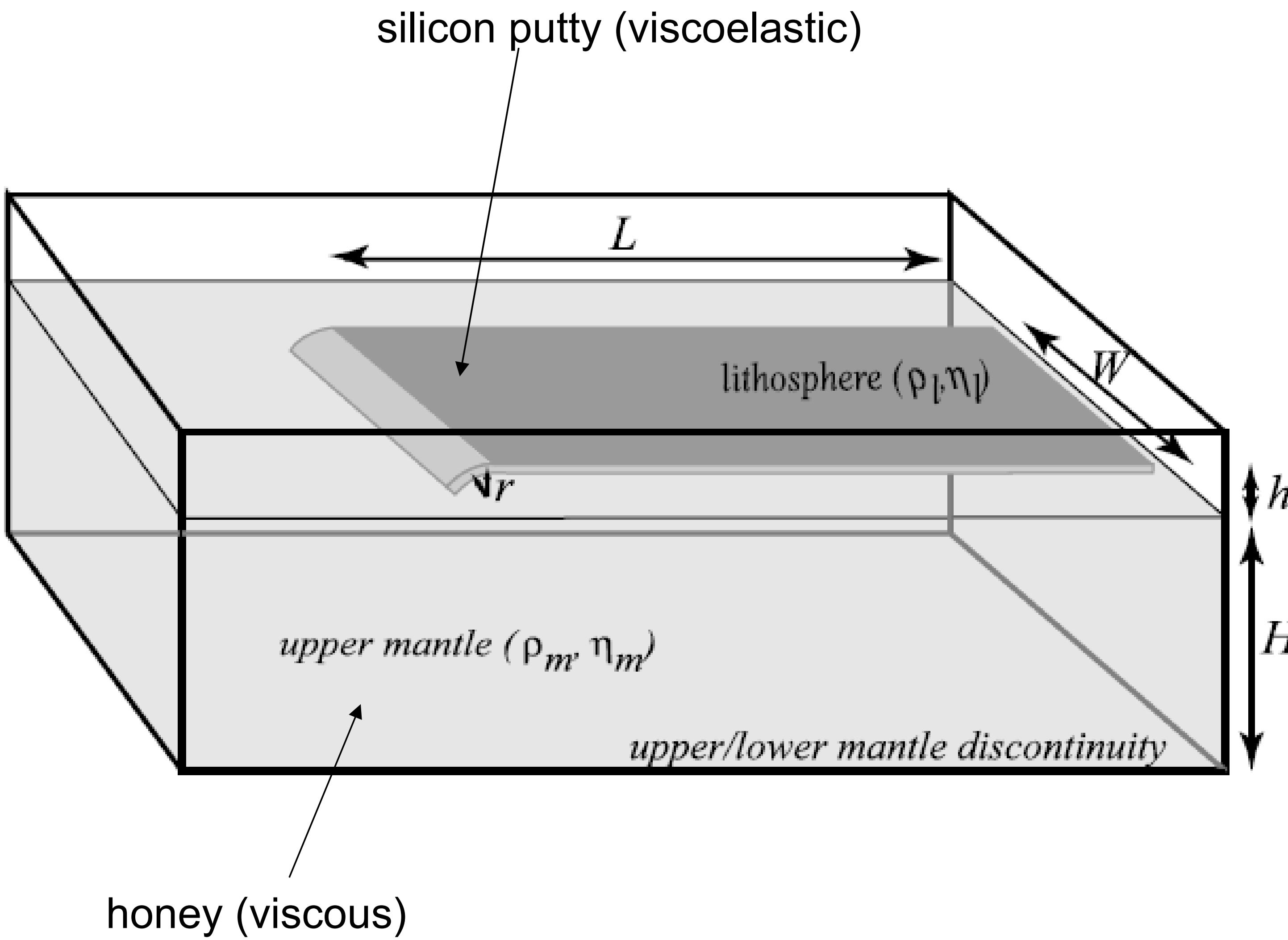

Bellahsen et al., JGR, 2005

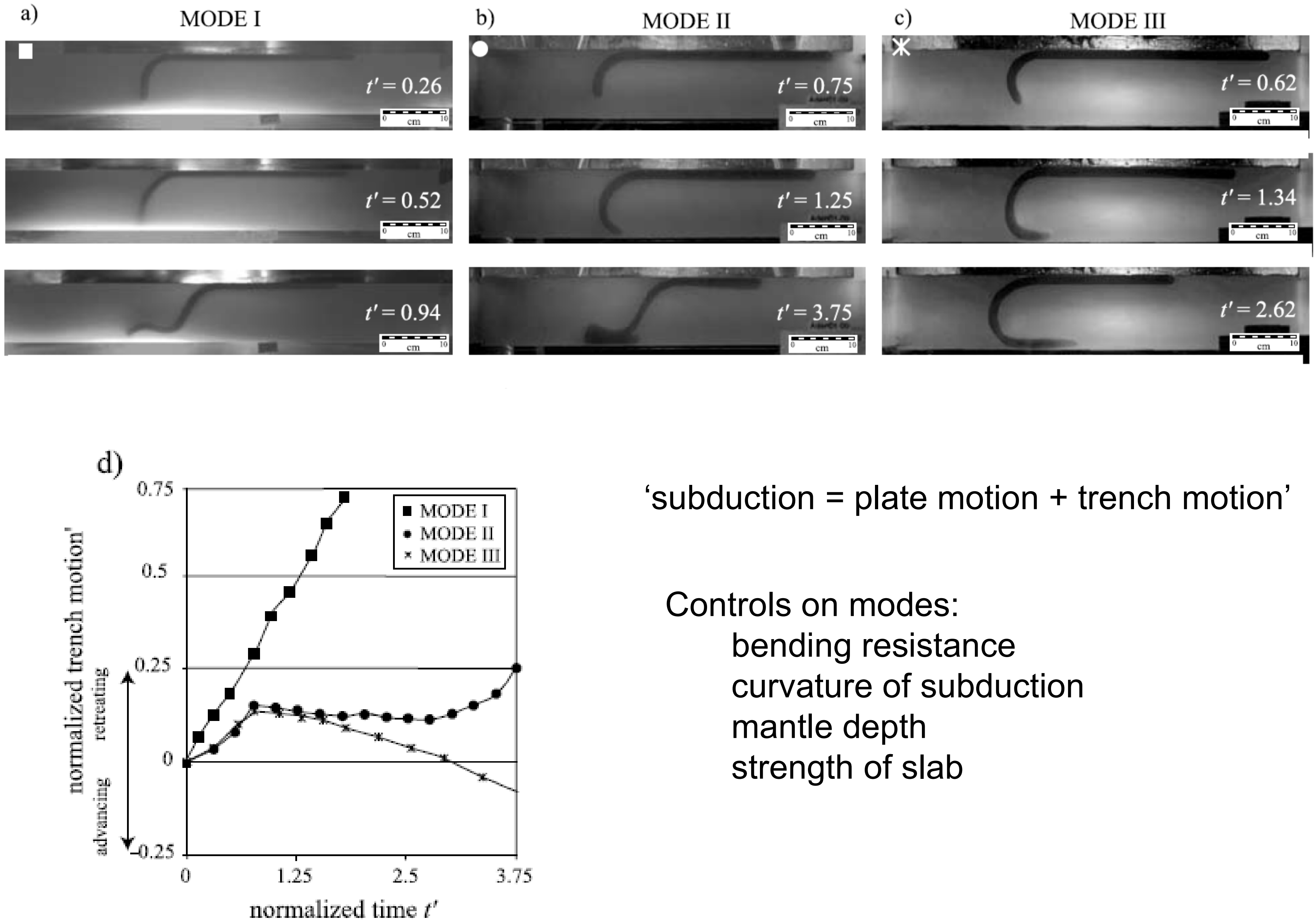

'subduction = plate motion + trench motion'

Controls on modes:
- bending resistance
- curvature of subduction
- mantle depth
- strength of slab

Bellahsen et al., JGR, 2005

Strong slab trench dynamics

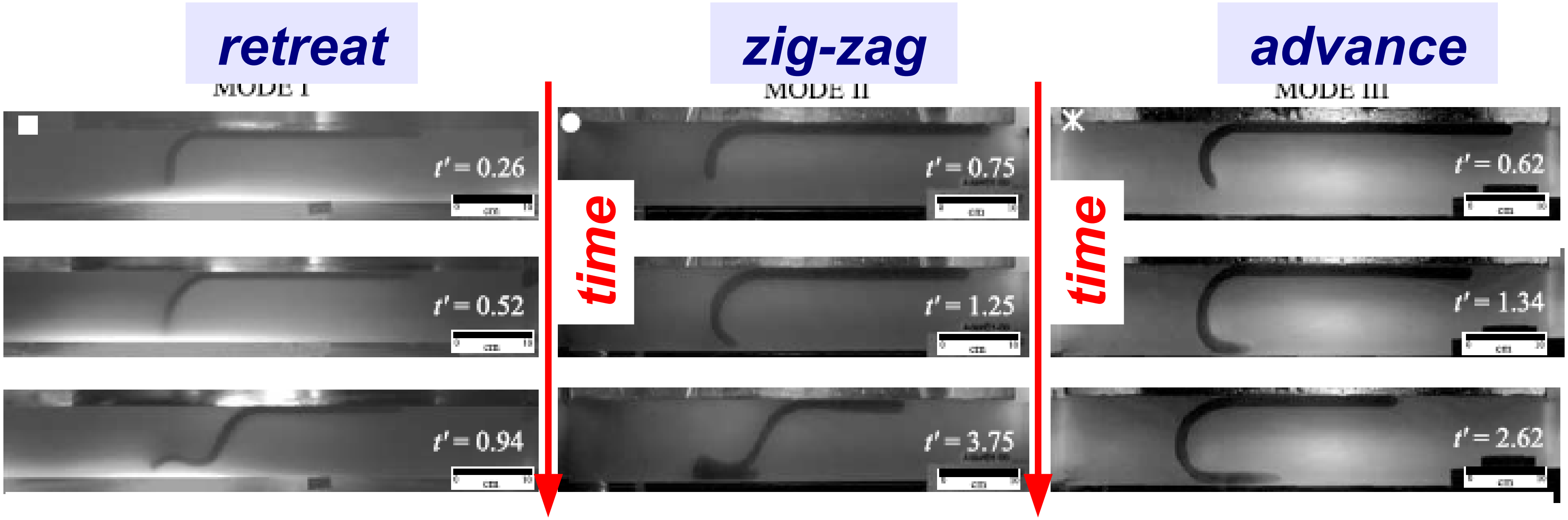

- For slabs with η' ~ 2,00 – 10, 000, a mixed mode regime with advance and retreat exists for free slab models
- Analyze a wide set of experiments with different slab widths, viscosities, thickness, etc. (cf. Enns et al., 2005)

Bellahsen et al. (2005)

Subduction velocity scaling

slab bending

mantle drag

slab pull

$$V' \approx \Delta\rho g h L / [2\eta_l (h/r)^3 + 3\eta_m A]$$

$$V^\circ = (\Delta\rho^\circ g H^\circ h^\circ)/\eta_m{}^\circ$$

$$V = V'/V^\circ$$

$$= (hL/h^\circ H^\circ)[1/(2(\eta_l/\eta_m)(h/r)^3 + 3A)]$$

- Subduction velocity = modified Stokes velocity accounting for bending
- Conrad & Hager (1999); Becker et al. (1999)

Strong slab force balance

- Stiff slab experiments are dominated by bending vs. mantle drag
- cf. Buffett (2006) for proper force estimate (for *r* = *const.*)

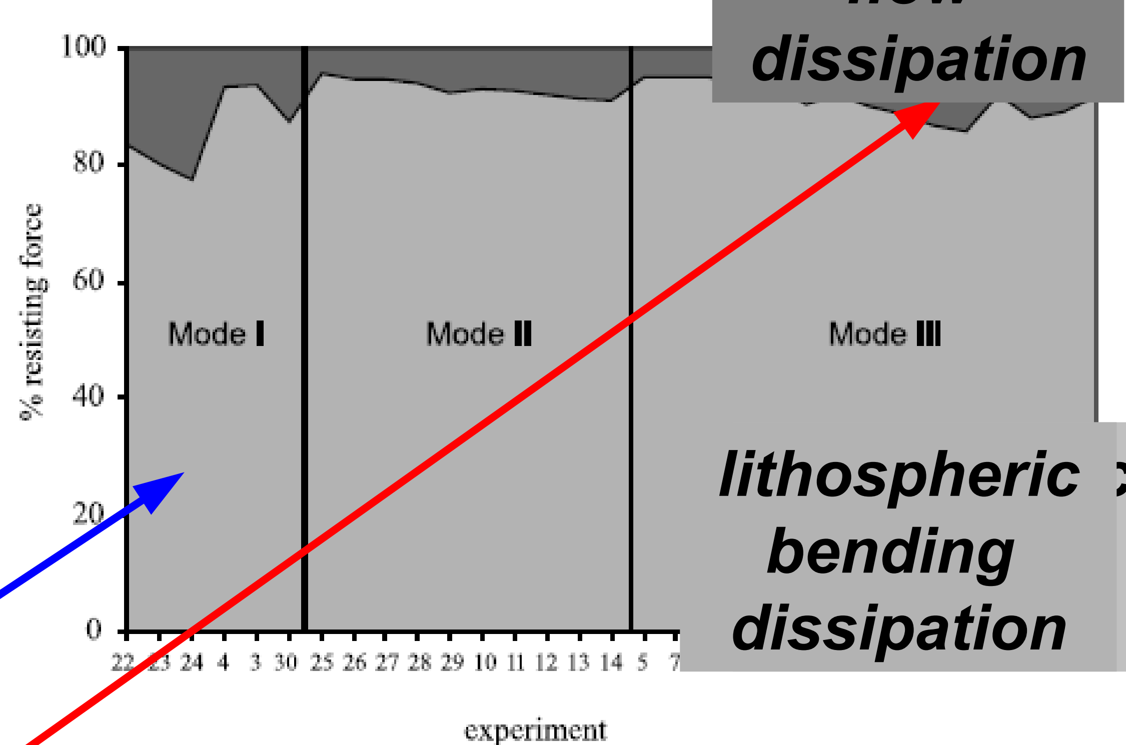

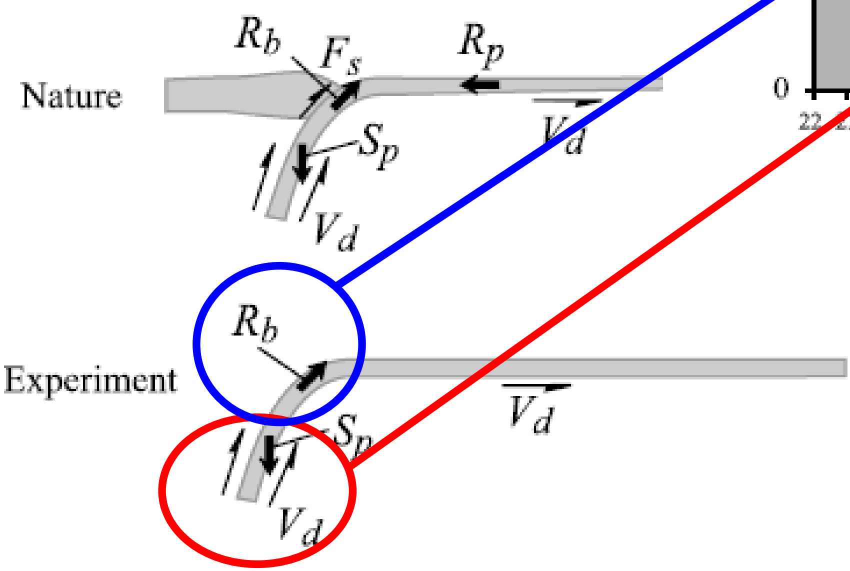

Bellahsen et al. (2005)

- It's a percentage numbers game, f(strength of slab), which is not well known

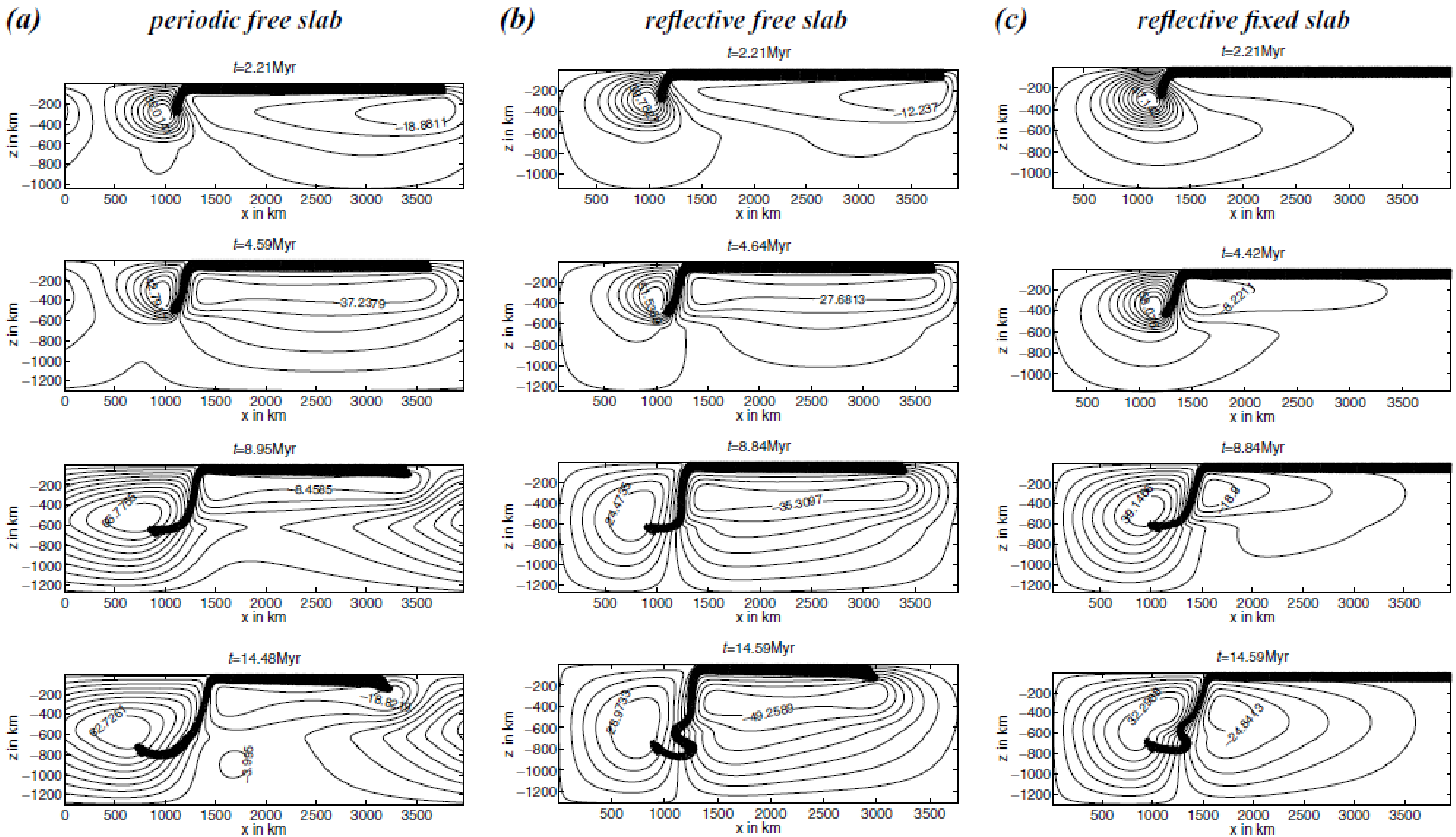

Enns et al. (2005)

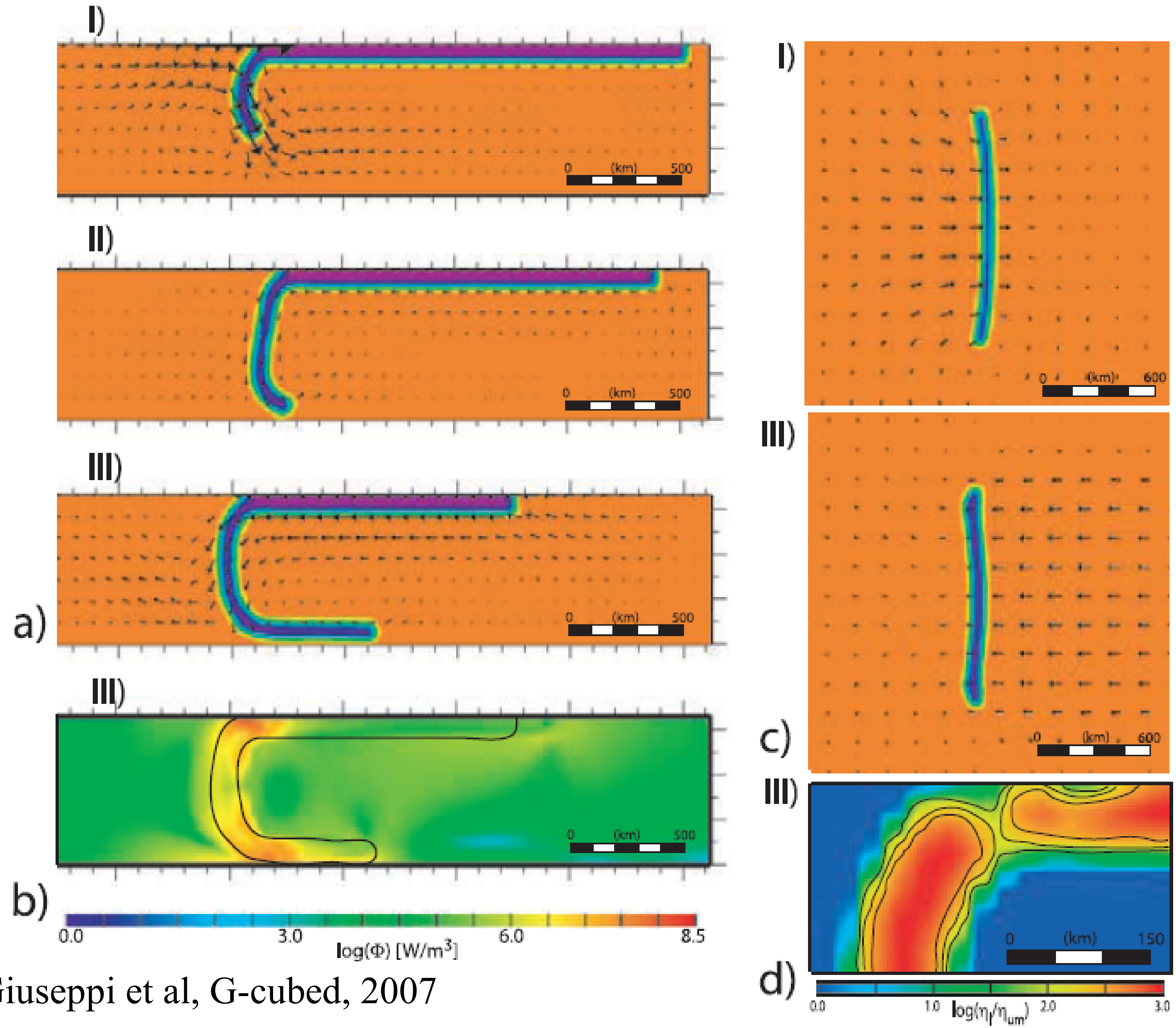

di Giuseppi et al, G-cubed, 2007

Top boundary conditions I

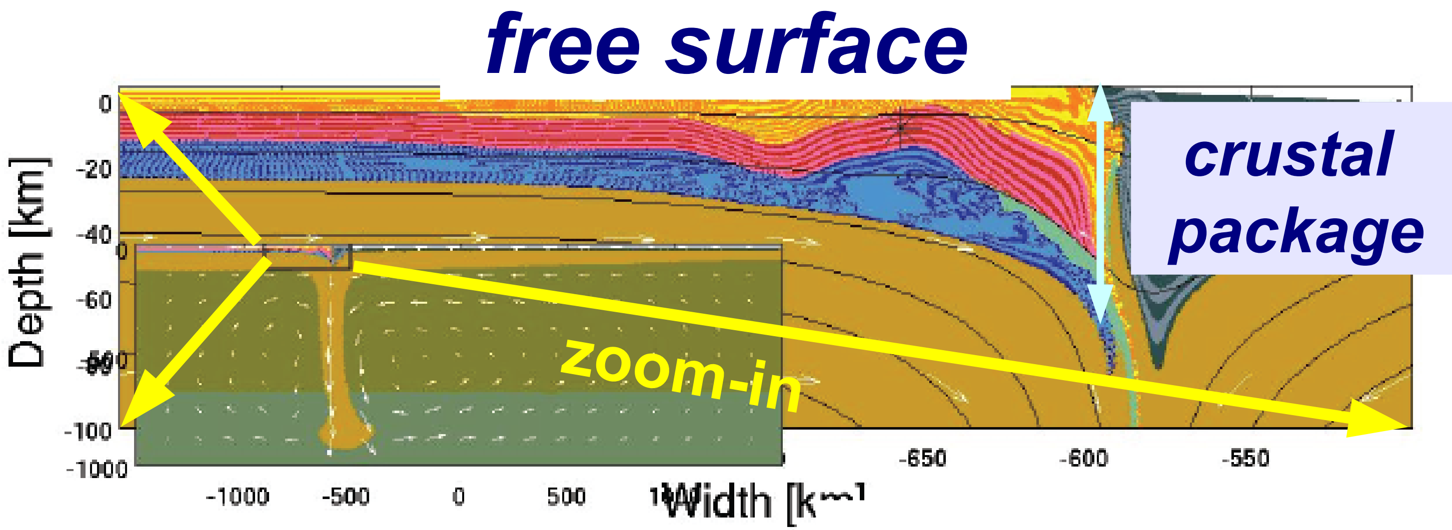

Elasto-visco-plastic rheology & erosion, finite elements (SloMo)

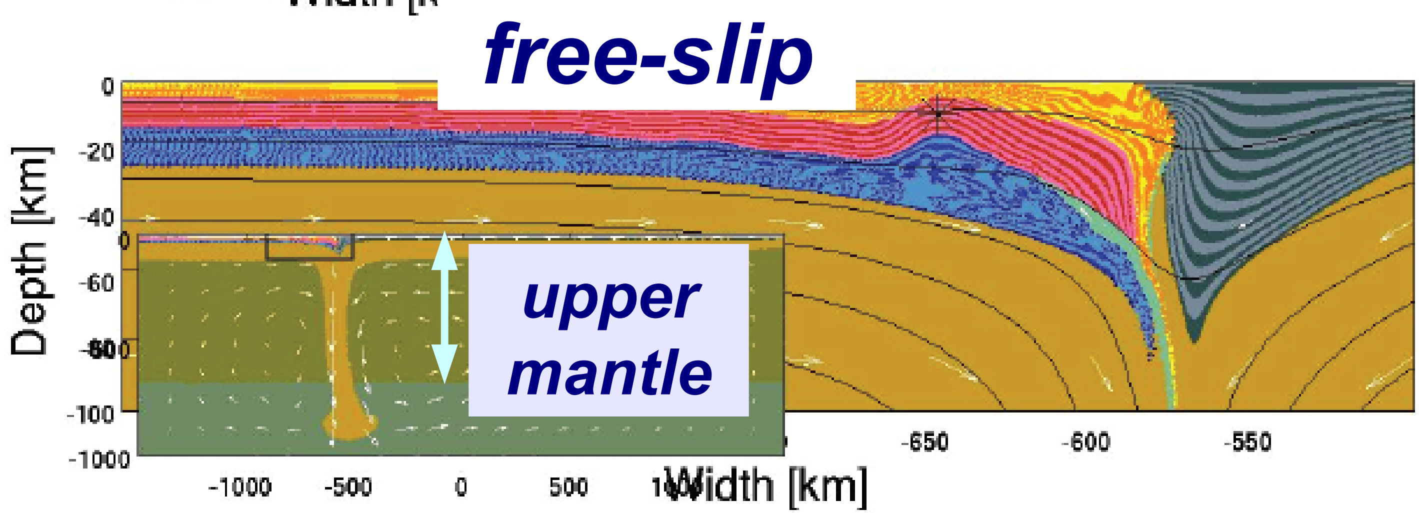

Kaus et al. (2008)

Top boundary conditions II

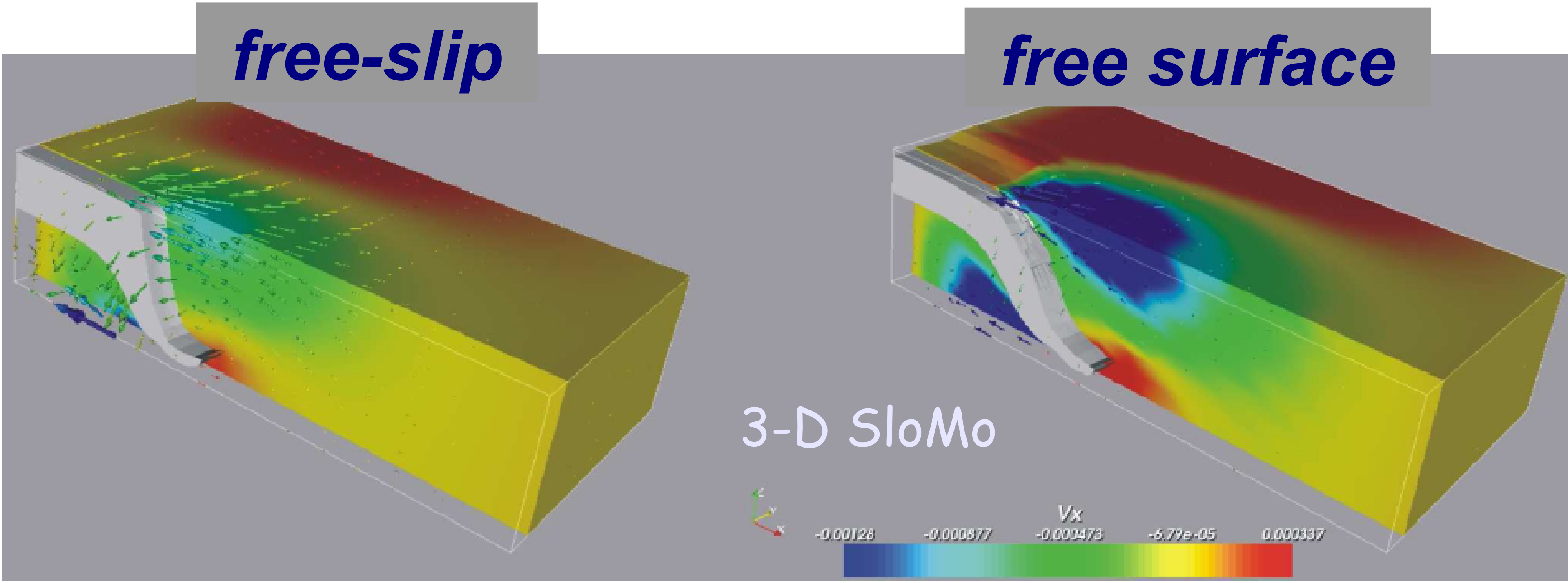

- Boundary condition important for isolated plate experiments (cf. Enns et al., 2005; Schmeling et al., 2006)
- Boundary condition not important for two-plate models (cf. Zhong, Moresi), and tests of Kaus et al. (20078)

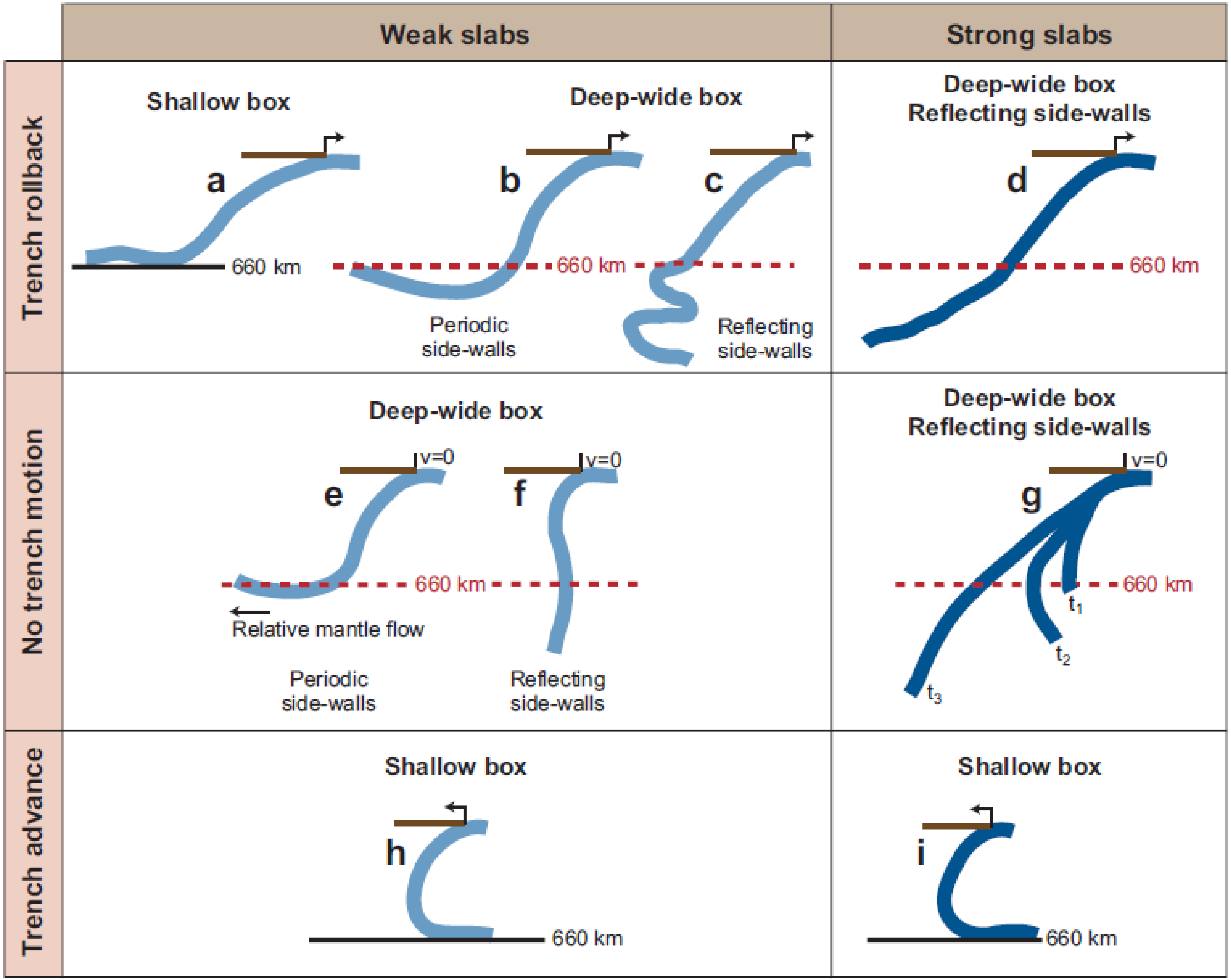

Weak slabs
Strong slabs
Trench rollback
Shallow box
Deep-wide box
Deep-wide box
Reflecting side-walls
a
b
c
d
660 km
660 km
660 km
Periodic
side-walls
Reflecting
side-walls
No trench motion
Deep-wide box
Deep-wide box
Reflecting side-walls
v=0
v=0
v=0
e
f
g
660 km
660 km
Relative mantle flow
Periodic
side-walls
Reflecting
side-walls
t_1
t_2
t_3
Trench advance
Shallow box
Shallow box
h
i
660 km
660 km

Billen (2009)

Effect of slab strength

- Toroidal power increases with viscosity contrast, i.e. flow becomes progressively less Stokes-sinker like (Piromallo et al., 2006)
- Subduction velocities (poloidal RMS) decrease with viscosity contrast, i.e. the slab strength has an important effect on mantle flow and subduction rates (Conrad & Hager, 1999; Becker et al., 1999; Bellahsen et al., 2005)
- Trench curvature is more convex for stiff slabs (cf. Funciello et al., 2004, Schellart et al., 2007)
- No elasticity needed to explain trench morphology (cf. Morra et al., 2006)

The moderately weak slab

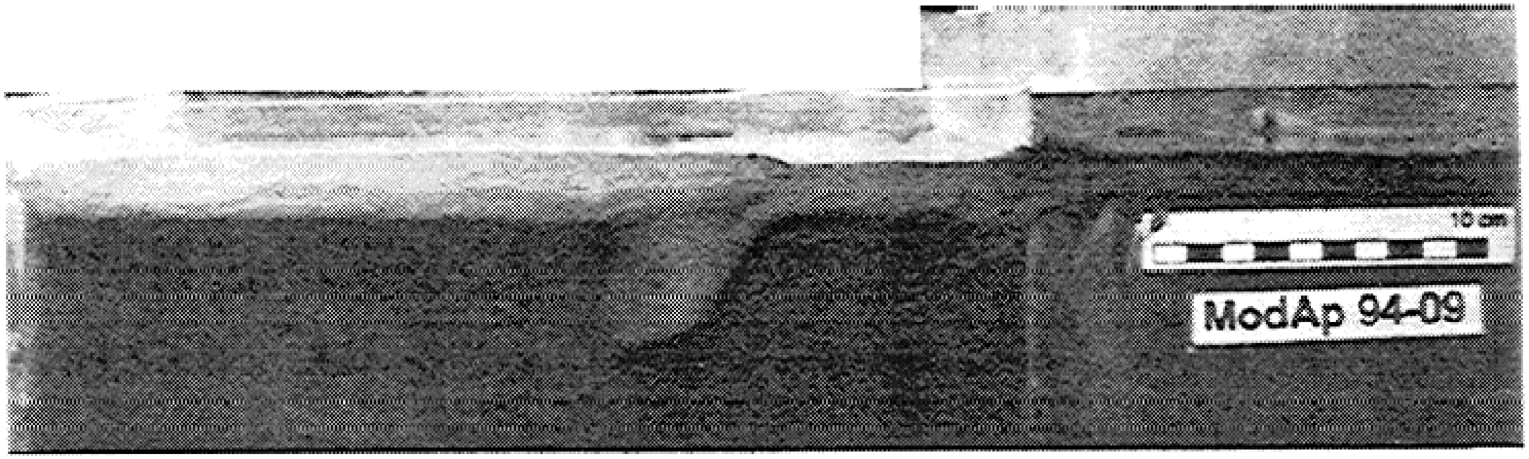

Becker *et al.* (1999)

- Consistent with
  - Becker et al. (1999) and Conrad & Hager (1999) bending related estimates which yielded upper bound of $\eta' \sim 500$
  - Moresi & Gurnis (1996) geopotential argument
  - Billen & Gurnis (2005) trench admittance work
  - ...

Lab model behavior as f (η')

η'

strength

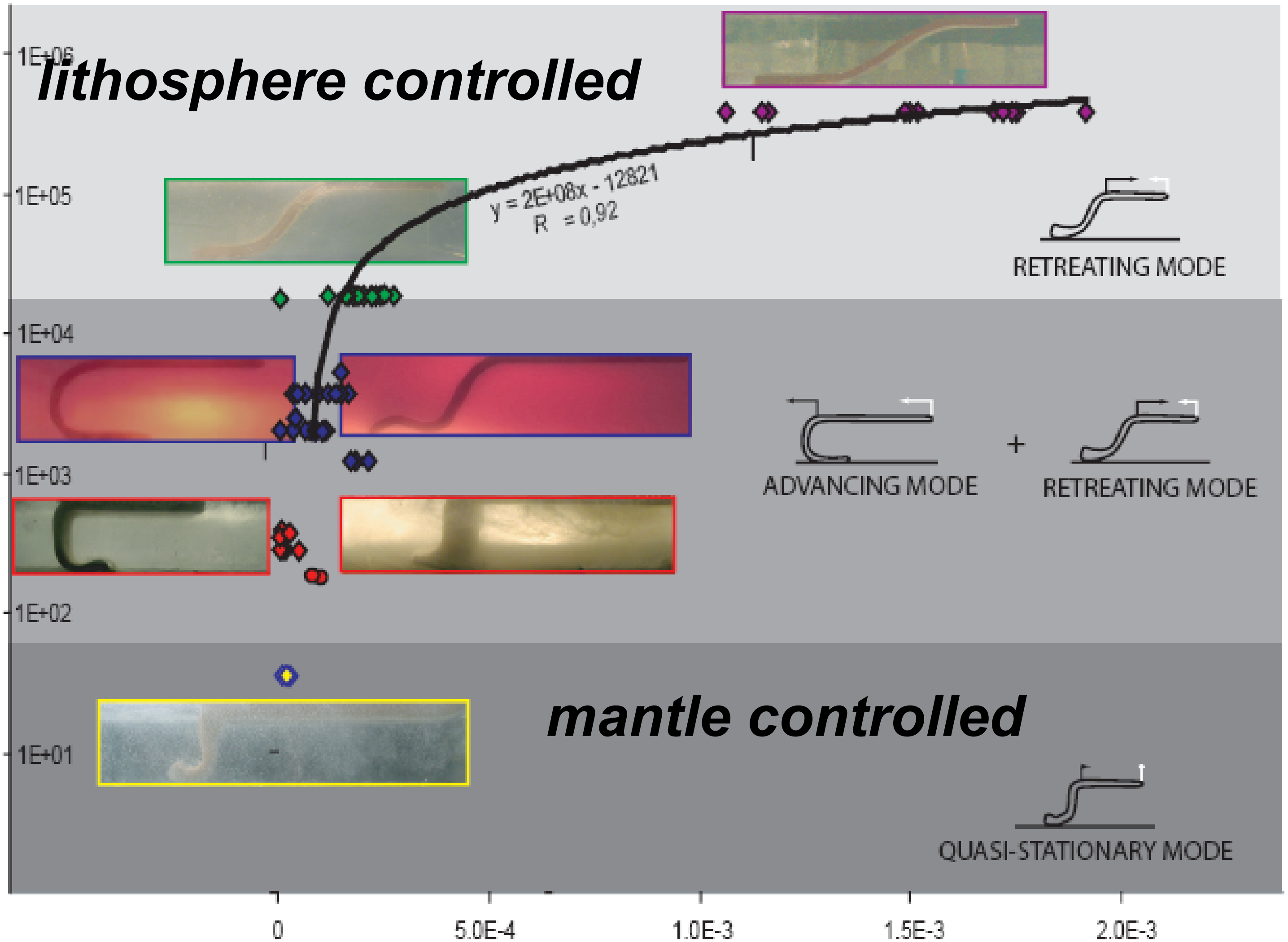

buoyancy

~V'

Funiciello et al. (2007) with data from Schellart (2004)

$$D^*_{\text{vis}} = \frac{D_{\text{vis}}}{\frac{1}{3}\eta_{\text{um}} H^3} = \frac{\eta_{\text{plate}}}{\eta_{\text{um}}}\left(\frac{h_{\text{plate}}}{H}\right)^3$$

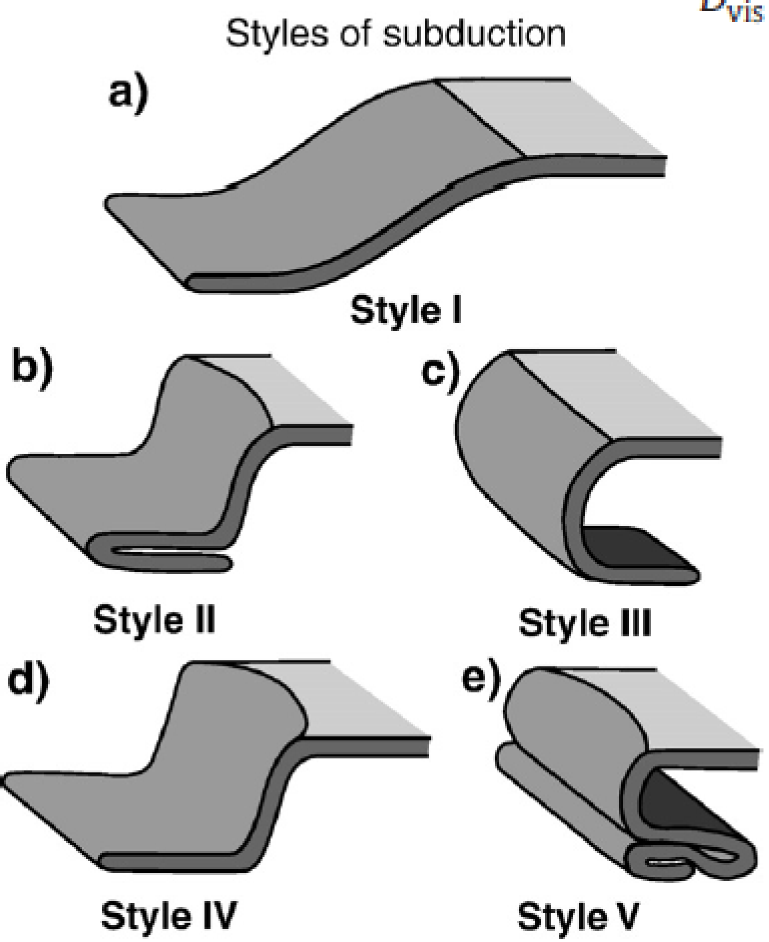

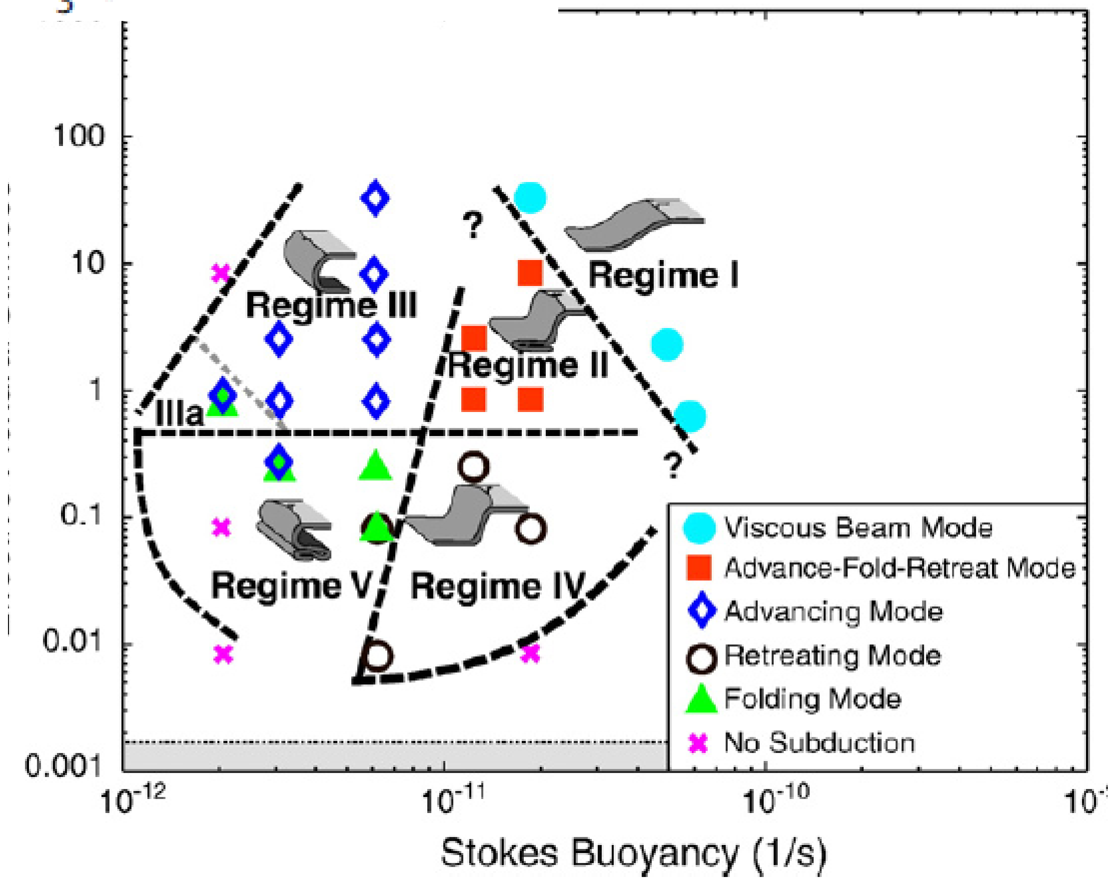

$$B_S = \frac{\Delta\rho g\, h_{\text{plate}}}{\eta_{\text{um}}}$$

Stegman et al. (2010)

Thin sheet BEM models of free slabs

Role of γ

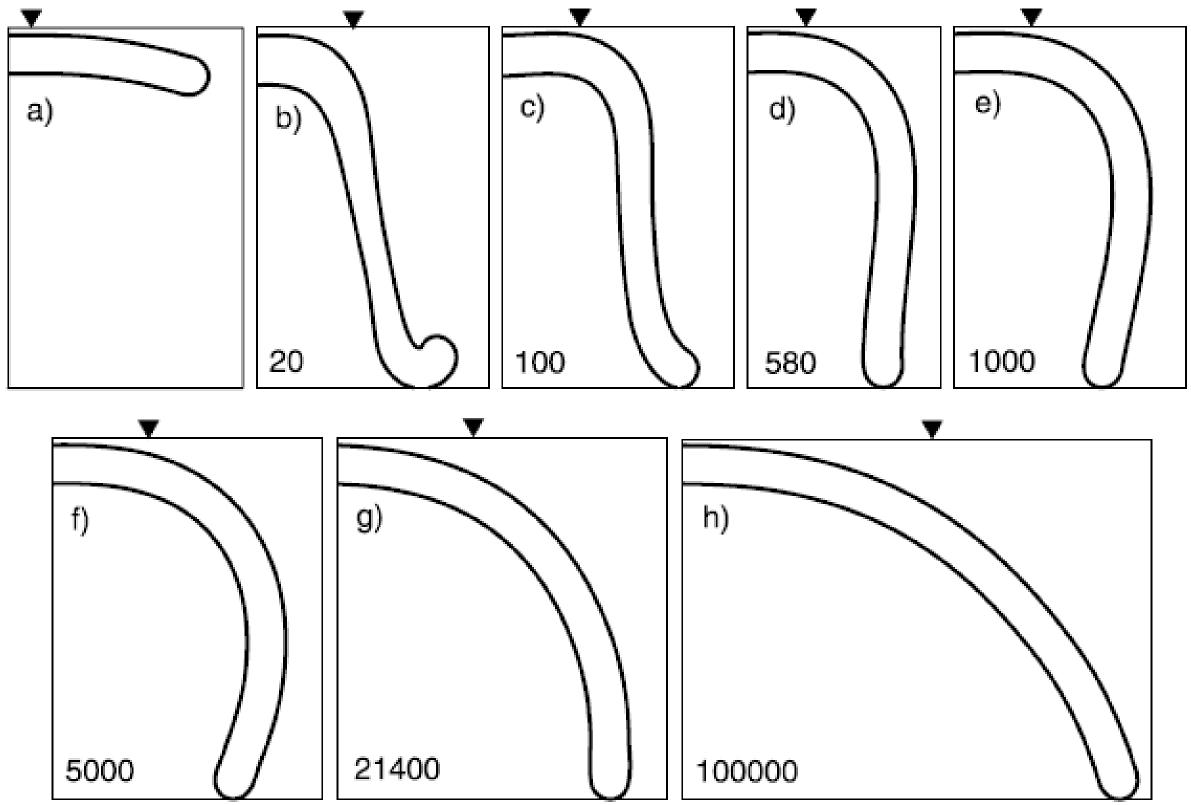

Figure 12. Shapes of subducting viscous sheets that have reached a depth $D = 9.17h$, starting from the initial conditions $L(0) = 16h$, $d/h = 0.2$, $\ell(0) = 4h$ and $\theta_0(0) = 15^\circ$ shown in panel a). The viscosity contrast γ is indicated at the lower left-hand corner of panels (b)–(h). The inverted triangles indicate the initial position of the trench.

Ribe (2010)

Thin sheet BEM models of free slabs

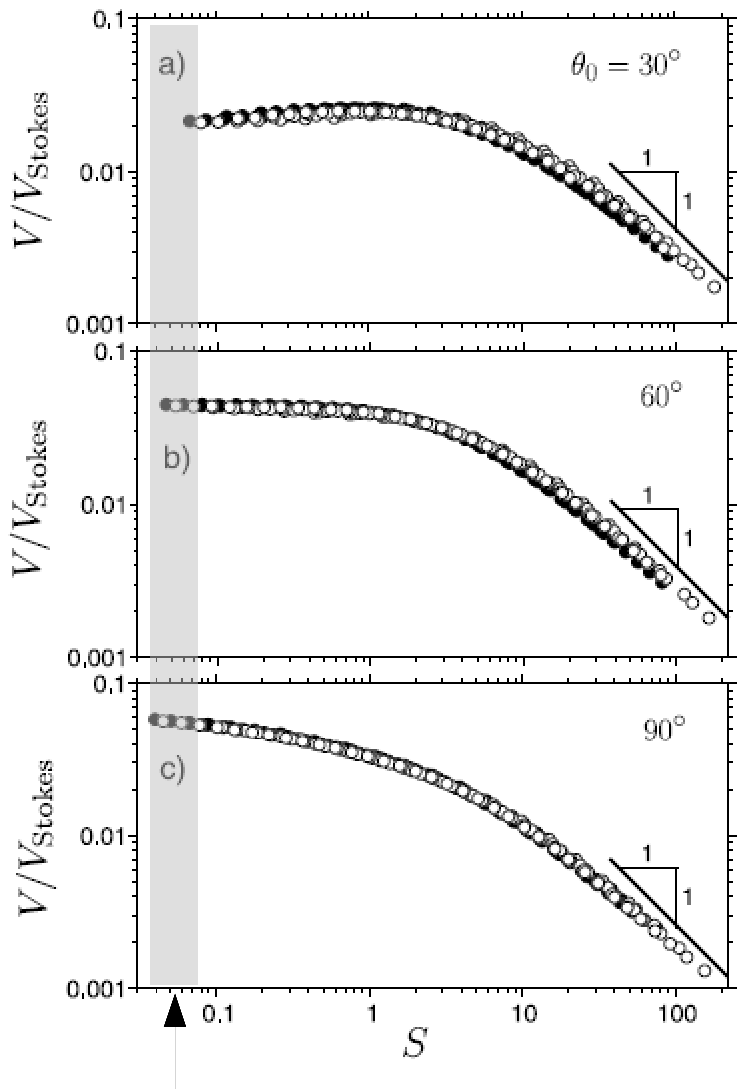

Capitanio et al. (2007) models

$$\gamma \left(\frac{h}{\ell_b}\right)^3 \equiv S.$$

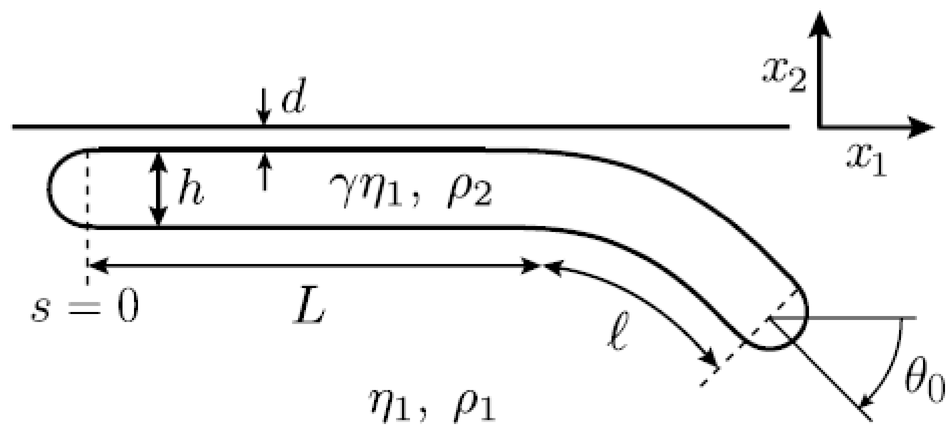

Ribe (2010)

Thin sheet BEM models of free slabs

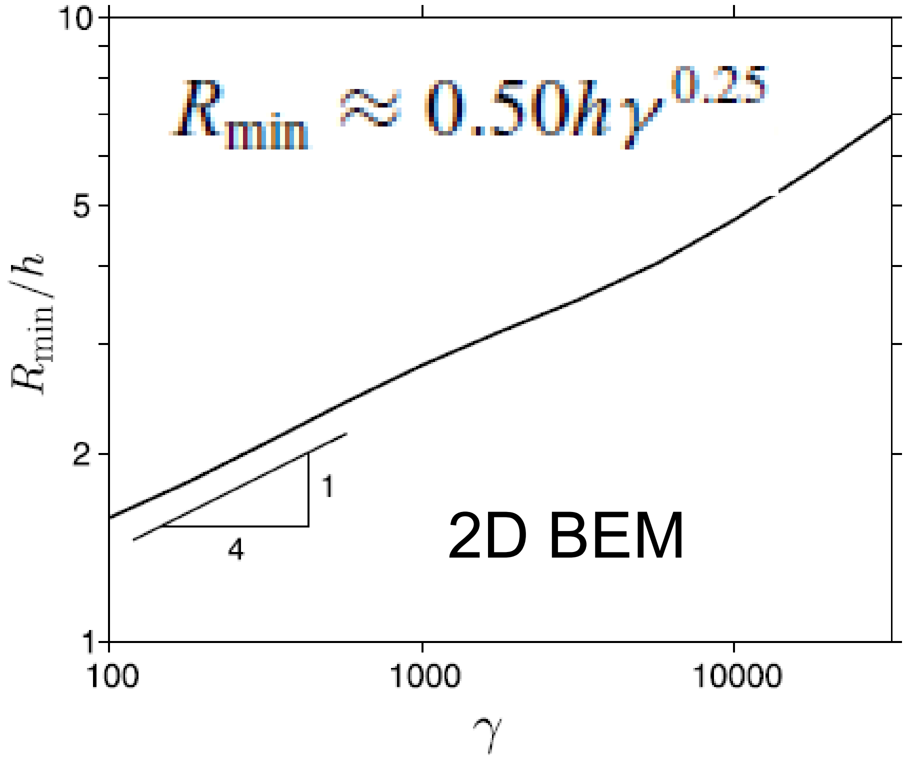

Figure 13. Minimum radius of curvature $R_{\min}$ of a subducting sheet at the time when its tip reaches a depth $D = 8.25h$, as a function of the viscosity contrast γ. The initial condition is the same as in Fig. 12(a).

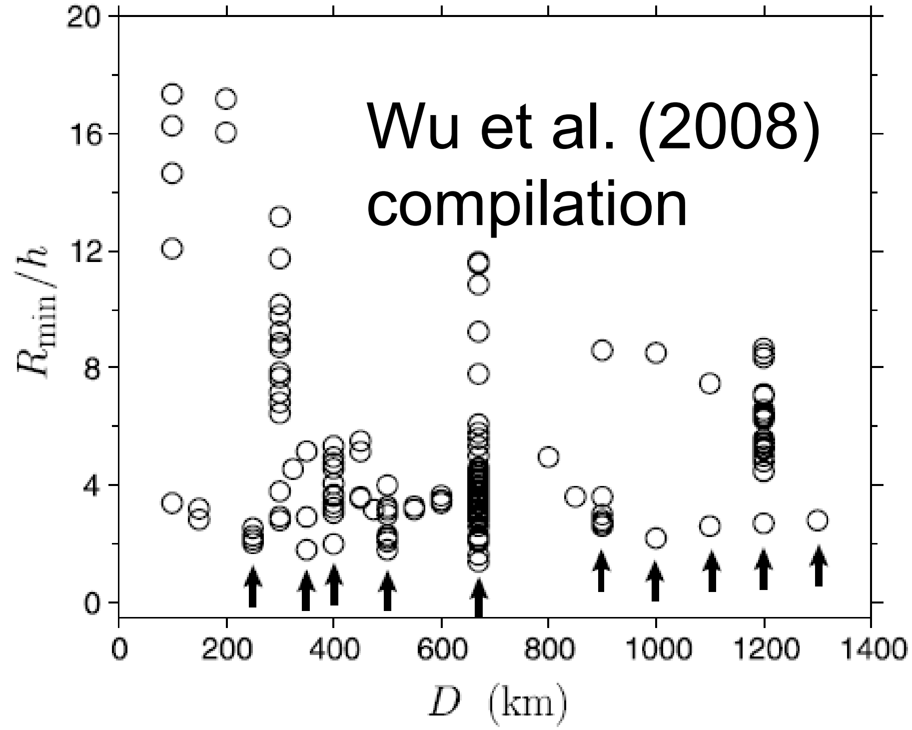

Figure 14. Normalized minimum radius of curvature $R_{\min}/h$ of subducting slabs on Earth as a function of the slab's maximum depth D (data from Wu *et al.* 2008). Arrows indicate the data points used to estimate the global minimum value of $R_{\min}/h$.

$$\gamma \in [140 ; 410]$$

Consistent with Funiciello et al. (2009)

$$\gamma \in [150 ; 500]$$

Ribe (2010)

Role of the dip at touchdown

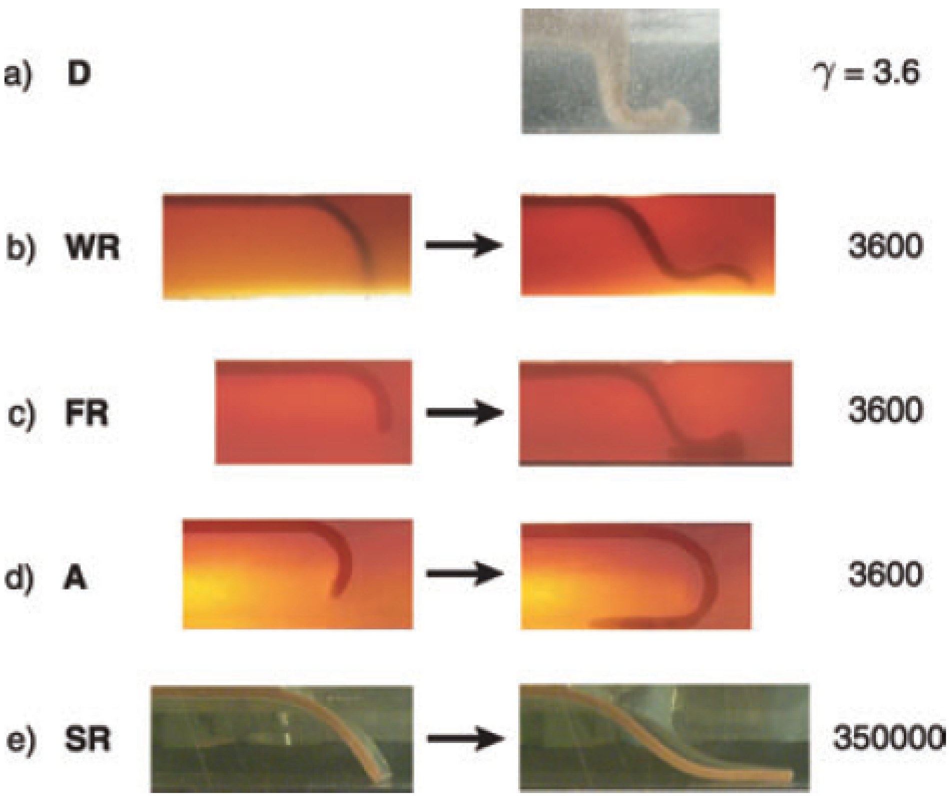

Figure 10. Modes of free subduction observed in analogue laboratory experiments. (a) 'dripping' (D) mode; (b) 'weak retreating' (WR) mode; (c) 'folding retreating' (FR) mode; (d) 'advancing' (A) mode and (e) 'strong retreating' (SR) mode. The photographs in the left-hand column were taken before the sheet's leading end reached the bottom of the experimental tank, and those in the right-hand column some time after. The viscosity contrast γ for each experiment is indicated at far right-hand side. The depths of the fluid layers are 9.4 cm for (a), 11 cm for (b)–(d) and 9.7 cm for (d). Photographs courtesy of F. Funiciello.

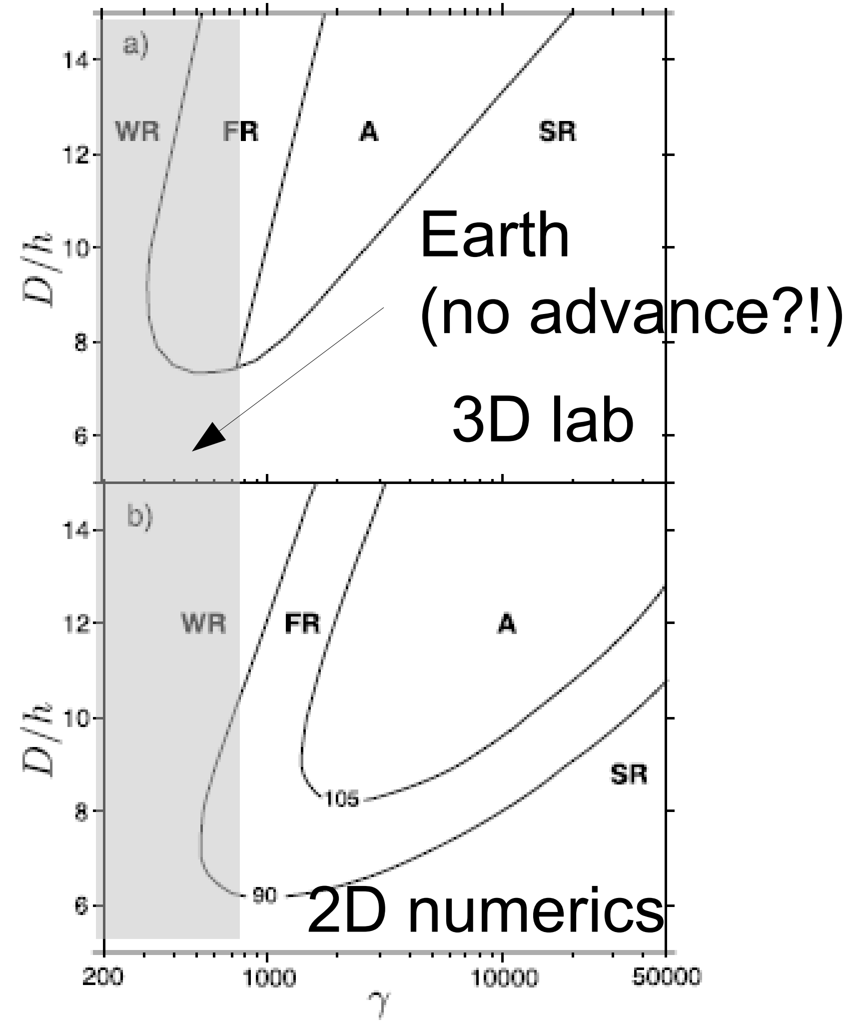

Figure 11. (a) Phase diagram showing the modes of free subduction observed in laboratory experiments as a function of the viscosity contrast γ and the ratio D/h of the layer depth to the sheet thickness (adapted from Fig. 13 of Schellart 2008). WR: weak retreating mode. FR: folding retreating mode. A: advancing mode. SR: strong retreating mode. (b) Contours of the dip θ_D (in degrees) of the tip of the slab at the time when it reaches the depth D, predicted numerically using the BEM model. The initial condition for the calculations is $\ell(0) = 0.455\ D$, $\theta_0(0) = 15°$, $L/h = 16$ and $d/h = 0.2$.

Ribe (2010)

Why not f(Δρ)?

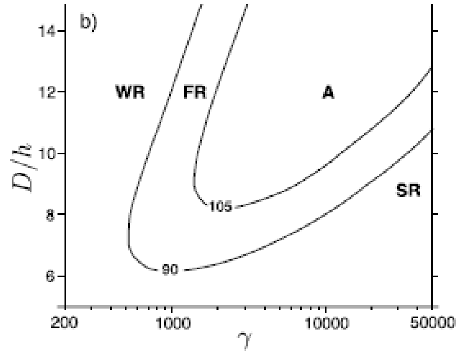

vs.

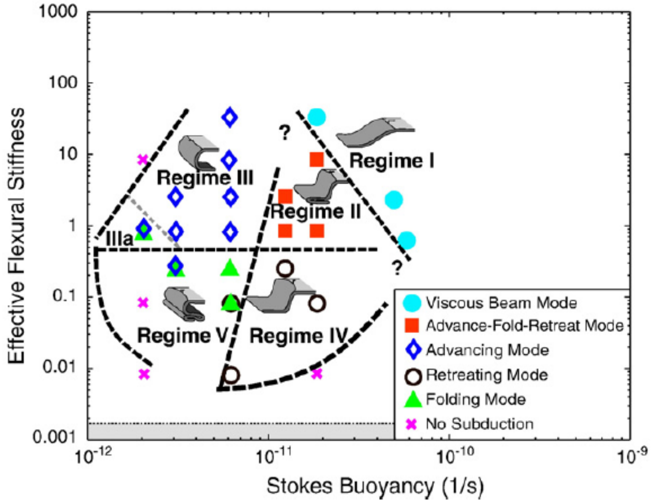

Lab: surface tension (Bellahsen et al., 2005)

$$Bo^{-1} = \frac{\sigma}{h^2 g \Delta\rho} \qquad Bo^{-1} \in [0.37\,;2.2]$$

Numerics: plastic yielding (Stegman et al., 2009)

$$\Pi = \frac{\tau}{hg\Delta\rho} \qquad \Pi \in [0.06\,;1.85]$$

Ribe (2010)

Real slabs aren't free

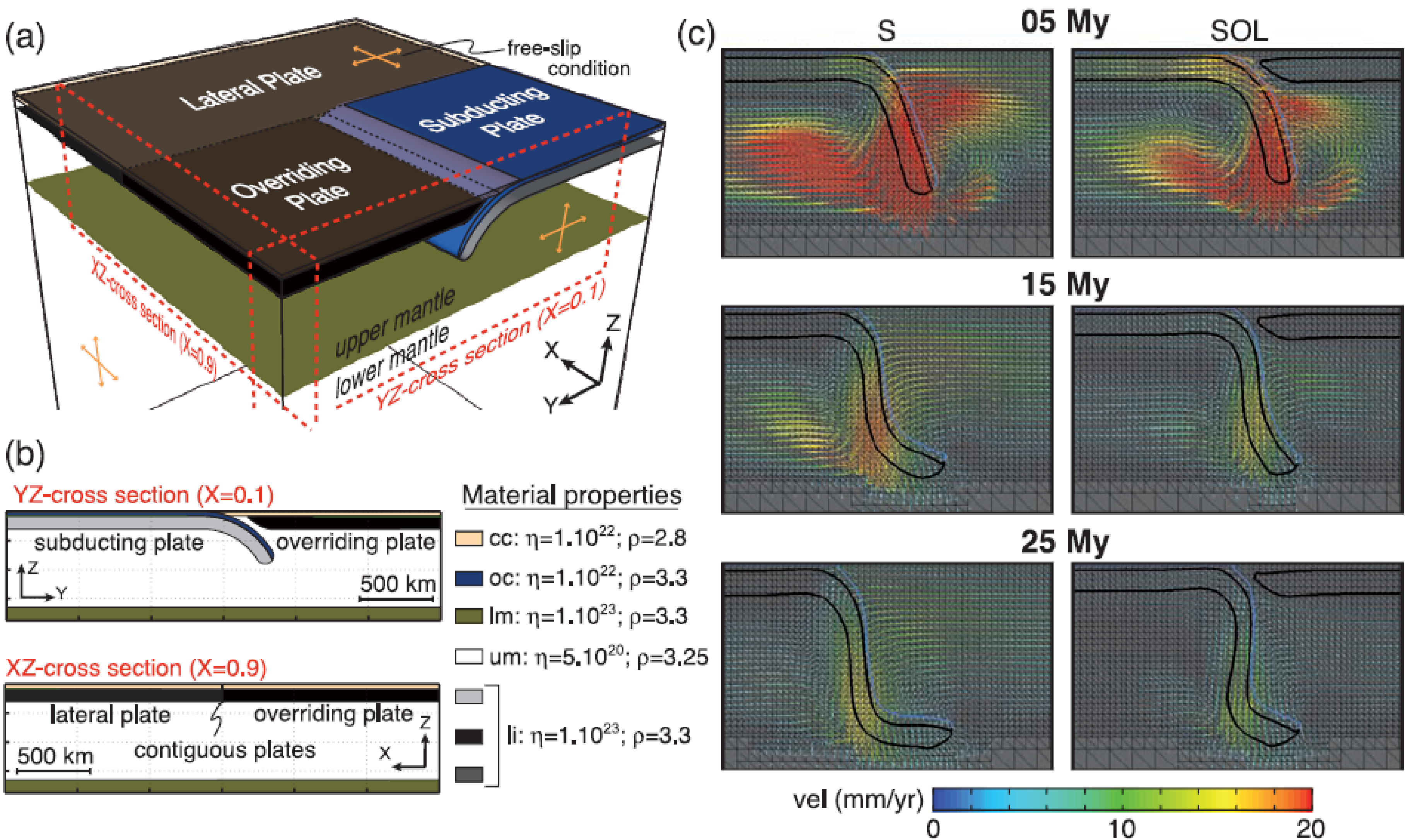

Yamato et el. (2009)

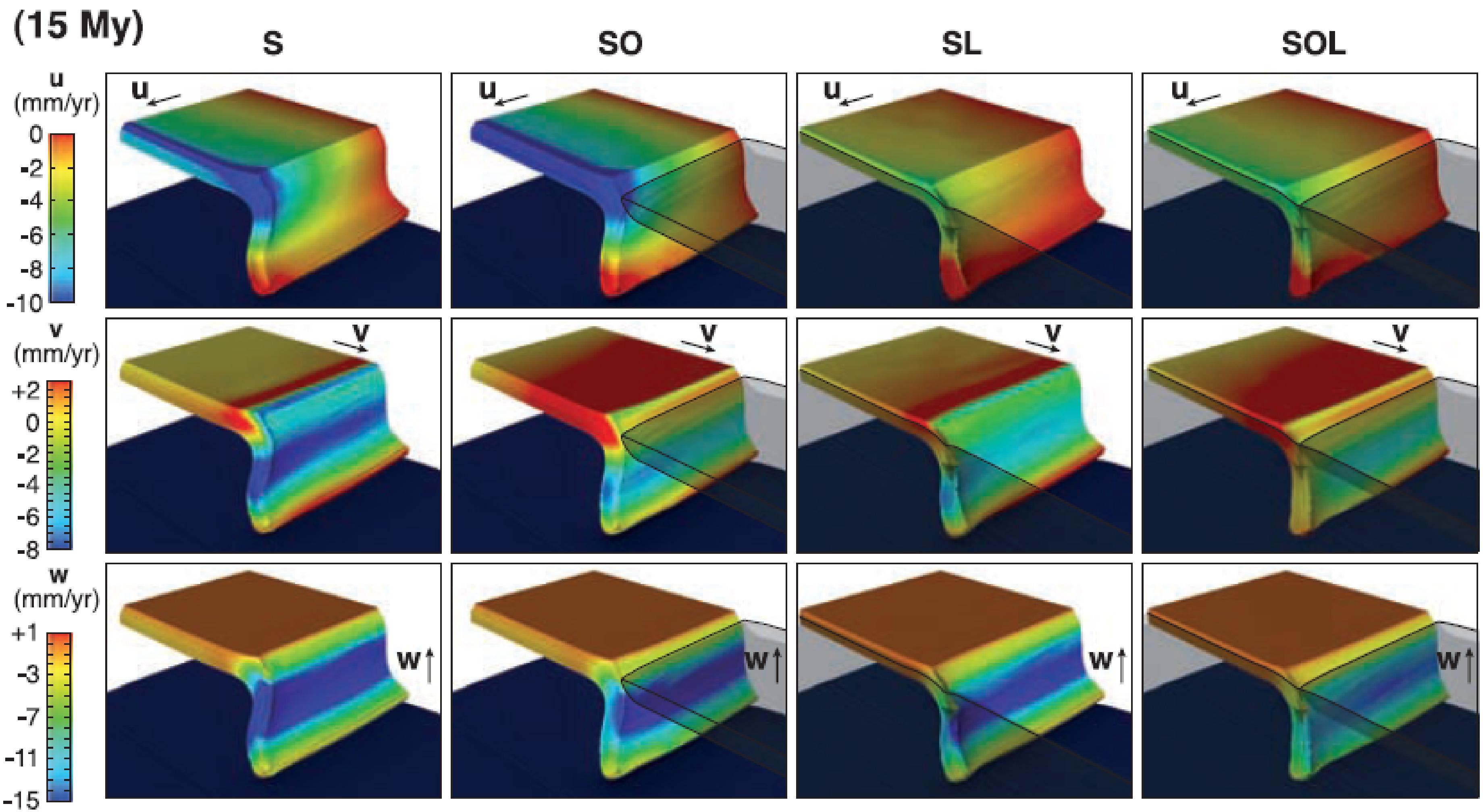

Yamato et el. (2009)

From regional to global

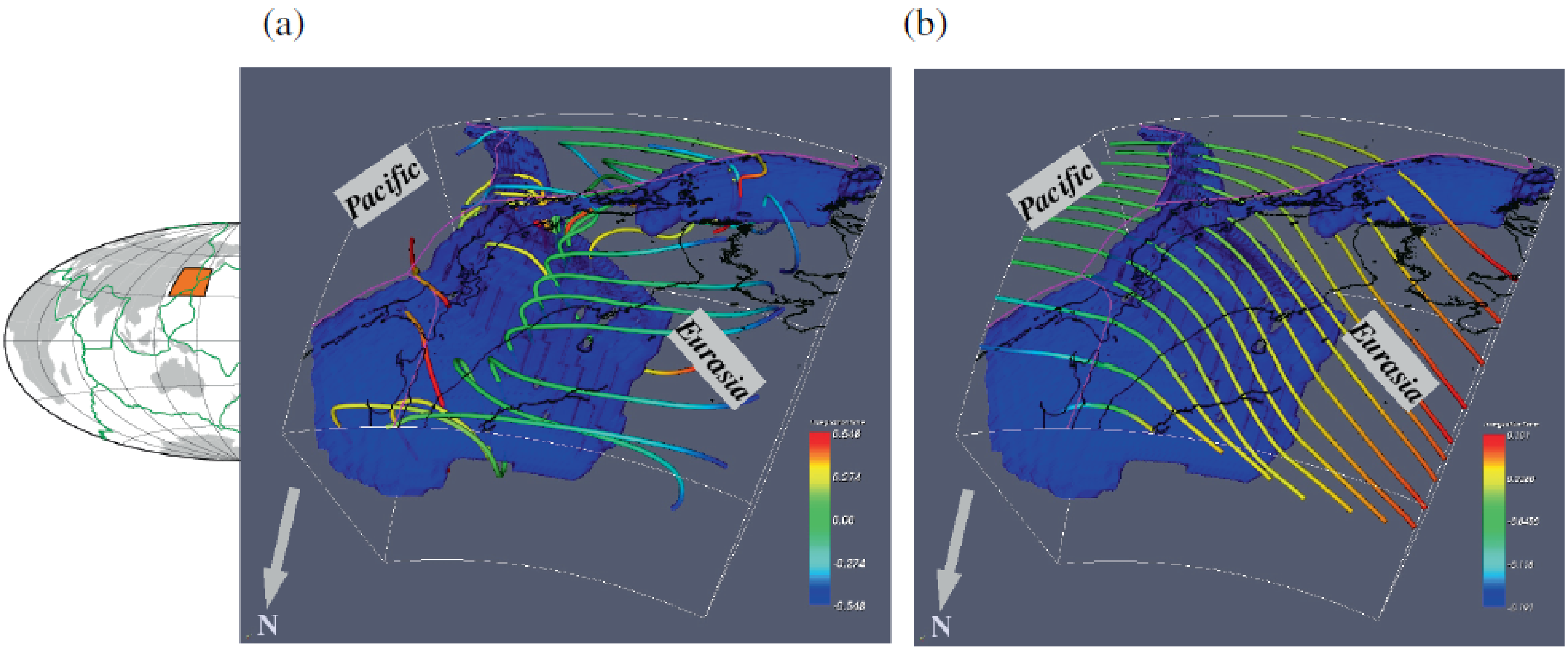

Becker & Faccenna (2009)